ACTION POTENTIAL SIMULATION OF THE *HIRUDO MEDICINALIS'S* RETZIUS CELL IN *MATLAB*

A Thesis

presented to

the Faculty of California Polytechnic State University,

San Luis Obispo

In Partial Fulfillment

of the Requirements for the Degree

Master of Science in Biomedical Engineering

By

Zechari Ryan Tempesta

December 2013

COMMITTEE MEMBERSHIP

TITLE:	Action Potential Simulation of the *Hirudo Medicinalis's* Retzius Cell in *MATLAB*
AUTHOR:	Zechari Ryan Tempesta
DATE SUBMITTED:	December 2013
COMMITTEE CHAIR:	Dr. Robert B. Szlavik, PhD Associate Professor of Biomedical Engineering
COMMITTEE MEMBER:	Dr. David S. Clague, PhD Associate Professor of Biomedical Engineering
COMMITTEE MEMBER:	Dr. Scott J. Hazelwood, PhD Associate Professor of Biomedical Engineering

ABSTRACT

Action Potential Simulation of the *Hirudo Medicinalis's* Retzius Cell in *MATLAB*

Zechari Ryan Tempesta

Modification of Hodgkin and Huxley's experimentally derived set of nonlinear differential equations was implemented to accurately simulate the action potential of the *Hirudo Medicinalis's* Retzius cell in *MATLAB* under analogous conditions to those found in the Retzius cell environment. The voltage-gated sodium and potassium channel responses to changes in membrane potential, as experimentally determined by Hodgkin and Huxley, were manipulated to suit simulation parameters established by electrophysiological Retzius cell recordings. Application of this methodology permitted additional accurate simulation of the *Hirudo Medicinalis's* P cell under analogous conditions to those found in the P cell environment. Further refinement of this technique should allow for the voltage-gated behavioral based simulation of action potential waveforms found in variety of neurons under simulation conditions analogous to the nerve cell environment.

ACKNOWLEDGMENTS

The Tempesta and Ruben Family

Dr. Robert Szlavik

Nicole Peretti

Chandra Miller

Erik Schlutter

Cindy Holton

TABLE OF CONTENTS

LIST OF TABLES xi

LIST OF FIGURES xii

LIST OF *MATLAB* SCRIPTS AND FUNCTIONS xv

ABLE OF SYMBOLS xvi

CHAPTER 1 INTRODUCTION 1

CHAPTER 2 THE NEURON 3
2.1 The Nervous System Overview 3
2.1.1 Nervous System Organization and Components 3
2.2 Nerves 3
2.2.1 Nerve Structure 4
2.2.2 Cell Body 4
2.2.3 Dendrites 4
2.2.4 Axon 5
2.2.5 Myelin 5
2.2.6 Synapses 6
2.3 Signaling in the Nervous System 6
2.3.1 Cellular Membrane 6
2.3.2 Ion Channels 7
2.3.3 Active Transporters 8

CHAPTER 3 RESTING POTENITAL 9
3.1 The Intracellular and Extracellular Environments 9
3.2 Factors that Move Ions 10
3.2.1 Passive Forces 10
3.2.2 Active Forces 11
3.2.3 Sodium- Potassium Pump 11
3.2.4 Resting Membrane Permeability 12
3.2.5 Selectivity 13

3.2.6 Membrane Conductance 13
3.2.7 Equilibrium Potential 14
3.3 Equations 14
3.3.1 Nernst Equation 14
3.3.2 Goldmann Equation 15

CHAPTER 4 THE ACTION POTENTIAL 16
4.1 Action Potential Overview 16
4.2 Generation of an Action Potential 17
4.2.1 Action Potential verses Graded Potential 17
4.2.2 Permeability 18
4.2.3 Voltage-Gated Ion Channels 18
4.3 Phases of an Action Potential 19
4.3.1 Resting Phase 19
4.3.2 Depolarization 20
4.3.3 Repolarization 21
4.3.4 Hyperpolarization 22
4.4 Properties of an Action Potential 22
4.4.1 Threshold 22
4.4.2 Summation 23
4.4.3 The Refractory Period 24

CHAPTER 5 THE HODGKIN-HUXLEY MODEL 26
5.1 Background 26
5.1.1 The Voltage Clamp 26
5.1.2 Membrane Conductance 26
5.1.3 Sodium Inactivation 27
5.2 Gating 28
5.2.1 Gating Particles 28
5.2.2 Rate Equations 29
5.2.3 Sodium Activation 30
5.2.4 Potassium Activation 32
5.2.5 Sodium Inactivation 33
5.2.6 Time Course of Conductance 34

5.3 Mathematical Description of the Hodgkin-Huxley Model 35
5.3.1 Ionic Conductance 36
5.3.2 Fitting Measured Data 37
5.4 Synthesis of the Hodgkin-Huxley Model 42
5.4.1 Voltage Control 42
5.4.2 Synthesis 43
5.4.3 Results 43

CHAPTER 6 *HIRUDO MEDICINALIS* AND DISSECTION PROTOCAL 46
6.1 The *Hirudo Medicinalis* 46
6.1.1 Anatomy 46
6.1.2 Leech Nervous System 47
6.1.3 Cell Selection 48
6.2 Ganglia Extraction Dissection Protocol 48
6.2.1 Equipment 49
6.2.2 Ganglia Extraction Procedure 49

CHAPTER 7 ELECTROPHYSIOLOGY OVERVIEW AND EXPERIMENTAL SETUP 52
7.1 Electrophysiology Recording Techniques 52
7.1.1 Current Clamp 52
7.1.2 Voltage Clamp 53
7.2 Experimental Procedure 54
7.2.1 Equipment 55
7.2.2 Equipment Setup 56
7.2.3 Calibration 56
7.2.4 Procedure Micropipette Preparation 57
7.2.5 Equipment Calibration 57
7.2.6 Procedure- Implementation 60

CHAPTER 8 EXPERIMENTIAL RECORDINGS OF THE RETZIUS CELL 64
8.1 Results 64

CHAPTER 9 IMPLEMENTATION OF THE HODGKIN-HUXLEY MODEL IN *MATLAB* 68
9.1 Setup 68
9.1.1 System of Nonlinear Ordinary Differential Equations 68
9.1.2 Initial Conditions 69
9.1.3 *MATLAB* 70
9.1.4 *MATLAB* Ordinary Differential Equation Solvers 70
9.2 Program Structure 72
9.2.1 Functions 72
9.2.2 The ODE Function 72
9.2.3 The Resting Potential Function 73
9.2.4 Initial Values of the Gating Variables 73
9.2.5 Gating Variable Rate Constants 73
9.2.6 Current 73
9.2.7 The Main Program 73
9.3 Results 73

CHAPTER 10 SIMULATING THE RETZIUS CELL 75
10.1 Initial Conditions Adjustment 76
10.1.1 Resting Potential 77
10.1.2 Pulse Characteristics 80
10.1.3 Threshold Potential 81
10.1.4 Gating Variable Initial Conditions 81
10.2 Steady State Analysis 82
10.2.1 The Rate Equations and Resting Potential 82
10.2.2 Time Constant and Gating Parameter Manipulation 84
10.2.3 Time Constant Relationship at Steady State 91
10.2.4 System Manipulation 92
10.2.5 Interaction Manipulation 95
10.3 Transient Analysis 96
10.3.1 Sodium Activation 96
10.3.2 Waveform Duration 97
10.3.3 Action Potential Peak Adjustments 97
10.3.4 Repolarization 98
10.4 Functions of Transient Analysis 98

10.4.1 Gating Behavior Manipulation 98
10.4.2 Rate Equation 99
10.4.3 Time Constant 100
10.4.4 Final Value of the Gating Variables 100
10.4.5 Ordinary Differential Equation Solver 101
10.4.6 Sodium Activation 102
10.4.7 Period Extension 109
10.4.8 Reducing Maximum 112
10.4.9 Reducing Peak Duration 115
10.4.10 Repolarization Increase 117

CHAPTER 11 RESULTS AND CONCLUSION 120
11.1 Results 120
11.2 Conclusions 123

REFERENCES 124

APPENDIX A 125

LIST OF TABLES

Table 3.1 Mammalian intracellular and extracellular ionic concentrations 10

Table 3.2 Squid axon ion concentration and their Nernst potentials 15

Table 8.1 Waveform characteristics of the Retzius cell recordings displayed in figure 8.1 64

Table 8.2 Waveform characteristics of the Retzius cell recordings displayed in figure 8.2 65

Table 8.3 Waveform characteristics of the Retzius cell recordings displayed in figure 8.3 66

Table 8.4 Average values of Retzius cell recordings in leech ganglia 1-3 67

Table 9.1. *MATLAB* nonstiff solvers 71

Table 9.2. *MATLAB* stiff solvers 71

Table 10.1 Values of *m_bc* and *m_ac* which shift the time constant along the steady state membrane potential axis 103

LIST OF FIGURES

Figure 2.1 Nerve diagram of relevant structure 4
Figure. 2.2 ATPase pumps and ion exchangers 8
Figure. 3.1 Mammalian cellular ionic concentration of intracellular and extracellular fluid 10
Figure 3.2 Driving forces and membrane permeabilities of sodium, potassium and chloride 12
Figure 4.1 Diagram of a neuron 16
Figure 4.2 Graded and action potential elicitation 17
Figure 4.3 Phases of an action potential generated in a mammalian motor neuron 19
Figure 4.4. Sodium and Potassium gates at the resting potential 20
Figure 4.5. Sodium and Potassium gates during the depolarizing phase 21
Figure 4.6. Sodium and Potassium gates during the repolarizing phase 21
Figure 4.7. Sodium and Potassium gates during the hyperpolarization phase 22
Figure 4.8. Spatial summation 24
Figure 4.9 Temporal summation 24
Figure 5.1. A diagram of the sodium channel protein, showing the gating particles for both the activation and the inactivation gates 29
Figure 5.2. Hodgkin-Huxley Model equivalent circuit of a patch of membrane 35
Figure 5.3. Conductance value of sodium and potassium at *Vm* 37
Figure 5.4. Rate constant behavior of the *m* gate at steady state voltages 39
Figure 5.5. Rate constant behavior of the *n* gate at steady state voltages 40
Figure 5.6. Rate constant behavior of the *h* gate at steady state voltages 40
Figure 5.7 Gating parameter values at steady state 41
Figure 5.8. Time constant values at steady state 41
Figure 5.9 Membrane potential and gating parameter responses as determined by solving the set of nonlinear ordinary differential equations (5.2, 5.5, 5.8, 5.41) 44
Figure 5.10. Sodium and potassium conductance response to the action potential shown in figure 5.9 45
Figure 6.1. Cross section of the *Hirudo Medicinalis* 46
Figure 6.2. Ganglia of the *Hirudo Medicinalis* 47
Figure 6.3. Nerve cell bodies within a midbody *Hirudo Medicinalis* ganglion 48
Figure 6.4. Step three of dissection protocol 50
Figure 6.5. Step seven in dissection protocol 51
Figure 7.1 Current clamp circuit diagram 53
Figure 7.2. Voltage clamp circuit diagram 54

Figure 7.3 Voltage clamp conceptual representation 54
Figure 7.4 Conceptual equipment setup 56
Figure 7.5. Axoclamp Commader Software Interface 58
Figure 7.6. Bridge balance 59
Figure 7.7. Electrophysiological recording 60
Figure 7.8. Leech ganglion under 100x magnification 61
Figure 7.9. Identifying the Retzius cell in the leech ganglion 62
Figure 7.10. Micropipette insertion into Retzius cell 62
Figure 8.1. Retzius cell recordings in leech ganglion 1 64
Figure 8.2. Retzius cell recordings in leech ganglion 2 65
Figure 8.3. Retzius cell recordings in leech ganglion 3 66
Figure 8.4 Enhanced individual Retzius cell recording 4 in leech ganglion 3 67
Figure 9.1. Conceptual representation of the electrophsysiological setup with an idealized cicuit, derived from the Hodgkin-Huxley Model 68
Figure 9.2. *MATLAB* simulation of an action potential waveform utilizing the Hodgkin-Huxley Model 74
Figure 9.3. *MATLAB* simulation of an *m, h,* and *n* during an action potential waveform utilizing the Hodgkin-Huxley Model 74
Figure 10.1. The Retzius cell action potential which will guide simulation parameters 75
Figure 10.2. The P cell action potential will guide simulation parameters 76
Figure 10.3. Steady state values of a_h, $b_{h,}a_n$, b_h at V_{rest} = -60mV 83
Figure 10.4 Steady state values of a_h, $b_{h,}a_n$, b_h at V_{rest} = -30mV 83
Figure 10.5. Steady state values of a_m, b_m at V_{rest} = -60mV 83
Figure 10.6. Steady state values of a_m, b_m at V_{rest} = -30mV 84
Figure 10.7. The relationship of $cosh(x)$, $e^x$and e^{-x} 85
Figure 10.8. The relationship of $cosh(x)$ and $sech(x)$ 86
Figure 10.9. The relationship of $sech(x)$, $\left(\frac{e^x}{2}\right)^{-1}$ and $\left(\frac{e^{-x}}{2}\right)^{-1}$ 87
Figure 10.10. The relationship of τ_m, , $(a_m)^{-1}$ and $(b_m)^{-1}$ 87
Figure 10.11. The relationship of $(\tau_m)^{-1}$, $(a_m)^{-1}$ and $(b_m)^{-1}$ 88
Figure 10.12. The function $k^{-1}(\tau_x)$ at steady state 89
Figure 10.13. Shifting the time constant at steady state with varying values of *h* equal to *a* 90
Figure 10.14. The relationship of τ_m, τ_h, and $\tau_n$at steady state 92
Figure 10.15. Uniform adjustment of τ_m, τ_h, and $\tau_n$at steady state using equations 10.8 for varying values of *k*.. 93
Figure 10.16 Uniform adjustment of τ_m, τ_h, and $\tau_n$at steady state using equations 10.8 for varying values of *h* .. 93
Figure 10.17 The gating parameters m_∞, h_∞, and n_∞ at steady state, with a resting potential of -60mV 94

Figure 10.18. Uniform adjustment of m_∞, h_∞, and n_∞ at steady state using equations 10.8 for varying values of *h* 95
Figure 10.19. The Retzius cell membrane potential generated while shifting τ_m using the Sodium activation function 107
Figure 10.20. An enhanced look at figure 10.19 where the initial activation of an action potential of the Retzius cell is observed 108
Figure 10.21. The initially activated action potential form figures 10.19 and 10.20 of the Retzius cell 108
Figure 10.22. The initially activated action potential of the P cell 109
Figure 10.23. Extension of the action potential period observed in the Retzius cell 109
Figure 10.24. Extension of the action potential period observed in the Retzius cell to a *duration* value of 0.25 111
Figure 10.25. Extension of the action potential period observed in the P cell to a *duration* value of 0.45 111
Figure 10.26. Peak reduction of the action potential observed in the Retzius cell 112
Figure 10.27. An enhanced depiction of figure 10.26 113
Figure 10.28. Peak reduction of the action potential observed in the Retzius cell to a *tau_m_reduction* of 8 114
Figure 10.29. Peak reduction of the action potential observed in the P cell to a *tau_m_reduction* of 0.9 114
Figure 10.30. Peak duration reduction of the action potential observed in the Retzius cell 115
Figure 10.31. Peak duration reduction of the action potential observed in the Retzius cell to *h* value of -15 116
Figure 10.32. Peak duration reduction of the action potential observed in the P cell to *h* value of -1 117
Figure 10.33. Repolarization increase of the P cell 117
Figure 10.34. Repolarization increase of the P cell with the value of *n_x* equal to -0.0061 119
Figure 11.1. An experimental recording of a Retzius cell action potential from the data gathered in Chapter 8 120
Figure 11.2 Multiple experimental recordings of a Retzius cell action potentials from the data gathered in Chapter 8 121
Figure 11.3. The stimulated action potential of a Retzius cell 121
Figure 11.4 Recording of a P cell action potential 122
Figure 11.5. The simulated action potential of a P cell 122

TABLE OF *MATLAB* SCRIPTS AND FUNCTIONS

V_r 77
Nernst_from_V_r 78
Pulse Information 80
Find_threshold 81
Gating initial conditions 81
Rate equation 99
Time constant 100
Final Value of the Gating Variables 100
Invoke ODE solver 101
Odefun 101
Tau_m_shift 104
Sodium activation 106
Period Extension 110
Reducing Maximum 112
Reducing Peak Duration 115
Repolarization Increase 118

TABLE OF SYMBOLS

$E_{ion\ x} =$ equilibrium potential (mV) for ion x
$[X_{ion}]_{out}$ = extracellular concentration of ion x
$[X_{ion}]_{in}$ = intracellular concentration of ion x
z = valence of ion x
R= Ideal gas constant (8.3145$\frac{J}{mol*T}$)
T = temperature (K)
F = Faraday's constant (9.6485e4 $\frac{C}{mol}$)
$p_{ion} =$ Membrane permeability
$i_k =$ Membrane current (A)
$I_m =$ Current across the membrane (A)
I_C = Capacitance current (A)
I_{Leak} = Leakage current (A)
C_m = Membrane capacitance (F)
$g_k =$ Conductance of the membrane (S)
$\overline{G_{ion}} =$ Maximum possible sodium conductance (S)
V_m= Potential across the membrane (V)
$a_x =$ Rate constant
$b_x =$ Rate constant
$m =$ Portion of gating particles that are able to interact with the *m* gate binding sites
m_0 = Initial value of *m*
m_∞ = Final value of *m*
$t =$ Time (s)

CHAPTER I: INTRODUCTION

Advances in computing over the last half-century have permitted accessible simulation of neural activity to the scientific community. Modern applications include artificial neural networks, disease modeling, machine learning, machine brain interface and many, many more.

The neural simulation technique was established in 1952 by Alan Lloyd Hodgkin and Andrew Huxley with the development of the Hodgkin-Huxley model. Hodgkin and Huxley based this model on a set of nonlinear differential equations which were systematically developed from an elegant series of electrophysiological studies that clarified the ionic mechanisms underlying initiation and propagation of action potentials in the giant axon of the Loligo squid. The experiments have provided the mathematical framework for modern biophysically based neural modeling and rewarded Hodgkin and Huxley with the 1963 Nobel Prize in Physiology.

This study modifies the original Hodgkin and Huxley experimentally derived set of nonlinear differential equations to simulate the action potential of the *Hirudo Medicinalis's* Retzius cell in *MATLAB*. Altering these equations allows manipulation of votlage-gated sodium and potassium channel responses to changes in membrane potential, permiting control of the temporal behavior of membane potential during an action potetnial.

Extensive electrophysiological studies were conducted in the *Hirudo Medicinalis's* Retzius cell to guide and establish simulation parameters. This simulation was generated under analogous conditions to those found in the Retzius cell, including cellular dimension, intracellular and extracellular ionic concentrations, ionic electrochemical grandients, ionic membrane permeabilies, membrane capacitance, stimulation parameters, threshold potential and function of voltage-gated ion channels. The resulting waveform is able to accurately represent many aspects of actual Retzius cell electrophysiological recordings, including: waveform amplitude, period, peak duration and decay.

The methodology developed during this study proves to have diverse application in waveform stimlation, providing an additional accurate simulation of action potentials recorded in the P cell of the *Hirudo Medicinalis* under analogous P cell conditions. Further application and refinement of this technique should allow for the voltage-gated behavioral based simulation of many action potential-like waveforms under simulation conditions analogous to the cellular environment. Simulations of this nature could provide helpful insight regarding the voltage sensitivity and dependence of voltage-gated ion channels in an array of organisms.

CHAPTER II: THE NEURON

2.1 The Nervous System Overview

The nervous system is an organized network of specialized, excitable cells and tissues which receive sensory information and orchestrate coordinated responses in all vertebrate and most invertebrate species. Proper function of the nervous system is essential to the survival of the organism. The nervous system monitors the organism's external and internal environment by interpreting and processing collected sensory information and triggering an appropriate motor response to maintain homeostasis.

2.1.1 Nervous System Organization and Components

Vertebrate and invertebrate species have fundamental differences in nervous system organization and complexity. The human nervous system, alike all other vertebrate, is anatomically divided into two parts: the central nervous system (CNS) and the peripheral nervous system (PNS). The CNS consists of the brain, spinal cord and complex neural networks. It receives sensory information gathered by the primary sensory organs, spinal nerves and peripheral nerves from all parts of the body. This information is integrated and processed by neural networks in the brain which formulate an appropriate response. A motor command is now generated and relayed out via spinal and peripheral nerves to be executed. The PNS is formed by all nerves and ganglia outside the brain and spinal cord. It provides the CNS with sensory information concerning external stimuli and internal organs and carries information from the CNS to organs muscles and glands [1, 2].

2.2 Nerves

The most fundamental part of the nervous system is the neuron. The neuron is an electrically excitable cell which receives and transmits electrical and chemical signals to target cells, tissue and organs.

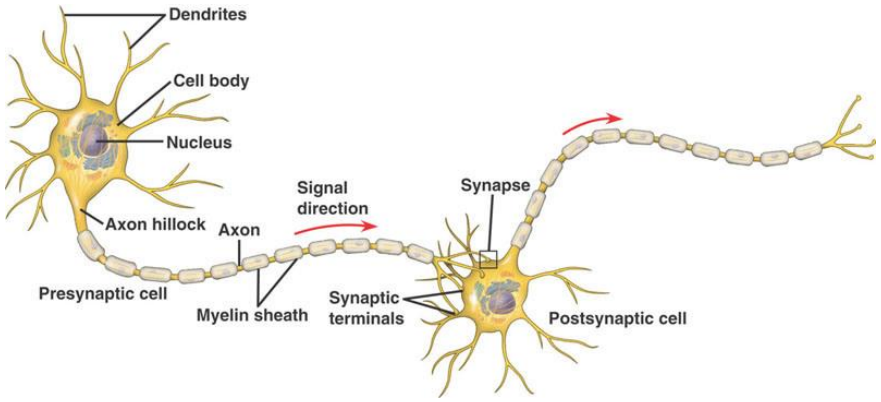

Figure 2.1. Nerve diagram of relevant structures [2]

2.2.1 Nerve Structure

Neurons are diverse in structure and function. The following characteristics represent common elements found in mammalian nervous systems:

2.2.2 Cell Body

The cell body, soma or perikaryon, is the central part of a neuron; it is responsible for protein synthesis and generation of metabolic energy to maintain normal neuron function. The cell body contains the nucleus, mitochondria, Golgi apparatus, Nissl granules, polyribosomes, and the axon hillock [1]. It is connected to dendrites and the axon via the axon hillock.

2.2.3 Dendrites

The dendrites act as the neuron's receivers. Each receives information from other neurons and transmits this information to the soma in the form of electrical signals [2]. Dendrites branch off from the cytoplasm of the cell in all directions to increase cellular surface area. A larger area increases the number of potential neural connections, known as synapses.

2.2.4 Axon

The axon is a specialized structure which conducts electrical signals from the cell body to the synaptic terminal and eventually other neurons. Most neurons have many dendrites but only a single axon. Axons can range in length from a few microns (as in interneurons) to over a meter (as in lumbar motor neurons which project from the lumbar section of the spinal cord to motor units in the foot) [2].

The axon is a cylindrical tube of cytoplasm covered by the axolemma membrane. A cytoskeleton consisting of microtubules and neurofilaments runs through the axon, providing a framework for axonal transport. The axon arises from the axon hillock in the cell body. The initial segment contains a high density of sodium channels in the axolemma; this area acts as a trigger zone for the electrical signal or action potential to be initiated and be transmitted down the length of the axon. Eventually the signal will reach the terminal axonal branches and trigger synaptic activity; this will allow the neuron to signal other neurons via synaptic transmission [1].

2.2.5Myelin

Myelin is an insulting layer which surrounds the length of the axon and serves to increase conduction speed. Myelin has multiple lipid rich membranes which are produced by Schwann cells in the peripheral nervous system and oligodendrocytes in the central nervous system. The myelin sheath is divided into one millimeter long sections with one micrometer gaps, known as the nodes of Ranvier, where myelin is absent. These gaps are uninsulated and capable of generating electrical activity. This capacity allows electrical signals to be successfully propagated down the length of the axon [1,3].

It should be noted that not all neurons contain myelin; axons without myelin are perfectly capable of conducting electrical signals. Myelin facilitates conduction speed to increase, resulting in quicker interaction between neurons.

2.2.6 Synapses

The synapse, or synaptic gap, is a special interneuronal area in which a neuron can transmit electrical or chemical signals to another neuron or neurons. Once an electric signal travels down the length of the axon and axonal branches it reaches the axon terminal. The axon terminal is the transmitting and presynaptic side of the synaptic junction; the receptive region of the receiving neuron is the post synaptic side. Transmission at most synaptic junctions involves the release of chemical transmitters, known as neurotransmitters, from the presynaptic neuron. However, other sites can communicate information by passing current directly from presynaptic cells to postsynaptic cells through specialized electrical synapses or gap junctions. Electrical synapses are common in invertebrate nervous systems but rare in vertebrate systems [1, 2, 3].

2.3 Signaling in the Nervous

The nervous system utilizes intricate networks of neurons to receive, process and exchange vast amounts of information. Neurons are able to respond to stimuli by generating and conducting electrical impulses, known as action potentials. These electrical signals can then be communicated to other neurons and neural networks. The following cellular structures aid nerve cells in generating action potentials.

2.3.1 Cellular Membrane

The cellular membrane separates the intracellular environment from the extracellular environment and regulates permeability of molecules and ions. The selectivity of the membrane allows exchanges of nutrients and wastes needed to sustain metabolism and allows passage of electrical currents created by the movement of ions through the membrane.

The cellular or plasma membrane is composed of a thin polar membrane made up of two lipid layers with embedded integral proteins which span the membrane. Generally, 98% of the molecules which make up the membrane are lipids, 75% of which are phospholipids. Phospholipids are a class of

lipids ideally suited to form lipid bilayers; each is characterized by their two hydrophobic tails and hydrophilic head. When exposed to water, these phospholipids orient into a two layered sheet with the polar, hydrophilic head pointing outward and the non-polar, hydrophobic tails inward. This formation creates an impermeable barrier to most water-soluble molecules [3].

The integral proteins which span the membrane are the remaining 2%. These proteins provide structures for essential cellular function; including: channels, transporters, pumps, receptors, enzymes, structural support and many others. We are most interested in the proteins that act as pumps, channels or transporters from one side of the impermeable membrane to the other. These proteins regulate the fluctuation of cellular ionic concentration and therefore the conduction of electrical current in and out of the membrane, which is fundamental to in neural communication [3,4].

2.3.2 Ion Channels

Ion channels are intrinsic membrane proteins which contain aqueous pores that can be opened or closed. When open, these channels selectively permit ions to diffuse from one side of the membrane to the other in accordance with the electrochemical gradient. When closed they are impermeable to ion flow. Ion channels can have single, multiple or no gating mechanisms. The gating mechanisms which open and close in response to a certain stimulus. These ion channels can be identified by the type of stimuli that causes the channel gates to open or close. Some channels are opened by particular chemicals inside or outside the cell, such as neurotransmitters or other cytoplasmic messenger molecules. Other channels are sensitive to changes in voltage across the membrane, and still others respond to various kinds of sensory stimuli [1].

Each channel also shows selectivity in the ions to which they are permeable. Some are constructed to only permit a specific type, such as sodium, potassium, chloride or calcium ions. Others have fewer restrictions permitting broader groups of ions, such as monovalent cations or all cations to pass through. These two characteristics, gating sensitivity and ion selectivity, are commonly utilized to

describe and classify different types of channels. The most common forms of stimuli that ion channel gates selectively respond to are the binding of ligands to the integral protein and changes in voltage across the membrane; these are known as ligand-gated ion channels and voltage-gated ion channels respectively. Leak channels are selective ion channels which are always open, do not have gates and do not require stimuli. Sodium, potassium, chloride and calcium ions all have individual channels, abundant throughout the body, which have prominent roles in neural firing and muscle contraction [4].

2.3.3 Active Transporters

Active transporters are a class of intrinsic plasma membrane proteins which selectively transport ions across the membrane and against their concentration gradient. Active transporters bind with ions to form complexes, which are then translocated across the membrane and released. This process takes several milliseconds causing ion translocation by active transport to be much slower than ion movement through ion channels. Actively transporting ions uphill also requires the consumption of energy. Neural transporters fall into two classes based on their energy sources: ATPase pumps and ion exchangers.

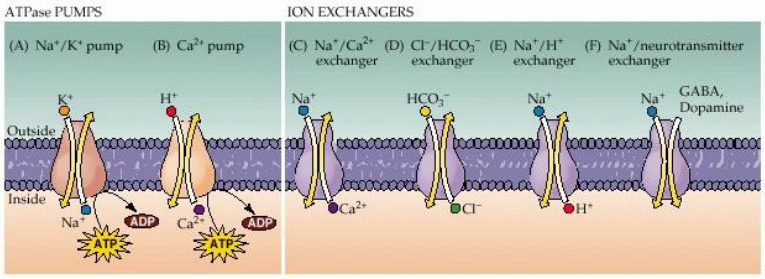

Figure. 2.2 ATPase pumps and ion exchangers [1]

ATPase pumps receive energy directly from the hydrolysis of ATP. Ion exchangers utilize the concentration gradients of other ions as an energy source to move a desired ion across the membrane. This type of transporter carries one ion up its electrochemical gradient while simultaneously carrying another ion down its electrochemical gradient. Abundant examples include the Na+/K+ pump and the Na+/Ca+ exchanger. [1, 6, 8].

CHAPTER III: RESTING POTENTIAL

Neurons are excitable cells which can generate electrical signals in response to stimuli. In order to achieve this phenomenon an electric potential must be maintained across the cell membrane at rest. Without the resting membrane potential it no nerve impulse can occur. A nerve cell is considered in a state of rest or equilibrium when it is not generating or recovering from an action potential and it is maintaining a consistent membrane potential. The electric potential across the membrane during this state is known as the resting membrane potential. The following factors allow a nerve to maintain a resting potential across its membrane.

3.1 The Intracellular and Extracellular Environments

The intracellular and extracellular environments of mammalian neurons consist mostly of water, proteins, amino acids, phospholipids, inorganic ions and organic ions as shown below in figure 3.1. The intracellular proteins, phosphate groups of ATP and other organic molecules are negatively charged at the pH of the cell cytoplasm and impermeable to the membrane. This presence of non-diffusible negatively charged molecules cause the intracellular environment to be negatively charged relative to the surrounding extracellular environment. At rest, the intracellular environment has a high concentration of potassium ions and membrane impermeable anions, while the extracellular environment has a high concentration of sodium and chloride ions. The concentrations of chloride, potassium and sodium ions will remain consistent at rest and slightly fluctuate during an excited state [2,4 ,9].

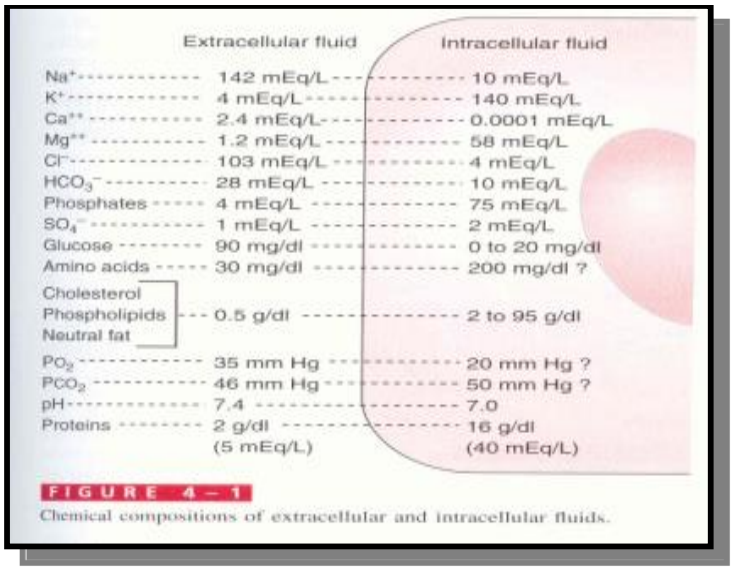

Figure. 3.1 Mammalian cellular ionic concentration of intracellular and extracellular fluid [9]

TABLE 3.1

MAMMALIAN INTRACELLULAR AND EXTRACELLULAR IONIC CONCENTRATIONS [4]

Ion	External(mM)	Internal(mM)	Permeable to Membrane
K+	5	125	Yes
Na+	120	12	No
Cl-	125	5	Yes
A-	0	108	No
H2O	55,000	55,000	Yes

3.2 Factors that Move Ions

3.2.1 Passive Forces

There are two forces which move ions and influence ionic equilibrium across the membrane without requiring energy, the chemical concentration and electrical gradient. Together these forces make up the electrochemical gradient and describe the ability of an ion to move across a membrane [3, 4, 9].

Ionic diffusion is a product of chemical concentration gradient. Diffusion is the random movement of particles from an area of high concentration to low concentration. If the cellular

environment of a neuron could be left unregulated, this force would move sodium and chloride ions into the cell and potassium out of the cell. However, the membrane repels this diffusive force, storing energy in the form a chemical potential across the membrane [1,3,9].

The electrical gradient is generated by the electrostatic forces which ions exert on one another. When ions with like charges are in the presence of each other they will exhibit electrostatic repulsion; if ions with opposite charges are in the presence of one another they will exhibit electrostatic attraction. In a neural environment there is an extracellular excess of positive ions separated from the negatively charged intracellular fluid by the cellular membrane. A difference in charge across the cellular membrane causes an electrical gradient to exist across the membrane [1,3,9].

3.2.2 Active Forces

Diffusive and electrostatic forces transport ions according to the direction of the electrochemical gradient. However, to maintain a proper resting potential the membrane must also have the ability to move ions against the gradient. In neurons, Na+/K+ ATPase pumps actively facilitate transport of sodium and potassium ions against their electrochemical gradient to maintain resting potential [1,9].

3.2.3 Sodium–Potassium Pump

The sodium–potassium pump is a carrier protein which actively extrudes three sodium ions from the cell as it transports two potassium ions into the cell. This process is energy dependent because it acts against the sodium and potassium concentration gradients. Energy is provided by the conversion of ATP to ADP and Pi by the carrier protein ATPase enzyme [1].

Each nerve cell has leak channels which passively allow sodium or potassium to flow down their concentration gradient. The cell membrane has many potassium leak channels, which allow potassium ions to leave the cell. The sodium-potassium pump counteracts this effect by restoring potassium into cell.

This counteraction of the sodium-potassium pump permits nerve cells to have a relatively constant intracellular concentration of sodium and potassium ions and a constant membrane potential [1].

3.2.4 Resting Membrane Permeability

The concentration differences between ions on the inside and outside of the cell generate potential across the membrane and influence the direction ions want to flow. However, ionic mobility is limited by the permeability of the cell membrane to specific ionic species. Together, the electrochemical force and membrane permeability influence ionic fluctuation and distribution across the membrane.

The most influential membrane permeable ions in nerve communication are sodium and potassium. The cellular membrane is made up of more potassium channels than any other type of ion channel, which also makes it the most permeable to potassium [4, 9]. This is demonstrated in the resting membrane permeability ratio of sodium to potassium ($\frac{p_{Na}}{p_K}$) which is 0.02 as shown below in figure 3.2.

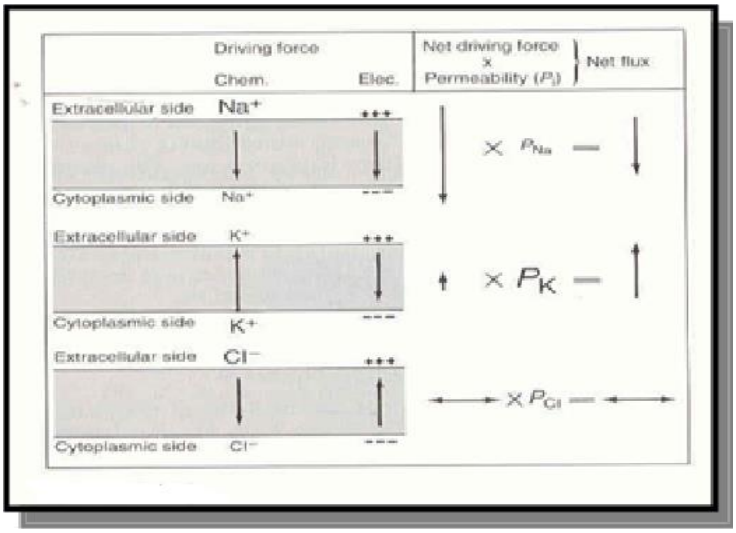

Figure 3.2 Driving forces and membrane permeabilities of sodium, potassium and chloride [9]

3.2.5 Selectivity

Sodium and potassium ion channels are highly selective of the ions that will pass through. Each channel protein spans the lipid membrane, with an aqueous pore connecting the external medium to the internal cytoplasm. The narrowest region of this pore is the selectivity filter, which only allows ions of a particular species to proceed through when open. The selectivity filter must be narrow enough to permit direct ion contact with the pore walls, limiting passage to ions of a specific dimension. The filter is hydrophobic which removes the hydration shell around the incoming ion: oxygen atoms from the filter's electronegative carbonyls align around the ion, replacing the oxygen atoms of the previously surrounding water molecules. The ion, if compatible, may then be bound to the channel protein at the ion binding site and released into the internal cytoplasm. [3, 7]

3.2.6 Membrane conductance

Membrane conductance of a particular ion is the index of an ion's ability to carry current across the membrane. Conductance quantifies the ease at which a particular ionic current flows through the cell membrane in response to a change in membrane potential. Conductance is analogous to the reciprocal of the resistance of an electrical circuit to current flow, as shown below:

$$i_k = G_k(E_m - E_k) \tag{3.1}$$

Here, g_k is the conductance of the membrane to potassium ions, measured in Siemens; $(E_m - E_k)$ is the driving force which governs net movement of potassium ions across the membrane, measured in Volts, and i_k is the outward membrane current, measured in Amperes. Similar equations can be written for sodium and chloride.

$$i_{Na} = G_{Na}(E_m - E_{Na}) \tag{3.2}$$

The membrane conductance of an ion is closely related to its membrane permeability, but is not identical. Conductance is proportional to the rate at which ions are crossing the membrane; this rate is

dependent on both permeability and the number of available ions [4]. Membrane permeability remains consistent in the presence of low and high concentrations of permeable ions, while conductance varies according to the concentration of permeable ions present. Together, these membrane properties provide helpful insight when evaluating the state ionic flow.

3.2.7 Equilibrium potential

Concentration gradients cause an unequal distribution of ionic charge that generates a bioelectric potential across the membrane, similar to a tiny battery with the positive pole outside of the cell and the negative pole inside. Concentration gradients are maintained by homeostatic processes such as the sodium potassium pump [1, 3, 4].

At rest, an equilibrium potential exists for each membrane permeable ion. An ion is at equilibrium when the diffusive and electrical forces are equal and opposite. In this state the electrochemical gradient is zero, allowing no net movement of ions through their channels. At rest, a membrane potential exists which encompasses interacting electrochemical gradients of sodium and potassium ions and membrane permeability to the specific ionic species. The electrochemical gradients of these individual ions are not equal to zero, meaning there still is some movement of ions through their open channels and down their electrochemical gradient when the membrane is at resting potential. An equilibrium potential can also represent the theoretical voltage that would be produced across the cellular membrane for a species of ion to return from resting potential to equilibrium if it were the only diffusible ion [4].

3.3 Equations

3.3.1 Nernst equation

The equilibrium potential of an ion is described by the Nernst Equation:

$$E_{ion\,x} = \frac{RT}{zF} \ln\left(\frac{[\mathrm{X_{ion}}]_{\mathrm{out}}}{[\mathrm{X_{ion}}]_{\mathrm{in}}}\right) \tag{3.3}$$

TABLE 3.2

SQUID AXON ION CONCENTRATION AND THEIR NERNST POTENTIALS [9]

Ion	External(mM)	Internal(mM)	Nernst Potential (mV)
K+	20	400	-75
Na+	440	50	+55
Cl-	560	40	-66

Here, the Nernst potentials for potassium, sodium and chloride in a squid axon are depicted.

3.3.2 Goldmann equations

The Goldmann equation expresses the contributions that ionic concentrations and membrane permeability have on membrane potential. The Goldmann equations describing a membrane which is permeable to potassium, sodium and chloride can be written as:

$$Vm = \frac{RT}{F} ln \frac{P_K[K^+]_{out} + P_{Na}[Na^+]_{out} + P_{Cl}[Cl^-]_{out}}{P_K[K^+]_{in} + P_{Na}[Na^+]_{in} + P_{Cl}[Cl^-]_{in}} \quad (3.4)$$

Here, P_{ion} is the membrane permeability to a particular ion; the remaining constants are the same as the Nernst equation [4]. Both the Goldmann and Nernst equations serve as useful tools in determining nerve cell characteristics from intracellular and extracellular ionic concentrations.

CHAPTER IV: THE ACTION POTENTIAL

Neurons are electrically excitable cells. This characteristic allows neurons to respond to stimuli by generating and conducting electrical impulses, known as action potentials. Action potential generation facilitates the onward propagation of nervous information to other neurons. This process provides the basis for all nervous communication.

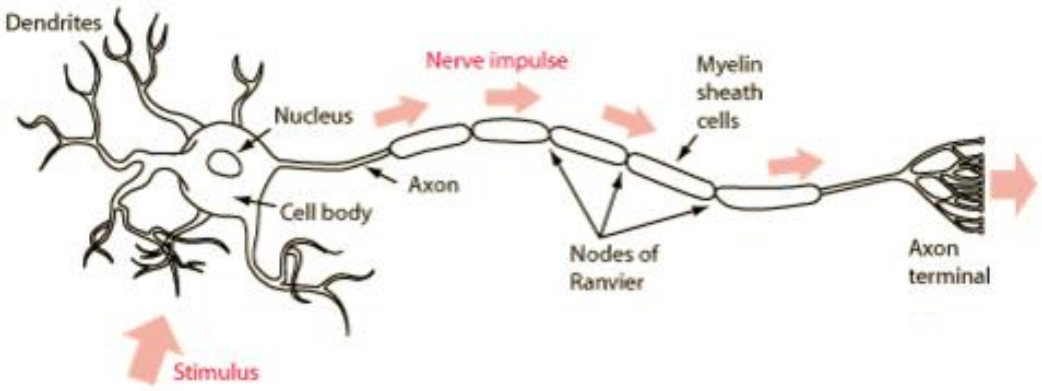

Figure 4.1 Diagram of a neuron [10]

4.1 Action Potential Overview

The cell body's dendrites are a common postsynaptic site for coupled presynaptic neurons. These presynaptic neurons are providing incoming information which is either excitatory or inhibitory. The dendrites pass all incoming information to the cell body via electrical impulses where, if sufficiently stimulated, an action potential is generated. The action potential will be conducted form the "trigger zone" in the cell body down the axon to the axon terminal endings. An action potential reaching the axon terminal endings will trigger the release chemical or electrical signals into the synaptic gap. The neuron is releasing these signals from the presynaptic side of the synaptic gap; these signals will travel across the synapse onto the coupled neuron's postsynaptic site, restarting the entire process again.

4.2 Generation of an Action Potential

4.2.1 Action Potential vs. Graded Potential

When a stimulus current of a sufficient magnitude is passed through the cellular membrane of an electrically excitable cell, a change in membrane potential called an action potential is generated. However, if a stimulus current is not of sufficient magnitude to elicit an action potential, a smaller change in membrane potential, called a graded potential, is generated. Thus, nerve cells have to capacity to generate a graded potential or action potential dependent on stimulus current magnitude [5].

The mechanism generating these potentials also differs in the relationship between stimulus magnitude and membrane potential: graded potentials show a continuous relationship between stimulus magnitude and membrane potential, while action potentials show a discontinuous relationship between stimulus magnitude and membrane potential. Graded potentials cannot activate voltage-gated ion channels and are therefore subjected to a dependent relationship. Action potentials drastically change membrane permeability by activating voltage-gated ion channels, allowing membrane potential to independently change with respect to stimulus magnitude [5]. The membrane response during a graded potential and action potential is depicted in figure 4.2.

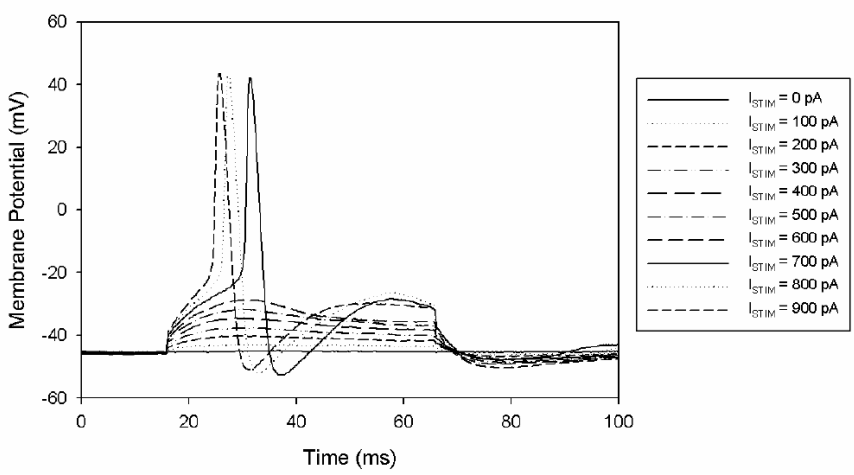

Figure 4.2 Graded and action potential elicitation [5]

4.2.2 Permeability

The distribution of charged ions across the cell membrane fluctuates during the 'all or nothing' progression of an action potential, generating the change in transmembrane voltage described in figure 4.2 and 4.3. This fluctuation is due to shifts in ionic permeability and results in ionic movement. Intervals of membrane permeability change can be divided into four basic phases: rest, depolarization, repolarizaton, and hyperpolarization. The changes in ion permeability during each phase are a result of activation and deactivation of voltage-gated ion channels [5, 10].

4.2.3 Voltage-Gated Ion Channels

Voltage-gated ion channels are a class of ion channels which open or close in response to changes in transmembrane potential. Voltage-gated sodium channels respond to stimulus currents to initiate an action potential; once an action potential has commenced voltage-gated sodium and potassium channels govern changes in ion permeability until the membrane is repolarized back to resting potential [3].

These channels have gates which regulate ion passage. Voltage-gated sodium channels have two independent gates, known as the *m* and *h* gate. The *m* gate, or sodium activation gate, is located on extracellular side of the membrane protein and is closed at resting potential. The *h* gate, or sodium inactivation gate, is located on the intracellular side the membrane protein and is open at resting potential. Voltage-gated potassium channels only have one gate, known as the *n* gate. The *n* gate, or potassium activation gate, is located on extracellular side of the membrane protein and is closed at resting potential. These gates respond to particular changes in membrane voltage and open or close at different rates [3,4]. Following the initial depolarizing step, *h* and *n* gates will respond slowly, while the *m* gate will react quickly [3,4]. The response of these channels and their gates during different phases of an action potential in a mammalian motor neuron is outlined below. Please note the location of these gates are presented for conceptual purposes, voltage-gated ion channels are three dimensional transmembrane proteins that undergo conformational changes to either inhibit or accommodate ion passage. The location of these gates

are not necessarily permanent, as the channel protein position and geometry distort during conformational change [25].

4.3 Phases of an Action Potential

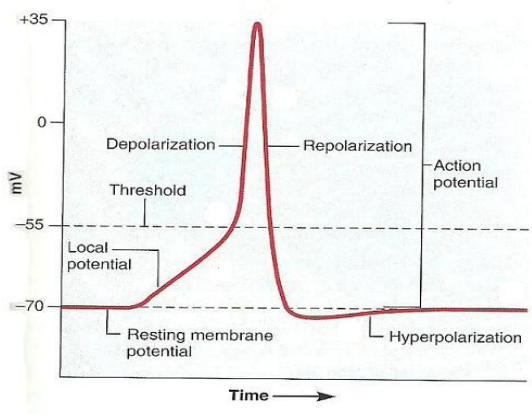

Figure 4.3 Phases of an action potential generated in a mammalian motor neuron [11]

4.3.1 Resting phase

The resting phase occurs when the nerve cell is in a steady state, maintaining resting membrane potential. In this state, the cell has the capacity to respond to sufficient stimulus current and generate an action potential. The resting potential of a mammalian motor neuron nerve cell exists between the Nernst potential for potassium (-80mV) and the Nernst potential for sodium (+58mV). Potassium's Nernst potential has a significant influence on resting potential because of its dominance in membrane permeability over sodium. During this phase, the *m* gate and *n* gate are closed while the slow *h* gate is open [4].

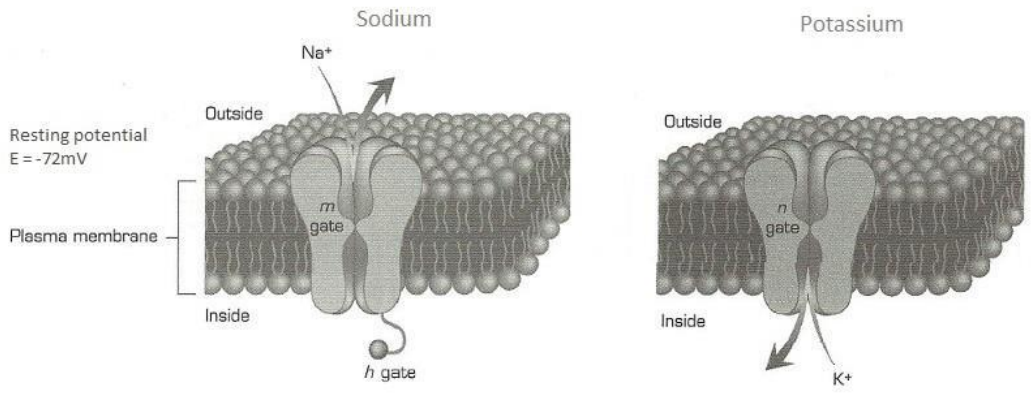

Figure 4.4. Sodium and Potassium gates at the resting potential [4]

4.3.2 Depolarization

The depolarization phase, or rising phase, occurs once when a stimulus current of sufficient magnitude is passed through the cellular membrane of a nerve cell in resting state. The stimulus current increases membrane potential above threshold. The threshold is the value of the minimum membrane potential which generates an action potential. Once threshold is reached, the fasting acting *m* gate rapidly opens, the slow acting *n* gate begins to open and slow acting *h* gate start to close. This change in membrane sodium permeability allows extracellular sodium to flow down its electrostatic gradient, into the negative intracellular environment of the neuron. The massive sodium influx increases the membrane potential to a peak near sodium's Nernst potential, marking the end of the depolarization phase [4].

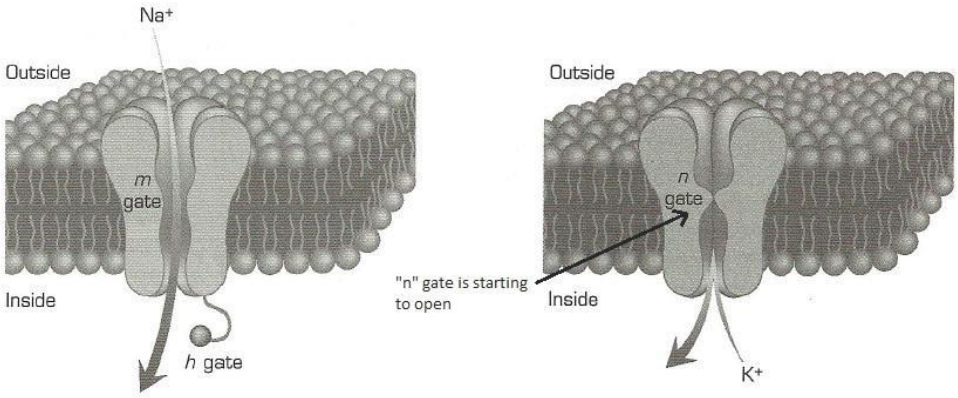

Figure 4.5. Sodium and Potassium gates during the depolarizing phase [4]

4.3.3 Repolarization

As the membrane potential reaches its maximum, the repolarization phase, or falling phase, begins. The slow acting *h* gate closes, inactivating the influx of sodium ions into the cell and ceasing the increase in membrane potential. Now the potassium channels' slow *n* gate is fully open, allowing potassium ions to flow down their electrostatic gradient from the newly positive intracellular environment of the neuron and into the more negative extracellular environment. The potassium *n* gate repolarizes the cell membrane potential, remaining open until resting potential is reached [4].

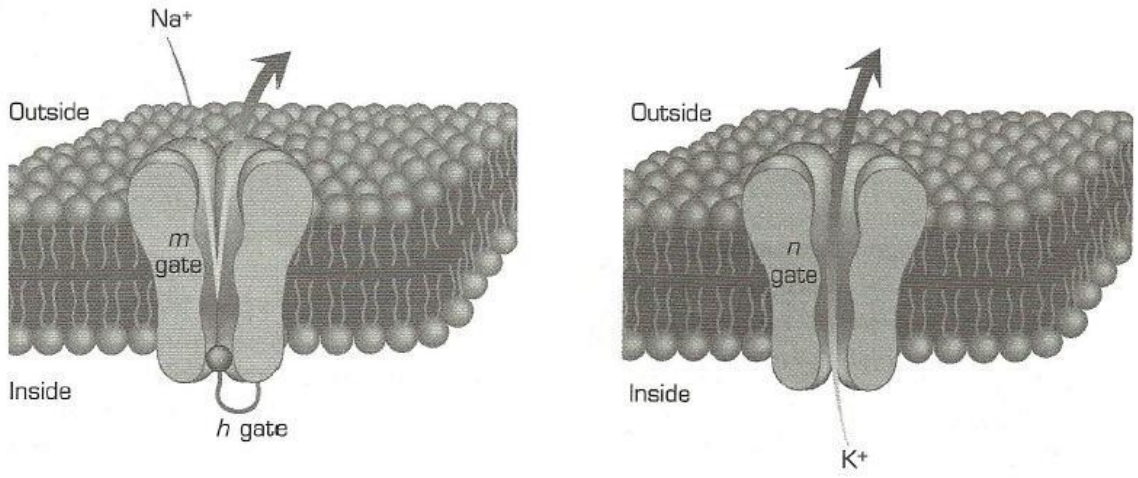

Figure 4.6. Sodium and Potassium gates during the repolarizing phase [4]

4.3.4 Hyperpolarization

During the repolarization, or refractory, phase the membrane potential becomes more negative due to the efflux of intracellular potassium ions. The membrane potential continues to decrease and undershoots resting potential while the *n* gate fully closes and *h* gate beings to open again [4].

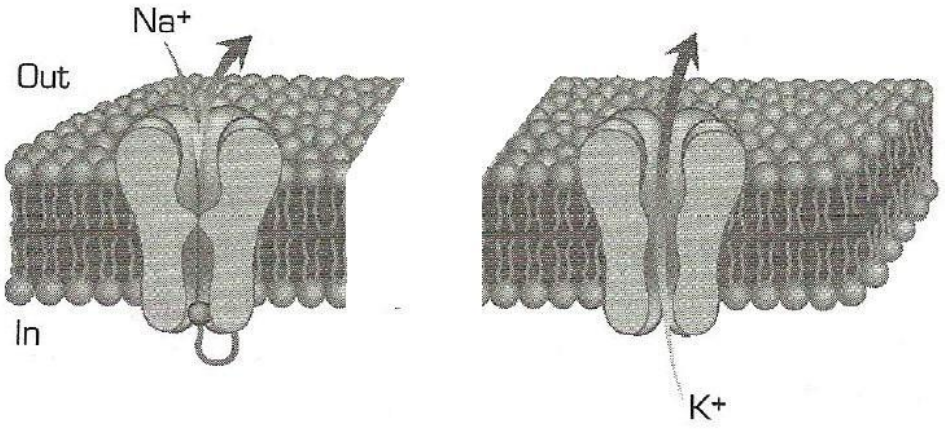

Figure 4.7. Sodium and Potassium gates during the hyperpolarization phase [4]

4.4 Properties of an Action Potential

4.4.1 Threshold

To generate an action potential a stimulus current of sufficient strength must elevate membrane potential from resting potential to threshold potential. A nerve cell's threshold potential is the minimum value of membrane potential that will elicit an action potential. If a stimulus current is not of sufficient magnitude to reach the threshold potential a graded potential is generated [5].

Graded potentials open a small portion of voltage-gated sodium channels, slightly increasing sodium permeability. However, the resulting influx of sodium ions cannot overcome the opposing efflux of potassium ions. A net outward membrane current is produced, ceasing further depolarization and generation of an action potential. At threshold potential, the minimum amount of voltage-gated sodium

channels are open in order to overcome the efflux of potassium ions and produce a net inward current. This permits further depolarization causing sodium influx to dominate, resulting in an action potential [5].

The value of threshold potential for a particular neuron is influenced by the density of voltage-gated sodium channels in the plasma membrane and the sensitivity of those channels. A high density of voltage-gated sodium channels requires a smaller portion of channels to open to generate an influx of sodium which overcomes potassium efflux. An increased sensitivity in voltage-gated sodium channels will also requires a smaller portion of channels to open to generate an influx of sodium which overcomes potassium efflux. The lower the threshold potential, the more excitable a neuron is to incoming nerve impulses and the more actively it propagates signals to other neurons [3].

4.4.2 Summation

Neurons receive postsynaptic potentials from many other neurons, located at the synapse sites. To elicit an action potential, these signals must generate a resultant potential exceeding the threshold potential when reaching the neuron's trigger zone. These individual postsynaptic potentials will decay in time and space when traveling from the synapse sites to trigger zone. However, in certain conditions, postsynaptic potentials can summate spatially or temporally to combine potential and combat decay [11, 12].

Spatial summation occurs when graded postsynaptic potentials, generated at different synapse locations, occur within a single space constant of another. The space constant is the distance a particular potential will occupy before it decays. Temporal summation takes place when graded postsynaptic potentials occur within a single time constant of another. The time constant is the amount of time a particular potential will take to decay. Potentials which summate combine amplitudes to form a single impulse with an elevated magnitude. This elevation expands the distance postsynaptic potentials can occupy before decaying to zero. Summation of postsynaptic potentials increases the ability of a neuron to

produce a resultant potential which exceeds threshold at the trigger zone and generate an action potential [12]. Spatial and temporal summations are demonstrated in figures 4.8 and 4.9 respectively.

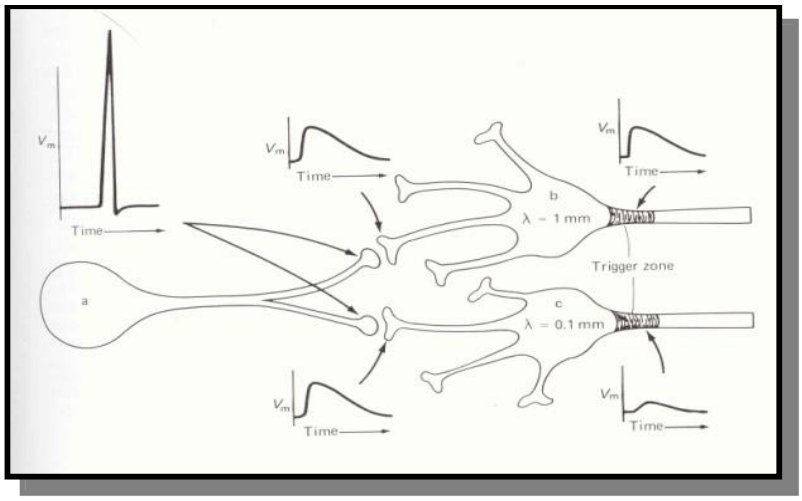

Figure 4.8. Spatial summation [12]

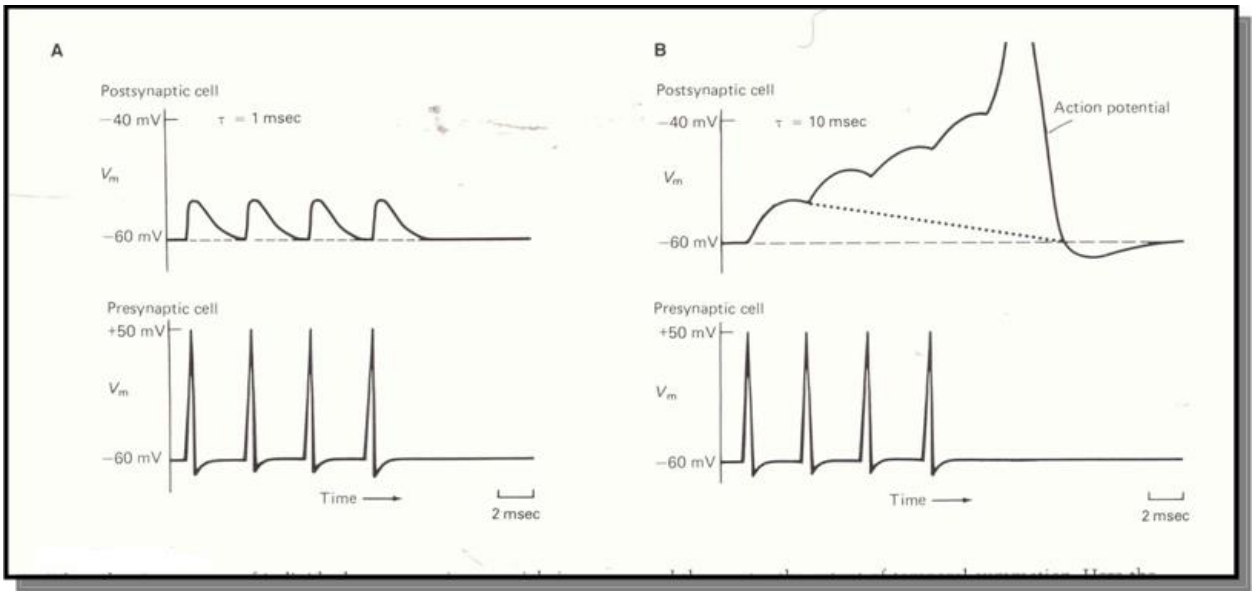

Figure 4.9 Temporal summation [12]

4.4.3 The Refractory Period

Immediately following the occurrence of an action potential, a nerve cell has a reduced ability to elicit a second action potential and is said to be refractory. For a brief interval, known as the absolute

refractory period, a second action potential cannot be elicited by any magnitude of stimulus. For intervals greater than the absolute refractory period, there is the relative refractory period in which a second action potential can be produced, but the threshold potential is elevated. Threshold elevation is dependent on a complex history of previous stimulation and response cycles of the axon. Absolute refractory periods occur on the order of a few milliseconds, while relative refractory periods have shown lasting effects, up to many minutes [5]. Together absolute and relative refractory periods limit the maximum frequency at which neurons can conduct information.

CHAPTER V: THE HODGKIN-HUXLEY MODEL

Alan Lloyd Hodgkin and Andrew Huxley were awarded the 1963 Nobel Prize in Physiology and Medicine "for their discoveries concerning the ionic mechanisms involved in excitation and inhibition in the peripheral and central portions of the nerve cell membrane" [13]. Their ground breaking work consisted of a series of five papers published in the Journal of Physiology in the 1950's; the culmination of this work was the Hodgkin-Huxley Model, published in the final paper in 1952 The Hodgkin-Huxley Model helped explain the ionic mechanisms underlying initiation and propagation of action potentials in the giant axon of the Loligo squid. Hodgkin and Huxley based this model on a set of nonlinear differential equations which were systematically developed from an elegant series of electrophysiological studies [14-18]. These experiments have provided the mathematical framework for modern biophysically based neural modeling and are considered the theoretical pillar of modern neurobiology [19].

5.1 Background

5.1.1 The Voltage Clamp

The voltage clamp is a recording technique which holds membrane potential at a constant value; membrane current adjusts to this change according to difference in membrane potential and the new 'clamped' potential. The amount of current flowing across the membrane to maintain this 'clamped' membrane potential is recorded [4]. This technique was utilized by Hodgkin and Huxley to uncover the time-course response of ionic conductance to step changes in membrane voltage. This subject will be revisited in great detail in the electrophysiology setup.

5.1.2 Membrane Conductance

Hodgkin and Huxley discovered that the peak conductance produced by a depolarizing voltage-clamp step is dependent upon the change in voltage. This established the voltage dependence of the sodium and potassium conductances within the nerve cell membrane. To account for voltage sensitivity of sodium and potassium conductances, Hodgkin and Huxley proposed that many individual ion channels, each with a small individual ionic conductance, determines the behavior of the whole membrane under

voltage-clamp analysis. Each of these channels has two conducting states: an open conducting state in which ions are free to pass through, and a closed, non-conducting state in which a channel is blocked. The transition between these two states behaves as though access to the channel were governed by gates. This system responds to changes in membrane potential by altering the probability that the channel gate will open and convert the channel from a non-conducting state into a conducting state. A depolarization step increases the probability that channel gates will open, converting a fraction of the total channel population into a conducting state and increasing total membrane conductance. If the depolarizing step is of sufficient strength, this effect will continue to increase probability and propagates until all channels are open and maximum conductance is reached [4, 5].

5.1.3 Sodium Inactivation

Hodgkin and Huxley performed a series of experiments to examine the voltage dependence of the sodium-inactivation process. The experiment established the magnitude for which sodium conductance increased in response to a fixed depolarizing step when preceded by a long prepulse whose amplitude could be varied. The experimental results demonstrated that a depolarizing prepulse reduced the amplitude of the depolarizing step while a hyperpolarizing prepulse increased the amplitude of the depolarizing step. Hodgkin and Huxley concluded that the depolarizing prepulses closed a portion of the sodium inactivation gates, hindering sodium accessibility and reducing the amplitude of the depolarizing step. The hyperpolarizing prepulses suggested that some of the sodium inactivation gates were are already closed a normal resting potential. By varying prepulse amplitude, Hodgkin and Huxley were able to establish the dependence of the inactivation gate on membrane potential [4].

5.2 Gating

5.1.1 Gating Particles

Hodgkin and Huxley theorized that voltage-gated ion channels contain charged entities, known as gating particles; each is associated with a channel protein and permits a gating response to transmembrane voltage fluctuation. When membrane potential is at resting potential, the charged gating particles of *m* and *n* gates are in a state which favors closed channels; when the membrane is depolarized these particles begin to assume a new state which favors an open channel. Gating particles are assumed to have a positive charge and are therefore attracted to the negative intracellular environment at resting potential. The electric field across the membrane influences the distribution of charged gating particles within the membrane and channel protein. At resting potential, these particles would be distributed close to the inner face of the membrane; upon depolarization, membrane potential increases, shifting the electric field and distribution of gating particles to the outer face of the membrane [4].

The channel protein is assumed to have a binding site on the outer portion of the membrane which controls the 'gating' portion of the channel. When the binding site is unoccupied, the gate is shut and the channel is closed. When the site binds to one of the gating particles, the gate begins to swing open. The voltage-gated sodium channel has two gates on each channel protein: sodium activation and sodium inactivation. Like the activation gate, the inactivation gate is controlled by a charged gating particle; when the binding site is occupied, the gate is open. Unlike the activation gate, however, the inactivation gate is located on the inner portion of the membrane and opens at resting potential and begins to close upon depolarization. This behavior can be properly modeled by locating the binding site on the inner face of the membrane. At resting potential, the positively charged gating particles occupy the inactivation gate's binding sites and hold the gate open. The potassium activation gate functions in a similar manner to the sodium activation gate; the binding site is located on the outer edge of the

membrane and is closed during depolarization [4]. The sodium gates and gating particles are shown below:

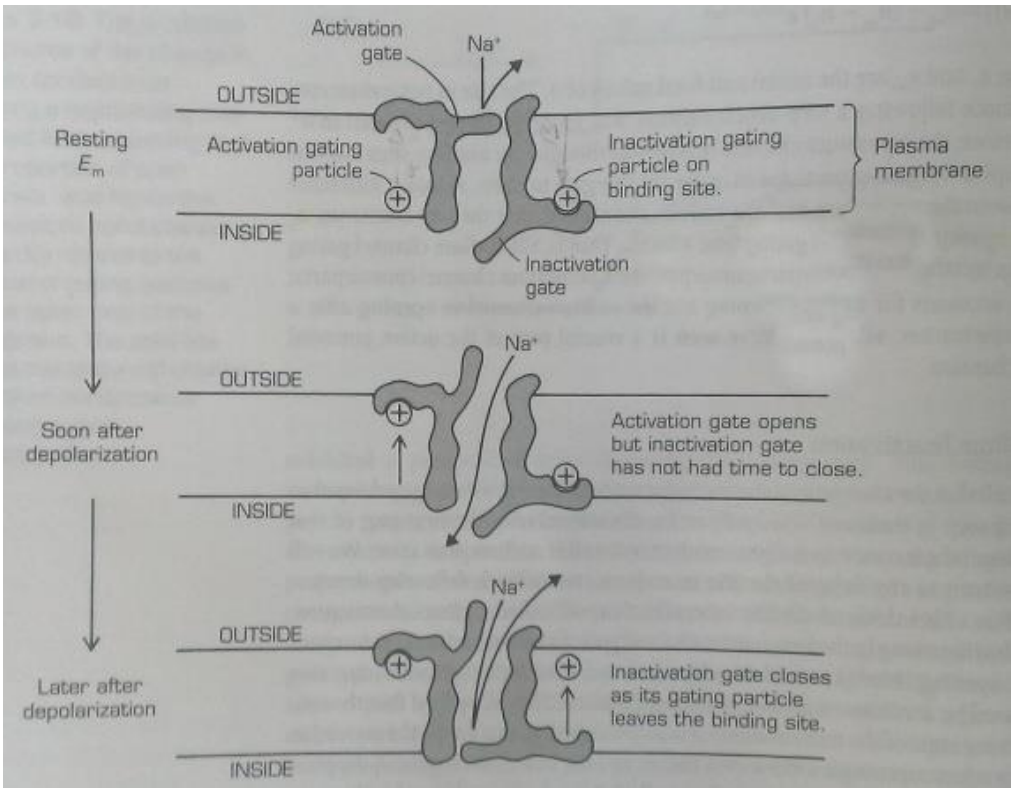

Figure 5.1. A diagram of the sodium channel protein, showing the gating particles for both the activation and the inactivation gates [4]

5.2.2 Rate Equations

The different rates at which the three types of voltage-sensitive gates respond to a step depolarization determine the fluctuations in membrane permeability and govern the form of the action potential. Hodgkin and Huxley assumed that the rate of change in the membrane conductance to an ion following a step depolarization is governed by the rate of redistribution of the gating particles within the membrane. The delay associated with the interaction of gating particles upon binding site arrival or departure is assumed to be negligible [4, 5].

5.2.3 Sodium Activation

The movement of gating particles within the membrane can be illustrated in the form of the following first-order kinetic model:

$$m \underset{b_m}{\overset{a_m}{\leftrightarrows}} (1-m) \tag{5.1}$$

This particular model described the kinetics involved in the opening of the sodium channel's *m* gate following a step depolarization. Here, *m* is the portion of gating particles that are able to interact with the *m* gate binding sites, located on the outer side of the channel protein within the membrane; 1-*m* is the portion of gating particles located on the inner side of the channel protein within the membrane, where no binding sites exist. The rate constant, a_m, describes the rate at which gating particles move from the inner face within the membrane to the outer face within the membrane, and $b_m$is the rate of reverse movement. During a change in membrane voltage, a gating response can be seen in the instantaneous change in the rate constants a_m and b_m. For instance, a depolarizing stimulus would increase a_m and decrease b_m, governing a net increase in *m* and net decrease in 1-*m* [4]. The following equation illustrates the rate at which gating particle redistribute following a change in the membrane potential:

$$\frac{\mathrm{d}m}{\mathrm{d}t} = a_m(1-m) - b_m m \tag{5.2}$$

Here, d*m*/d*t* is the net rate of change of the proportion of the gating particles on the outside face within the membrane (where the binding site is located). The term $a_m(1-m)$, is the rate at which particles are leaving the inside of the membrane and $b_m m$ is the rate at which the particles are leaving the outside surface. The difference between these rates is the net rate of the change in *m.* At a resting equilibrium, the rate at which particles move from inside to outside would equal the rate in the opposite direction and the net rate of the change in *m* would be zero. If a constant depolarization is maintained, the system will approach a new steady distribution of particles, with the rate governed by this equation [4].

The solution of a first-order kinetic expression structured as equation 5.2 is an exponential function. Following a step change in membrane potential, *m* will approach a new steady value in an exponential manner, described below:

$$m(t) = m_\infty - (m_\infty - m_0)e^{-(a_{m+}b_m)t} \tag{5.3}$$

A change in membrane voltage will cause *m* to change exponentially from its initial value (m_0) to its final value (m_∞) at the rate governed by the rate constants (a_m and b_m) of the gating particles at the new value of membrane potential [4].

Using this equation to determine the behavior of *m* over time after a step depolarization also allows insight into gating particle activity. The number of binding sites occupied by gating particles would be expected to be proportional to *m;* with this information the number of open channels can be determined. Assuming occupation of a single binding site causes the channel to open, the number of open channels would be expected to follow the same exponential manner as *m* after a step change in membrane potential [4].

To observe this effect, sodium conductance was measured following a voltage clamp step depolarization. Sodium conductance was chosen because it directly reflects the total number of open sodium channels. This experiment demonstrated that the kinetic behavior of sodium conductance following a step depolarization actually exhibits an S-shaped increase rather than the predicted exponential increase. This behavior can be attributed to the assumption that an occupation of a single binding site causes the channel to open, when in fact, it is a combination of several independent sites. The probability that all of a channel's binding sites are occupied is the product of the probabilities that each single site will bind a gating particle. Because these probabilities are proportional to *m,* it can be assumed that the probability of a channel opening is proportional to m^x, with *x* being the number of binding sites. The S-shaped rise in sodium conductance following a depolarizing step suggests proportionality to $m^3$for

the sodium channel. This finding suggests that the sodium channel behave as though three binding sites must be occupied by gating particles before the channel will open and conduct [4].

5.2.4 Potassium Activation

Like to the sodium system, the movement of potassium gating particles within the membrane can be illustrated in the form of the following first-order kinetic model:

$$n \underset{b_n}{\overset{a_n}{\leftrightarrows}} (1-n) \tag{5.4}$$

By analogy, *n* is the proportion of potassium gating particles that are able to interact with the *n* gate binding sites, located on the outer side of the channel protein within the membrane; 1-*n* is the portion of gating particles located on the inner side of the channel protein within the membrane, where no binding sites exist. The rate constant, a_n, describes the rate at which gating particles move from the inner face within the membrane to the outer face within the membrane, and $b_n$is the rate of reverse movement. When *n* is approached, the potassium activation gate is fully open, permitting potassium entry into the cell and initiating repolarization [4].

Potassium channel gating particle redistribution following a change in membrane potential is illustrated in the equation below:

$$\frac{\mathrm{d}n}{\mathrm{d}t} = a_n(1-n) - b_n n \tag{5.5}$$

The solution to equation 5.4 is in the exponential form:

$$n(t) = n_\infty - (n_\infty - n_0)e^{-(a_n + b_n)t} \tag{5.6}$$

Following a step change in membrane voltage, *n* changes exponentially from its initial value (n_0) to its final value (n_∞) at the rate governed by the rate constants (a_n and b_n) of the gating particles at the new value of membrane potential. The rise in potassium conductance following a step depolarization

suggests proportionality to n^4; therefore potassium channels behave as though four binding sites must be occupied by gating particles before the channel will open and conduct [4].

5.2.5 Sodium Inactivation

The sodium channel is controlled by two gates: the sodium activation gate, *m*, and sodium inactivation gate, *h*. The aforementioned equations involving *m* describe the increase in sodium conductance following depolarization, known as sodium activation. The delayed decline in sodium conductance following a depolarization is known as sodium inactivation and is governed by the movement of sodium inactivation gating particles within the membrane illustrated in the form of the following first-order kinetic model:

$$h \underset{b_h}{\overset{a_h}{\leftrightarrows}} (1-h) \tag{5.7}$$

Like the sodium activation gate, the inactivation gate is controlled by a positive gating particle: when the binding site is occupied, the inactivation gate is open. Unlike the sodium activation gate, however, the inactivation gate is open at resting potential and slowly closes in response to the initial depolarizing step. This behavior can be modeled as in figure 5.1, with the inactivation gate and its binding site on the inner side of the channel protein within the membrane [4].

In this configuration, *h* is the portion of inactivation gating particles that are able to interact with the *h* gate binding sites located on the inner side of the channel protein within the membrane; 1-*h* is the proportion of sodium inactivation gating particles located on the outer side of the channel protein within the membrane, where no inactivation binding sites exist. The rate constant, a_h, describes the rate at which gating particles move from the outer face within the membrane to the inner face within the membrane, and $b_h$is the rate of reverse movement [4]. Redistribution of sodium inactivation gating particles following a change in membrane potential is illustrated in the equation below:

$$\frac{\mathrm{d}h}{\mathrm{d}t} = a_h(1-h) - b_h h \tag{5.8}$$

The solution to equation 5.8 is in the exponential form:

$$h(t) = h_\infty - (h_\infty - h_0)e^{-(a_h+b_h)t} \tag{5.9}$$

Following a step change in membrane voltage, *h* changes exponentially from its initial value (h_0) to its final value (h_∞) at the rate governed by the rate constants (a_h and b_h) of the gating particles at the new value of membrane potential. Investigation into the relation of prepulse duration and peak sodium conductance during a depolarizing test step suggests number of closed channels would be expected to follow an exponential manner proportionate to h^1. This indicates that sodium inactivation behaves as though a single binding site must be occupied by a gating particle for the inactivation gate to remain open [4].

Introducing the *h* gate into the sodium channel system adds complexity when determining general gating and rate equation guidelines. To clarify, *m*, *h* and *n* represent the probability that gating particles will occupy their respective binding site; conversely, 1-*m*, 1-*h*, and 1-*n* are the probabilities that gating particles do not occupy their respective binding site. The alpha rate equations describes the rate at which gating particles move within the membrane from an unbound state to a bound state, in response to a change in membrane potential; the beta rate equations describes the rate at which gating particles move within the membrane from an bound state to a unbound state, in response to a change in membrane potential [4].

5.2.6 Time Course of Conductance

The gating parameters, *m*, *n* and *h* describe the redistribution rate of gating particles within the membrane over the course of an action potential. Activity of these gating particles specifies the change in sodium and potassium conductance following a depolarizing voltage-clamp step; these relationships are shown in equations 5.10 and 5.11:

$$G_{Na} = \overline{G_{Na}} m^3 h \tag{5.10}$$

$$G_K = \overline{G_K} n^4 \tag{5.11}$$

Here, $\overline{G_{Na}}$ and $\overline{G_K}$ are the maximum possible sodium and potassium conductance across the membrane and *m, n* and *h* are the gating parameters. Following a depolarization, the sodium conductance rises proportionately to the third power of the sodium activation gate parameter *m* and returns directly proportionate to the decline in the sodium inactivation gate parameter, *h*. The product of $m^3 h$ governs the time-course of the sodium conductance following depolarization. The potassium conductance rises proportionately to the fourth power of its activation parameter, *n*, and does not inactivate. The time-course of potassium conductance is governed by n^4 following depolarization [4].

5.3 Mathematical Description of the Hodgkin-Huxley Model

The Hodgkin-Huxley Model equivilant circuit of a patch of membrane is shown below:

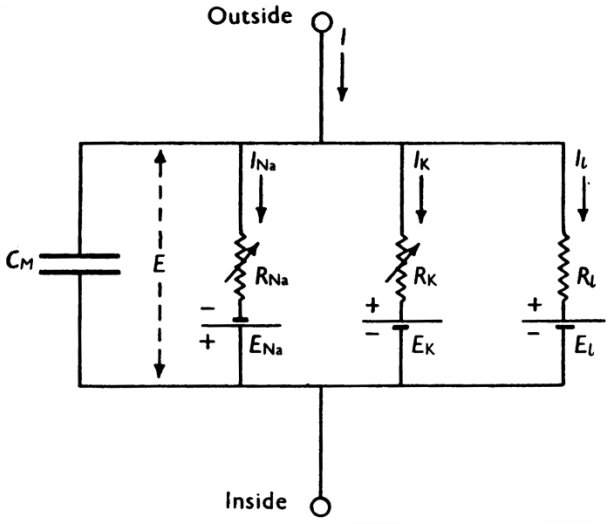

Figure 5.2. Hodgkin-Huxley Model equivalent circuit of a patch of membrane [15]

Here, membrane current, I_m, is related to the membrane potential, V_m. There are four branches of current, each branch representing different currents which effect membrane potential. The capacitance current, I_c, represents the displacement current through the membrane; the three remaining branches

represent ionic currents due to sodium, potassium and leakage. The leakage current signifies the sum of ionic membrane currents other than those flowing through sodium and potassium channels, including currents though the cut end of the dissected axon. Sodium and potassium currents are each represented by a change in conductance over time in series with the Nernst equilibrium potential for each ion. Conductance of sodium and potassium, G_{Na} and G_K, is now explicitly dependent on membrane potential and time, indicated by the arrow through the conductance. The leakage branch is characterized by a Thevenin network with a constant conductance, G_L, and equivalent battery [5]. Utilizing Kirchoff's current law, the membrane current, I_m, of the equivalent circuit is expressed below

$$I_m = I_C + I_{Na} + I_K + I_{Leak} \tag{5.12}$$

Substitution of Ohm's law into equation 5.12 for each of the conductances and capacitance yields:

$$I_m = C_m \frac{dV_m}{dt} + G_K(V_m, t)(V_m - V_K) + G_{Na}(V_m, t)(V_m - V_{Na}) + G_L(V_m - V_L) \tag{5.13}$$

Here, V_{Na} and V_K are the Nernst equilibrium potentials for sodium and potassium and C_m is the membrane capacitance. The term, $G_{ion}(V_m, t)$, specifies ion conductance as a function of membrane potential and time [5].

5.3.1 Ionic Conductances

Membrane potential may be predicted by the Hodgkin-Huxley model computed from equation 5.12 if the functions $G_{Na}(V_m, t)$ and $G_K(V_m, t)$ are known and boundary conditions are specified. To uncover these functions, Hodgkin and Huxley performed a series of experiments in which conductances were measured as functions of V_m and t [5].

5.3.2 Fitting Measured Data

Ionic conductances were obtained from direct ionic current measurements in voltage clamp studies:

$$G_K(V_m, t) = \frac{I_K(V_m,t)}{V_m - V_K} \tag{5.14}$$

and

$$G_{Na}(V_m, t) = \frac{I_{Na}(V_m,t)}{V_m - V_{Na}} \tag{5.15}$$

Conductance was calculated as a function of time for several different values of V_m from measurements of sodium and potassium currents as a function of time for several values of V_m, shown in figure 5.3. Following a specified step depolarization, sodium conductance rises rapidly along an S-shaped curve to a maximum and then decays exponentially to zero; potassium rises along an S-shaped curve to a steady final value and does not decay. The rate at which potassium conductance rises is roughly similar to the decay rate of sodium conductance. Both temporal behavior and amplitude of these conductance changes are dependent upon membrane potential [5].

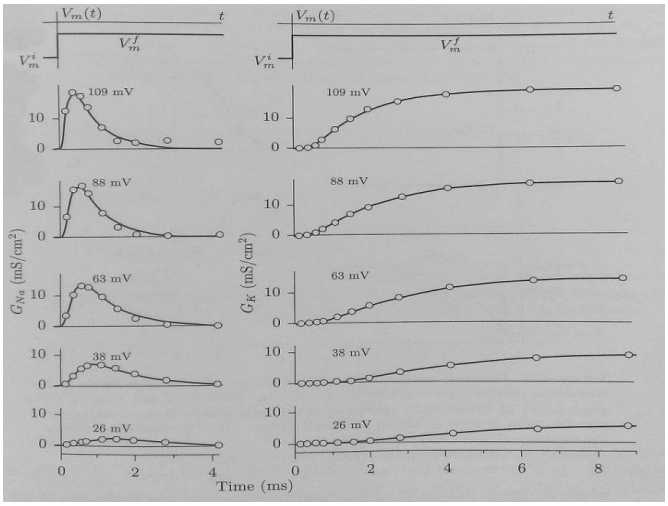

Figure 5.3. Conductance value of sodium and potassium at *Vm* [5]

Hodgkin and Huxley fit the ionic conductances with the gating parameters, *m, n* and *h*. Together these parameters describe the dynamic conductance response to membrane potentials changes and satisfy the first-order kinetic equations:

$$G_K(V_m, t) = \overline{G_K} n^4(V_m, t) \tag{5.16}$$

and

$$G_{Na}(V_m, t) = \overline{G_{Na}} m^3(V_m, t) h(V_m, t) \tag{5.17}$$

Here, $\overline{G_K}$ and $\overline{G_{Na}}$ are constants, representing maximum conductance and *m* ,*n* and *h* are solutions of first-order ordinary differential equations dependent on membrane potential.

The following two forms satisfy a first-order kinetic equation utilizing *x* as a generic gating parameter which could represent *m, n* or *h.* The first form is expressed in terms of rate constants:

$$\frac{\mathrm{d}x}{\mathrm{d}t} = a_x(1 - x) - b_x x \tag{5.18}$$

The second form is expressed in terms of a time constant and a final value:

$$\tau_x \frac{\mathrm{d}x}{\mathrm{d}t} + x = x_\infty \tag{5.19}$$

From these two forms the relationship of the final value of *x*, x_∞, and the time constant, τ_x, to the rate constants can be determined:

$$x_\infty = \frac{a_x}{a_x + b_x} \tag{5.20}$$

and

$$\tau_x = \frac{1}{a_x + b_x} \tag{5.21}$$

For Hodgkin and Huxley to completely characterize $G_{Na}$and $G_K$under voltage-clamp conditions, the variables dependent on membrane potential within the rate constants had to be determined; these dependent variables include: a_m, b_m, a_n, b_n, a_h and b_h [5]. The voltage dependence of the rate constants was recorded and fit with the following expressions:

$$a_m = \frac{-0.1(V_m-(-35))}{e^{-0.1(V_m-(-35))}-1} \tag{5.22}$$

$$b_m = 4e^{(-1/18)*(V_m—60))} \tag{5.23}$$

$$a_h = 4e^{(-0.05)*(V_m-(-60))} \tag{5.24}$$

$$b_h = \frac{1}{1+e^{-0.1*(V_m-(-30)}} \tag{5.25}$$

$$a_n = \frac{-0.01*(V_m-(-50))}{e^{-0.1(V_m-(-50)}-1} \tag{5.26}$$

$$b_n = 0.125e^{(-1/80)*(V_m—60))} \tag{5.27}$$

Here, $V_m$is expressed in mV and a_x and b_x are expressed in 1/ms. Figures 5.3-5.5 depict the experimental measurements of a_x and b_x while alteringV_m. Note that resting membrane potential lies at zero and the convention of charge across the membrane is opposite in directionality. The rise in negative membrane potential is analogous to rise in positive membrane potential in the aforementioned equations and examples [15].

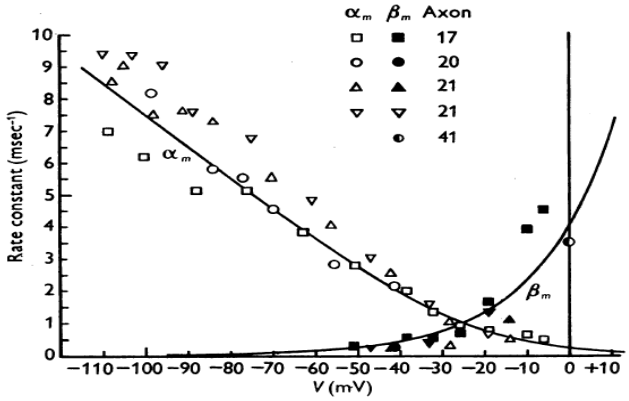

Figure 5.4. Rate constant behavior of the *m* gate at steady state voltages [15]

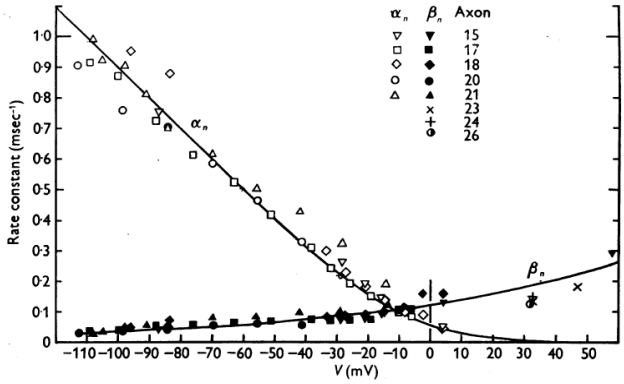

Figure 5.5. Rate constant behavior of the *n* gate at steady state voltages [15]

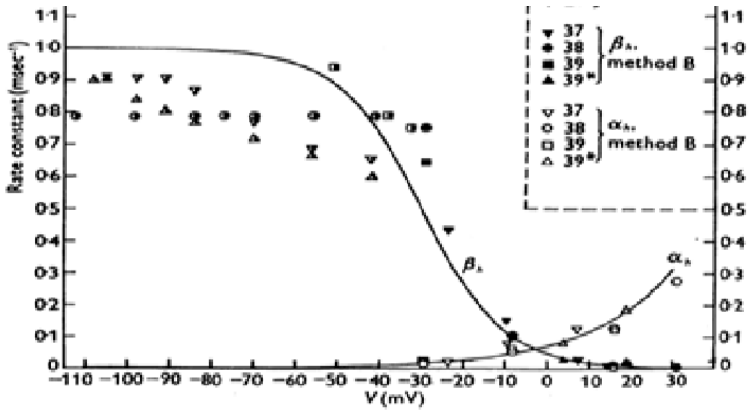

Figure 5.6. Rate constant behavior of the *h* gate at steady state voltages [15]

As steady state membrane potential rises, the rate constants a_m, a_n and $b_h$increase whileb_m, b_n and $a_h$decrease. The response of the rate equations to a linear increase in membrane potential, outlined in figures 5.4, 5.5, and 5.6, reflect the *m* and *n* gate opening and *h* gate closing.

With the response of the rate constants now known, it is possible to calculate the dependence on membrane potential of $m_{\infty,}n_{\infty}, h_{\infty,}\tau_m, \tau_n$and τ_h with the following equations:

$$m_{\infty} = \frac{a_m}{a_m+b_m} \tag{5.28}$$

$$h_{\infty} = \frac{a_h}{a_h+b_h} \tag{5.29}$$

$$n_{\infty} = \frac{a_n}{a_n+b_n} \tag{5.30}$$

$$\tau_m = \frac{1}{a_m+b_m} \tag{5.31}$$

$$\tau_h = \frac{1}{a_h + b_h} \tag{5.32}$$

$$\tau_n = \frac{1}{a_n + b_n} \tag{5.33}$$

With

$$m_\infty = \tau_m a_m \tag{5.34}$$

$$h_\infty = \tau_h a_h \tag{5.35}$$

$$n_\infty = \tau_n a_n \tag{5.36}$$

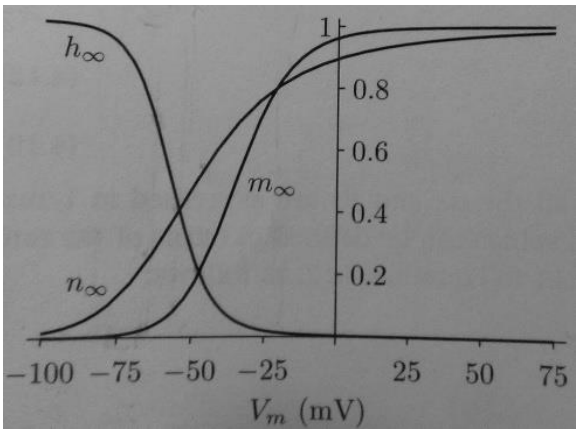

Figure 5.7 Gating parameter values at steady state [5]

Figure 5.7 depicts the gating parameter dependence on membrane potential. The values of m_∞ and n_∞ increase monotonically with membrane potential and are denoted as activation factors; conversely, h_∞ decreases monotonically with membrane potential and is denoted as an inactivation factor.

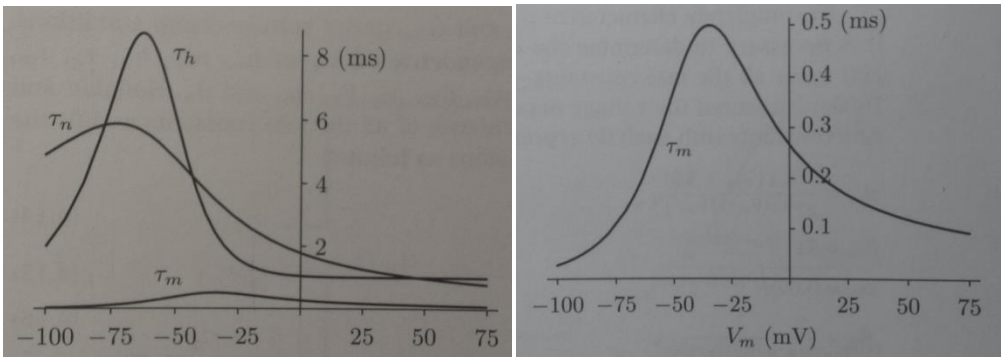

Figure 5.8. Time constant values at steady state [5]

Figure 5.8 illustrates the time constant dependence on membrane potential. Note that $\tau_m$is a factor of ten smaller than τ_h and τ_n. The magnitude of the time constant will dictate the pace at which each gate will respond; the smaller τ_m will decay quickly, indicating that the *m* gate will respond to initial depolarization more rapidly than *n* or *h*. The larger τ_h and $\tau_n$will decay more slowly, indicating a slower gating response to initial depolarization.

5.4 Synthesis of the Hodgkin-Huxley Model

5.4.1 Voltage Control

Combining equations 5.3, 5.6, 5.9, 5.16 and 5.17, Hodgkin and Huxley determined the voltage dependence of sodium and potassium conductance in a squid axon with the equations 5.34-5.37.

$$G_K(V_m, t) = \overline{G_K} n^4 \tag{5.37}$$

$$G_{Na}(V_m, t) = \overline{G_{Na}} m^3 h^1 \tag{5.38}$$

These dependences indicate that the membrane potential has two effects on the current carried by an ion:

$$I_K = \underbrace{G_K(V_m, t)}_{gating} \underbrace{(V_m - V_K)}_{driving\ force} \tag{5.39}$$

$$I_{Na} = \underbrace{G_{Na}(V_m, t)}_{gating} \underbrace{(V_m - V_{Na})}_{driving\ force} \tag{5.40}$$

The membrane potential acts as a driving force on sodium and potassium ions. Any fluctuation in membrane potential causes a response in the sodium and potassium current to the new electrochemical potential difference across the membrane, $V_m - V_{ion}$; this potential drives sodium and potassium ions across the membrane. The membrane potential also influences the passage of ions through voltage-gated ion channels by regulating gating activity. The state of the ion channels, determined by gating position, dictates the membrane conductance, $G_{ion}(V_m, t)$ and ionic current.

5.4.2 Synthesis

Substituting equations 5.13, 5.15, 5.16 into equation 5.12 compose the following expression:

$$0 = C_m \frac{dV_m}{dt} + \overline{G_K} n^4(V_m, t)(V_m - V_K) + \overline{G_{Na}} m^3(V_m, t) h(V_m, t)(V_m - V_{Na}) + G_L(V_m - V_L) \quad (5.41)$$

$$\frac{\mathrm{d}m}{\mathrm{d}t} = a_m(1 - m) - b_m m \quad (5.2)$$

$$\frac{\mathrm{d}h}{\mathrm{d}t} = a_h(1 - h) - b_h h \quad (5.5)$$

$$\frac{\mathrm{d}n}{\mathrm{d}t} = a_n(1 - n) - b_n n \quad (5.8)$$

Here, equation 5.41 is the solution of the Kirchhoff's current law at internal node of the circuit depicted in figure 5.2; the membrane current is equal to zero in order to determine change in membrane potential. A brief stimulus current is delivered to vary the initial membrane potential to any value and examine the resulting membrane potential change. The initial change in membrane potential is represented by $C_m \frac{dV_m}{dt}$, where C_m is the capacitance per cm^2 of the membrane and $\frac{dV_m}{dt}$ is the initial voltage step. Equation 5.39 along with equations 5.2, 5.5, and 5.8 represent the complete set of non linear ordinary differential equations of the Hodgkin- Huxley Model [5].

5.4.3 Results

The resulting action potential and gating parameters were determined by solving the set of nonlinear ordinary differential equations for V_m, *m, n,* and *h* is shown in Figure 5.9.

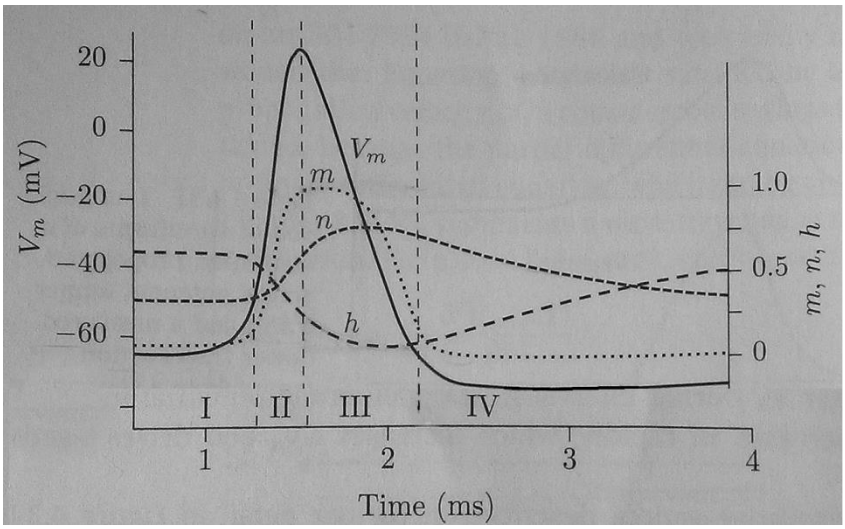

Figure 5.9 Membrane potential and gating parameter responses as determined by solving the set of nonlinear ordinary differential equations (5.2, 5.5, 5.8, 5.41) [5]

In figure 5.9 in may be observed that the membrane potential,V_m, changes dynamically. The four phases of an action potential are represented by roman numerals: interval I represents the resting phase for which V_m rests around -65mV, interval II represents the depolarization phase for which V_m rises from threshold potential (~ -55mV) to peak potential(+20 mV), interval III represents the repolarization phase for which V_m falls from peak potential down near resting potential and interval IV represents the hyperpolarization phase for which $V_m$drops below the resting potential to a minimum value of around -70mV.

The gating parameters, *m, n,* and *h* respond to the change in membrane potential over time. During the resting phase, *m, n* and *h* remain constant at their initial values until depolarization occurs. The *m* gate's (sodium activation) initial value is zero, meaning it is closed and sodium is inactivated. The *h* gate's (sodium inactivation) initial value is around .6, which is partially open but has no effect on resting potential because the *m* gate is closed. The *n* gate's (potassium activation) initial value is about 0.3, which is mostly closed, but still permits some potassium to pass into the cell.

During the depolarization phase, *m, n* and *h* begin to fluctuate in response to a sufficient stimulus which raises membrane potential above threshold potential (not depicted in figure 5.9). The *m* gate

rapidly opens, rising from 0 to 1 and allowing sodium to rush in and further depolarize the cell. The *n* and *h* gates slowly begin to react to the opening of *m*.

During the repolarization phase, *m* has reached its maximum and begins to fall; soon after *h* drops close to zero, closing the sodium inactivation gate and counteracting any further effect of *m* on the sodium channel. At roughly the same time, *n* arrives to its maximum of roughly 0.75 and fully opens the potassium activation gate; potassium begins to rush into the cell and repolarizes the membrane potential back near resting potential.

During the hyperpolarization phase, *m* reaches zero which closes the sodium channel and ceases sodium conductance. With only the potassium channel open and having an effect, V_m decreases to a minimum until *n* returns to its initial value.

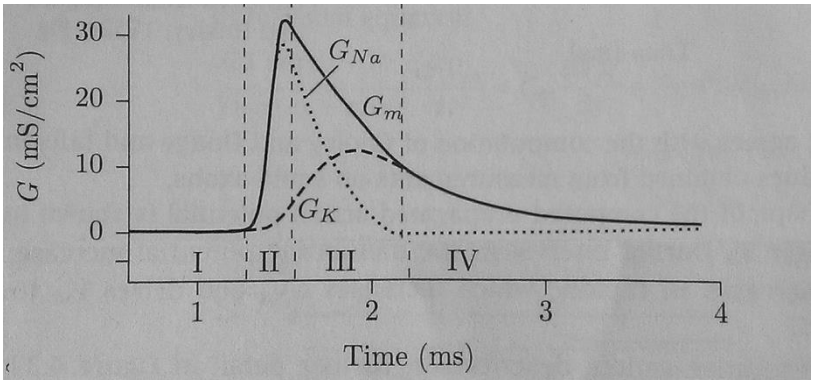

Figure 5.10. Sodium and potassium conductance response to the action potential shown in figure 5.9 [5]

Figure 5.10 illustrates the response of sodium and potassium conductance to changes in membrane potential during an action potential is illustrated. Note that sodium conductance only occurs during the depolarization and repolarization phases and potassium conductance only occurs during the repolarization and hyperpolarization phases; potassium conductance has a slight presence near the end of the depolarization phase but has a limited effect.

CHAPTER VI: *HIRUDO MEDICINALIS* AND DISSECTION PROTOCAL

To examine the dynamic behavior of electrically excitable cells, a species of the invertebrate leech was selected. The medicinal leech, or *Hirudo Medicinalis*, was readily available to record electrical signals in a reproducible manner.

6.1 The *Hirudo Medicinalis*

6.1.1 Anatomy

Leeches are a class of segmented worms with a fixed number of segments (32), know as annelids. The segments can be divided into groups based on location and function. The four most anterior segments, the 'head' region, are fused into a specialized structure including five pairs of eyes dorsally and a mouth surrounded by an anterior sucker. The seven most posterior segments, the 'tail' region, are also fused into a large caudal sucker. The 21 segments in between these two specialized structures represent the midbody section of the leech. The outer layer of skin in this section contains three layers of muscle fiber, permitting multi-directional contraction [20].

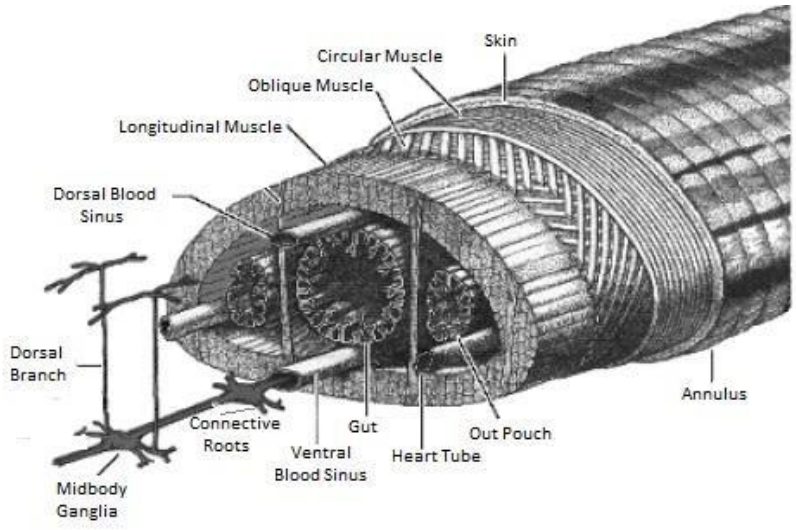

Figure 6.1. Cross section of the *Hirudo Medicinalis* [20]

6.1.2 Leech Nervous System

The nervous system reflects this segmented layout. It consists of a ventral nerve cord running down the length of the leech, associating a ganglion with each segment. The four most anterior ganglia are fused to form the anterior brain and seven most posterior are fused to form the posterior brain. Each ganglion has two paired connective roots which branch out laterally to innervate body wall musculature and anchor the ganglion. Segmented ganglia are linked to one another via an unpaired, median connective known as Farive's nerve. Each connective contains interganglionic axons and several longitudinal muscle fibers [20].

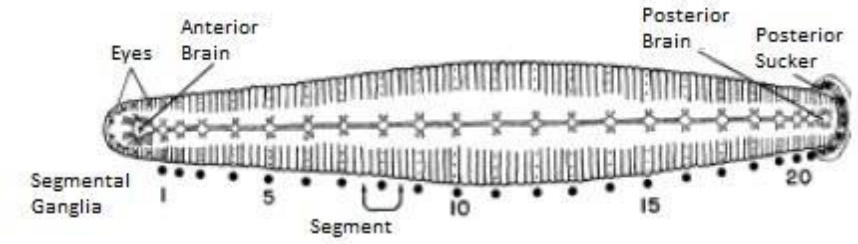

Figure 6.2. Ganglia of the *Hirudo Medicinalis* [20]

Each ganglion houses a variety of nerve cell bodies which perform a diverse set of functions. The type and function of the nerve cells within the ganglia are dependent upon the region in which the ganglia are located. The midbody region of the leech has been the most successfully mapped and categorized based nerve cell function. The major cell types which have been identified include: the Retzius cell, T cell, P cell, N cell and L cell shown in figure 6.3.

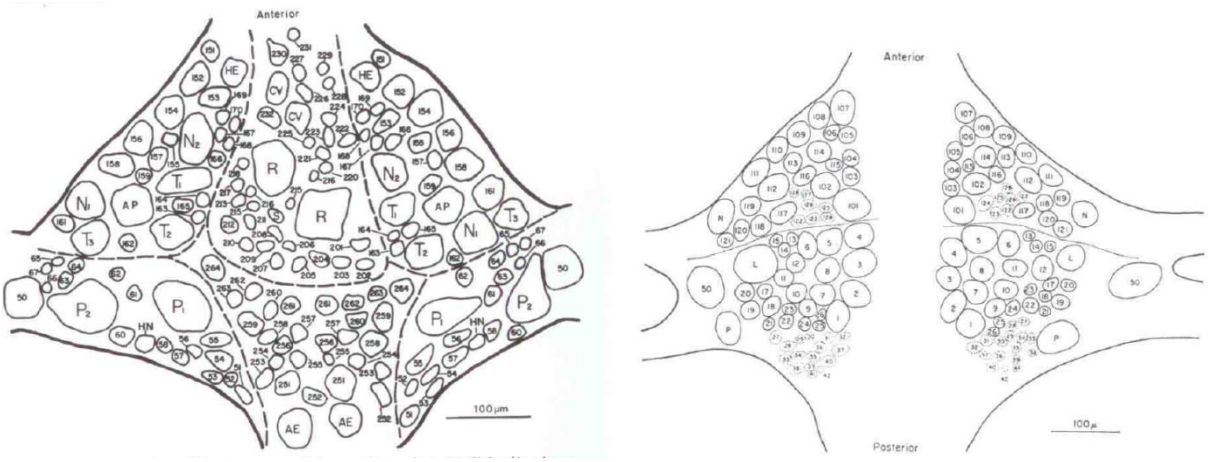

Figure 6.3. Nerve cell bodies within a midbody *Hirudo Medicinalis* ganglion [20]

The Retzius cell is a large, central cell which responds to stimulation by releasing serotonin to other nerve cells via interneurons. The rest of the identified cells are different types of mechanosensory cells, located laterally from the Retzius cell in the ganglion. The T cell is sensitive to tactile sensation, the P cell is sensitive to pressure, the N cell is sensitive to nociception and the L cell is sensitive to motor neuron propioception. As figure 6.3 depicts, the nerve cells within the ganglion are generally bilaterally symmetric with the exception of a few unpaired cells which send signals to Faivre's nerve [20].

6.1.3 Cell selection

In determining which cell type to record, the following factors were considered: experimental reproducibility, cell identification, and cell accessibility to recording equipment. The Retzius cell was the overwhelming favorite to be selected. Its size and location make it the simplest to identify and access; these qualities reduce the variability in the experimental procedure and permit more consistent results.

6.2 Ganglia Extraction Dissection Protocol

In order to record electrical signals from a Retzius cell, a midbody ganglion was extracted utilizing the dissection technique outlined in the following sections. To promote clarity, this procedure will be discussed in a step-by-step manner.

6.2.1 Equipment

The following items were used to extract a midbody ganglion from the leech in preparation for electrophysiological recordings:

10mm Micro Pins	Push Pins
Dissection Table	Refrigerator
Hirudo Medicinalis	Ringer's Solution (pH 7.4)
Large Silicon Filled Petri Dish	Small Silicon Filled Petri Dish
Leech Mobile Home	Surgical Tweezers
Light Source	Surgical Scissors
Microscope	Tongs
Paper Towels	

6.2.2 Ganglia Extraction Procedure

1. Using tongs, remove a leech from the leech mobile home onto the large silicon filled petri dish, so the leech is dorsal side up.
2. Insert one push pin through the anterior portion of the leech and into the silicon of the petri dish; make sure that pin placement is near an edge of the dish. This pin will anchor the leech to one side. Insert another push pin into the posterior portion of the leech; with this pin, spread the leech directly across the dish so its body is under light tension and insert it into the silicon. Cover the entire leech with ringer's solution.
3. With the surgical scissors carefully cut down the length of the midbody, slicing through the only dorsal layer of skin and muscle. Remove the leech blood with a paper towel. With the leech now sliced open, pin the skin on one side of the open cut into the petri dish with two or three pins. Make sure the cut is as open as possible and pins are sufficiently spaced out. Repeat for the other side of the cut. The leech should now be spread out taught over the petri dish with the push pins

placed in a rectangular fashion; the ventral nerve cord should be revealed. An example of this step is shown in figure 6.4.

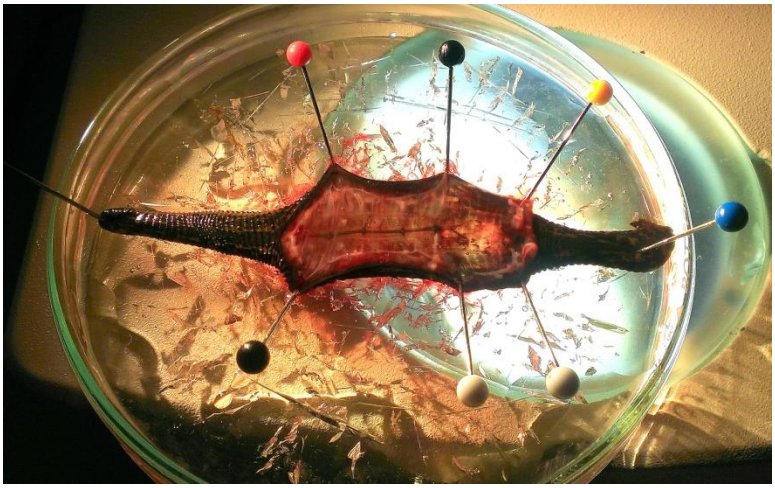

Figure 6.4. Step three of dissection protocol

4. Select an intact ganglion in the midbody which is easy to access. With the surgical tweezers and scissors, pull and cut away the surrounding dark tissue which covers the ventral nerve cord and any debris which impairs surrounding ventral cord exposure. The transparent ganglion and its extensions will start to be revealed; clear away as much of the surrounding tissue as possible without damaging the ganglion or detaching its roots.
5. Once this surrounding tissue is removed, cut the ventral nerve cord on both sides of the ganglion as far from the ganglion being extracted as possible. Cut the roots in the same manner.
6. Place the extracted ganglion into a droplet of ringer solution in the center of the small petri dish. This step limits the floating mobility of the extracted ganglion.
7. Now under the assistance of a microscope, use the surgical tweezers to orient the ganglion into the ventral aspect. Insert one micro pin though each of the ganglion's four extensions and into the silicon of the petri dish so the ganglion is spread out taught in each direction; the pins should be oriented as if each were the distal end of equilateral cross . Make sure the portion of the pins which are not in the silicon are flattened and pointed away from the ganglion, so not to interfere with recording equipment. Cover the entire ganglion with ringer's solution.

8. Place extracted ganglion in the refrigerator.

Figure 6.5. Step seven in dissection protocol

The dissection protocol is now complete; the nerve cells within the extracted leech ganglion are properly prepared for electrophysiological studies.

CHAPTER VII: ELECTROPHYSIOLOGY OVERVIEW AND EXPERIMENTAL SETUP

Electrophysiology is a branch of physiology which studies the electrical behavior of electrically excitable cells and tissues. Studies in this area utilize techniques which are capable of measuring the changes in ionic current or membrane potential during bioelectric event. The techniques associated with electrophysiology experiments may be broadly divided into the two categories of voltage clamp and current clamp type experiments.

7.1 Electrophysiology Recording Techniques

Most bioelectrical events cause independent responses in two variables: the membrane potential and transmembrane current flow. Electrophysiological studies aim to investigate excitable cell characteristics by measuring the effect or response behavior of these variables. However, membrane potential and transmembrane current flow often change at the same time and this dynamic adds complexity to these studies by reducing the ability to observe isolated bioelectric effects. The voltage and current clamp techniques resolve this issue by holding one of these variables constant.

7.1.1 Current Clamp

The current clamp technique controls or 'clamps' the membrane current to a predetermined value to monitor and induce changes in membrane potential. The desired current is sourced or sunk as a function of time through a micropipette in accordance with the study parameters. The membrane is either depolarized or hyperpolarized to a particular magnitude as current is sourced or sunk [4, 21]. The circuit suitable to perform current clamp measurements is shown in figure 7.1.

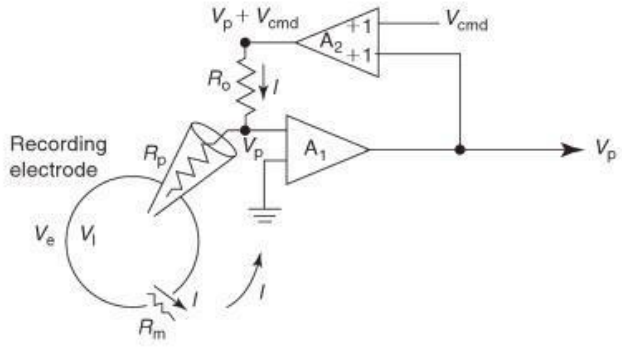

Figure 7.1 Current clamp circuit diagram [21]

7.1.2 Voltage Clamp

The voltage clamp technique controls or 'clamps' the membrane voltage to a predetermined value to observe and induce changes in membrane current. The ability to clamp an axon or cell at a particular voltage is dependent upon the electronic feedback system consisting of two intracellular electrodes, an amplifier and a current monitor. One electrode is used to measure the membrane potential and the other to inject current. The feedback amplifier measures the difference between the membrane potential and a reference potential. The amplifier sources current proportional to this difference back into the axon or cell through an intracellar electrode. The value of return current can be monitored to observe current behavior in response to the membrane voltage. This setup ensures any change in membrane potential will be neutralized by an opposing change in membrane current [4, 21]. A typical voltage clamp circuit is depicted in figure 7.2.

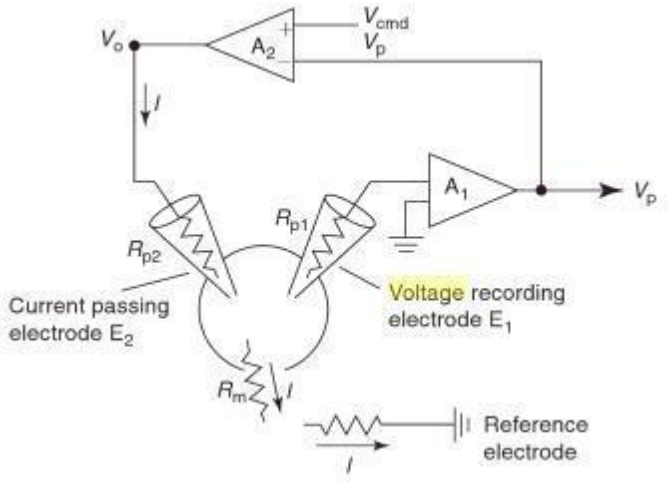

Figure 7.2. Voltage clamp circuit diagram [21]

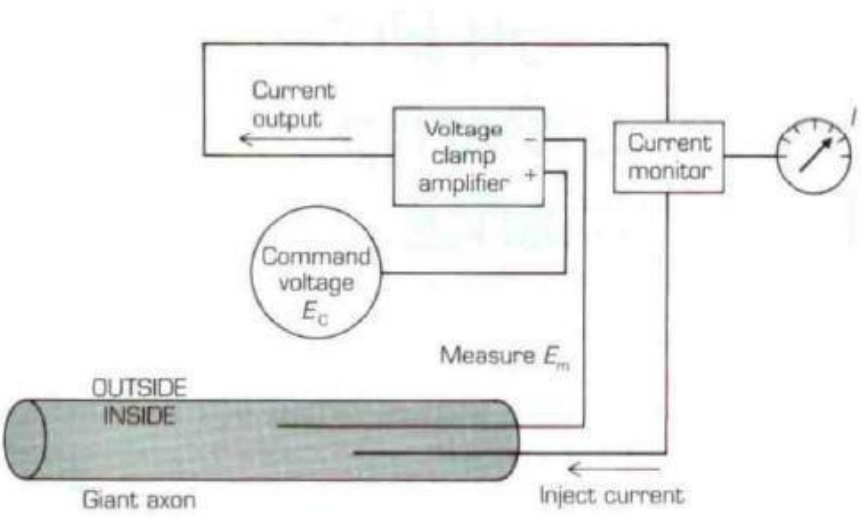

Figure 7.3 Voltage clamp conceptual representation [4]

7.2 Experimental Procedure

This electrophysiological study was designed to investigate membrane potential activity during an action potential in the Retzius cell of the *Hirudo Medicinalis*. In order to observe this phenomenon, a sufficient stimulus pulse was injected to excite the Retzius cell's membrane potential past threshold to recruit an action potential. For this reason, the current clamp technique was chosen. The current clamp

configuration can deliver a stimulus pulse into the membrane by holding membrane current to a particular amplitude for a designated amount of time. The difference in resting membrane current and the holding current is the amplitude of the pulse, the duration for which the membrane current is held is the pulse width.

7.2.1 Equipment

The following equipment was used to perform this electrophysiological study in the leech, *Hirudo Medicinalis*.

3M Potassium Chloride solution

Axoclamp 900A amplifier

Axoclamp 900A software

Clampex 10.2 software

Clampfit 10.2 software

Computer

Dark field microscope

Digidata 1440a DAQ unit

Extracted leech ganglia

Faraday cage

Headstage

Lighting

Mircofill

Micropipettes

Micropipette puller

Oscilloscope

Recording electrode

Ringer's solution

Silver silver-chloridized wire

Small petri dish

Syringe

7.2.2 Equipment Setup

To simplify the explanation of this electrophysiological equipment setup, we will treat the extracted ganglion simply as a recording site. The recording of electrical signals occurs at the recording site, under a dark field microscope and within a Faraday Cage. A recording electrode is placed in the recording site with the adjustable headstage. A reference electrode is placed in by hand. The recording and reference electrodes are configured as a current clamp on the Axoclamp 900A amplifier. The amplifier increases the signal's amplitude, which is then read by an oscilloscope, the computer and the Digidata 1440a DAC unit; the computer also reads the Digidata 1440a DAC unit's output. The information the computer receives from the amplifier and Digidata 1440a DAC unit can now be read, and analyzed by computer software. The Axoclamp software is used to calibrate all equipment and monitor electrode impedance. The Clampex and Clampfit software is used to observe and record membrane potential, inject current pulses and analyze the results. The equipment setup is shown in figure 7.4.

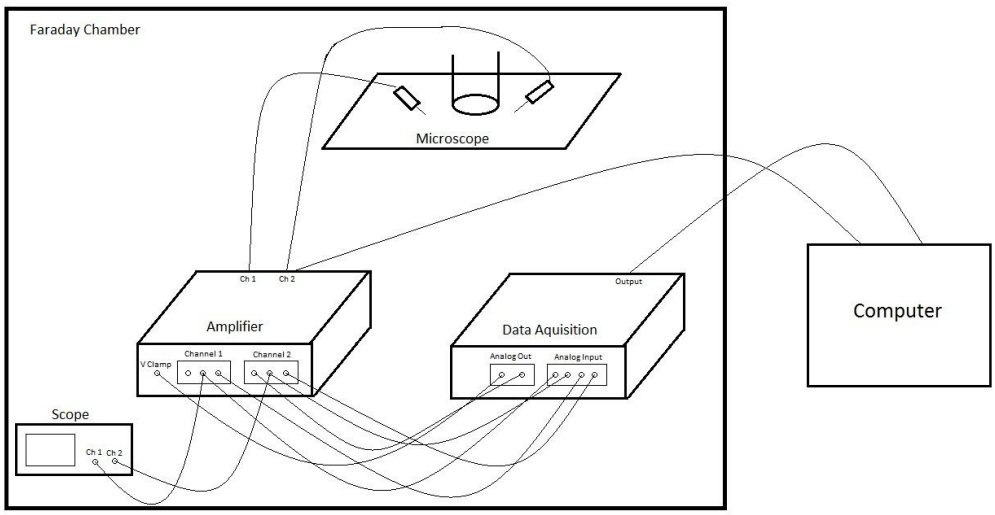

Figure 7.4 Conceptual equipment setup

7.2.3 Calibration

The electrical signals we intend to record occur in a small cell at very small amplitudes (mV and nA). A suitable electrode must penetrate the cell membrane without causing any appreciable damage and

remain sensitive enough to detect small signals. These issues were resolved by the use of glass capillary microelectrodes or micropipettes and a Faraday cage. Micropipettes are hollow glass cylinders which are heated and pulled to form a sharp tip. A chloridized silver wire is place in a micropipette that is filled with 3M potassium chloride solution. A paired, standard reference electrode is placed in the same ringer's solution bath as the micropipette to complete the circuit. The recording electrodes will pick up unwanted noise if not placed in a Faraday cage. Noise is generated by the computer, lighting and electrical outlets, and results in poor recordings. A Faraday cage reduces the amount of unwanted electrical noise which enter the recording site [21].

7.2.4 Procedure Micropipette Preparation

1. Ensure the Axoclamp amplifer is turned off before handling electrodes.
2. Pull two or more micropipettes with the micropipette puller.
3. Place a silver silver-chloride wire in the electrode headstage.
4. Attach the microfill onto a syringe filled with 3M KCL solution. Insert the mircofill into the hollow end of the micropipette to maximum depth and fill.
5. Slide the filled micropipette over the silver silver- chloride wire and attach it to the headstage.
6. Place a petri dish filled with ringer's solution near the headstage. Using the headstage adjustments, carefully insert the tip of the micropipette into the ringer's solution. Carefully place the reference electrode in the ringer's bath to complete the circuit.

7.2.5 Equipment Calibration

1. Turn on the computer, Digidata 1440a Data Aquisition unit, Axoclamp 900A amplifier and oscilloscope. Once the computer is running, open the Axoclamp 900A software.
2. From the Axoclamp Commader Software Interface (figure 7.5), select the IC and I-Clamp 1 tab for the first headstage.

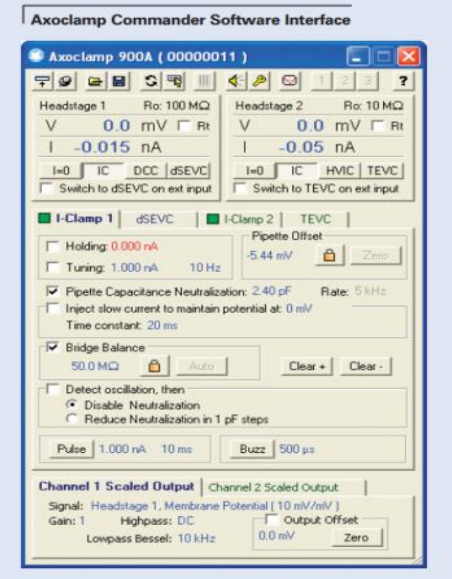

Figure 7.5. Axoclamp Commader Software Interface

3. Check the pipette resistance by checking the Rt box next to the displayed voltage. If the resistance is not between 20MΩ and 80MΩ it is not suitable for this application. Repeat the micropipette preparation procedure until the resistance of a micropipette is within this range.
4. Turn off Bridge Balance and Pipette Capacitance Neutralization by unchecking their respective boxes.
5. Zero the Pipette Offset voltage. This step positions the potential at zero.
6. Turn the test stimulus pulse train on the oscilloscope. Adjust trigger level, time base and volts/div as needed until a single pulse train is displayed.
7. Turn on the Pipette Capacitance Neutralization on the Axoclamp interface. Adjust the capacitance level until the rising edge of the pulse has a slight overshoot and is perpendicular to the time axis. This step removes stray capacitance which can negatively impact the bandwidth of the recording.
8. Readjust the oscilloscope's time base so there are multiple pulses displayed.
9. Turn on the Bridge Balance in the Axoclamp interface. Manually adjust the resistance until the pulse train waveforms display a flat base line with the offset voltage. This bridge balancing technique calibrates out the micropipette resistance (R_P). When current is passed

through a micropipette, a voltage drop across its resistance is produced ($I R_p$). To remove this voltage drop, it is subtracted from the total voltage (V_P) which isolates the membrane potential (V_m). This concept is shown in figure 7.6.

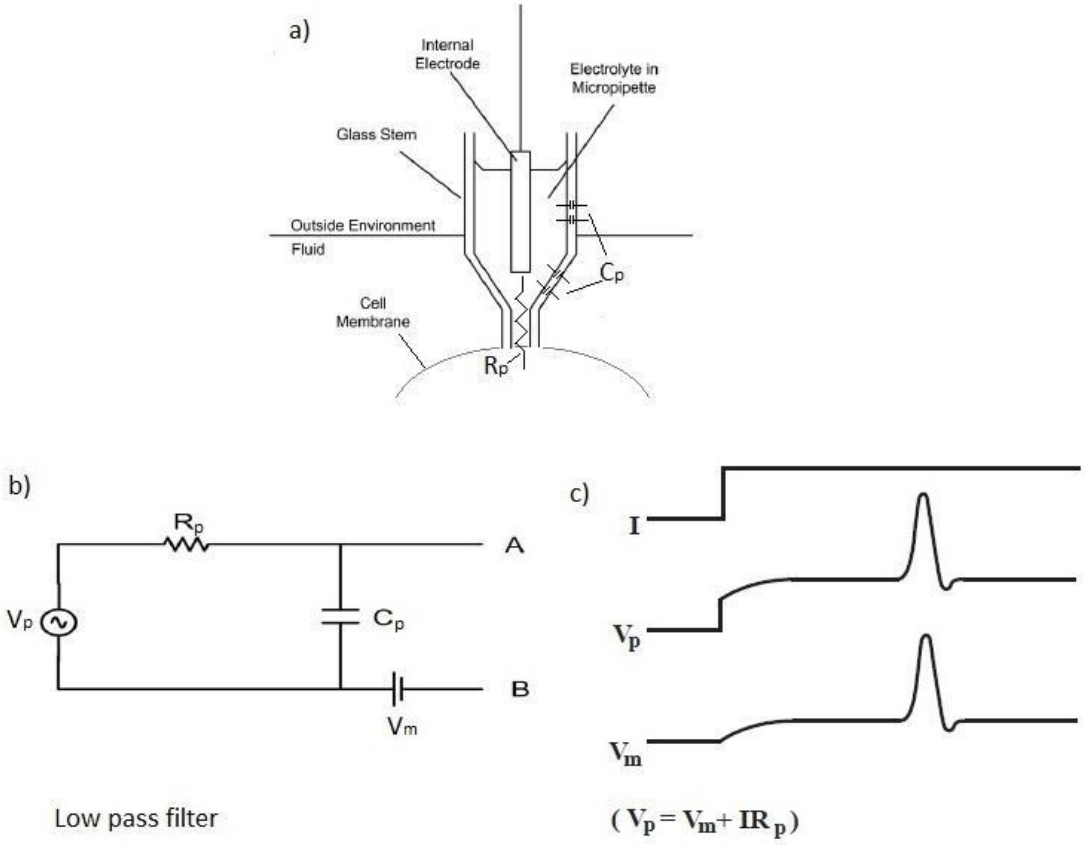

Figure 7.6. Bridge balance [21]

10. Turn off the test pulse train on the oscilloscope.

Calibration of electrodes is essential in recording electrophysiological signals. It removes the effect of electrode offset potentials, pipette capacitance and pipette series resistance. The pipette capacitance and series resistance create a low pass filter as shown above in figure 7.6. Calibrating out pipette capacitance creates an open circuit, removing the filtering effect and allowing use of a wider range of frequencies.

7.2.6 Procedure –Implementation

With the dissection and calibration protocol complete, the electrophysiological investigation of membrane potential activity during an action potential in the Retzius cell can commence.

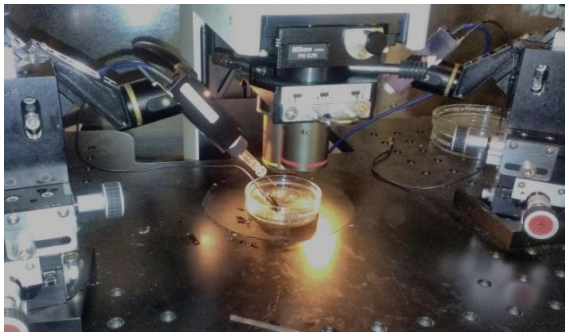

Figure 7.7. Electrophysiological recording

1. Turn off the Axoclamp amplifier.
2. Place the small petri dish with the pinned down extracted ganglion under the dark field microscope. Make sure the headstage arm which secures the micropipette is retracted enough to avoid contact during placement.
3. Under 40x magnification bring the ganglion into focus. Inspect the ganglion to ensure it has no appreciable damage or abnormalities. Repeat the dissection protocol if damage or abnormalities are found. Check the orientation of the micro pins. Make sure they are properly flattened and pointing outward, away from the center of the ganglion. Readjust the micro pins if they are not properly orientated.
4. Place the ganglion in the center of view. Orient the ganglion as shown in figure 7.8.

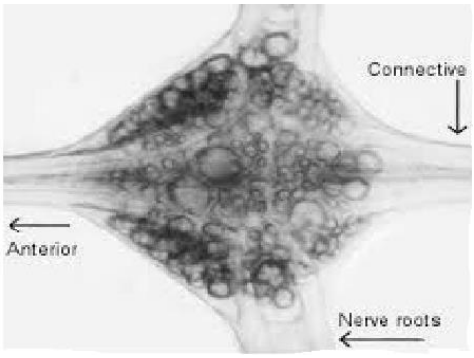

Figure 7.8. Leech ganglion under 100x magnification

5. Adjust lighting and focus so the nerve cell bodies within the ganglion are as sharp as possible. Retract the 4x eye.
6. Use the adjustable headstage to bring the tip of the micropipette into the ringer's solution of the petri dish between the headstage and ganglion. Insert the reference electrode into the bath, orientated so it does not interfere with ganglion or micropipette.
7. Turn on the Axoclamp amplifier and check the electrode impedance on the Axoclamp interface. Ensure electrode impedance is between 20MΩ and 80MΩ; if it is not, it is likely broken and unsuitable for use. Repeat micropipette preparation and calibration protocol for the replacement micropipette.
8. Engage the 4x eye. Using the fine adjustments of the headstage, bring the tip of the micropipette into view. The tip of the of the micropipette is just under the surface of the ringer's solution; to account for difference in focal length, adjustments in focus must be made to observe the micropipette when it first comes into view.
9. Continue to use the fine adjustments until the micropipette is directly over the center of the ganglion. Lower it down to where it almost touches the ganglion. Make adjustments in focus in accordance to these changes.
10. Retract the 4x eye and engage the 10x.
11. Identify the Retizius cell using the ganglion map and figure 7.9. Note that this map is not necessarily oriented as the ganglion.

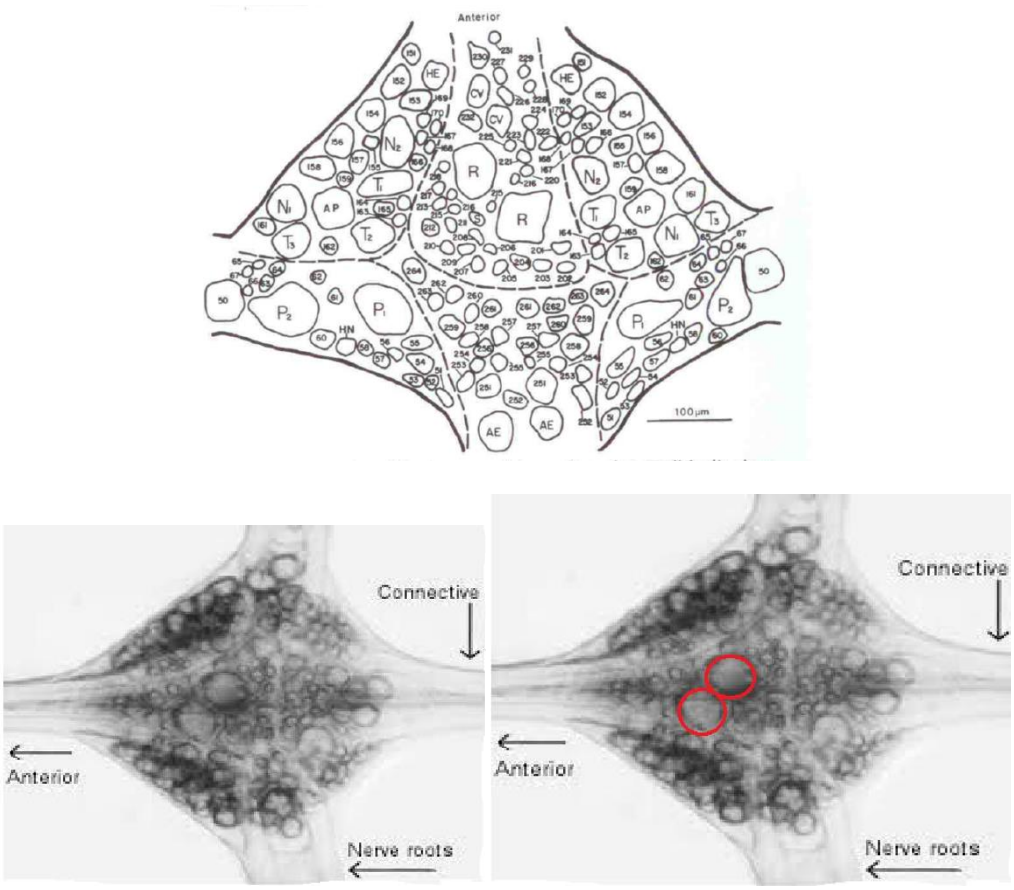

Figure 7.9. Identifying the Retzius cell in the leech ganglion

12. Using the fine adjustments, move the micropipette to the side of the chosen Retzius cell which is closest to the headstage. Show below in figure 6.15a:

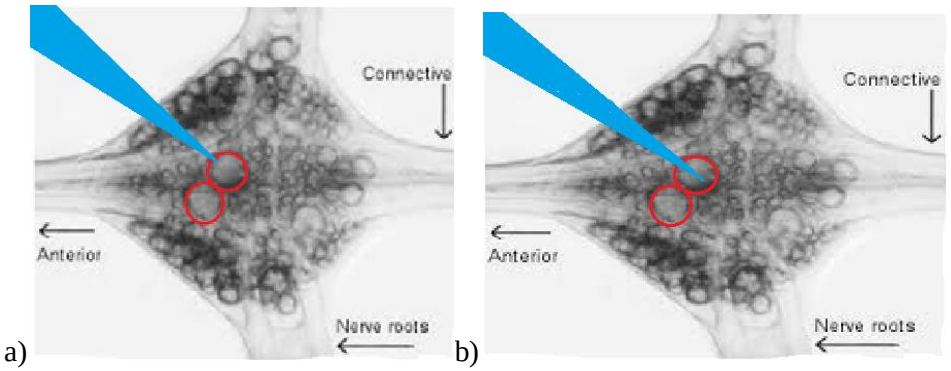

Figure 7.10. Micropipette insertion into Retzius cell

13. Puncture the Retzius cell with the micropipette using the fine adjustments of the head stage as shown in the figure above in 7.10a. and b

14. If the micropipette has entered the cell, a drop in membrane potential to the Retzuis cell's resting potential will be observed on the oscilloscope. This should be on the order of -30 to -40mV. Spontaneous depolarizations may occur without stimulation.
15. Using the Clampex software, stimulate the Retzius cell with incremental increases in pulse amplitude to recruit an action potential. Once a minimum elicitation stimulus pulse is discovered, begin recording. Repeat as necessary.

CHAPTER VIII: EXPERIMENTAL RECORDINGS OF THE RETZIUS CELL

The following information was gathered in a series of electrophysiological recordings of the Retzius cell of the *Hirudo Medicinalis* in three separate specimens. Each Retzius cell was stimulated at 700 *p*A for 50 milliseconds.

8.1 Results

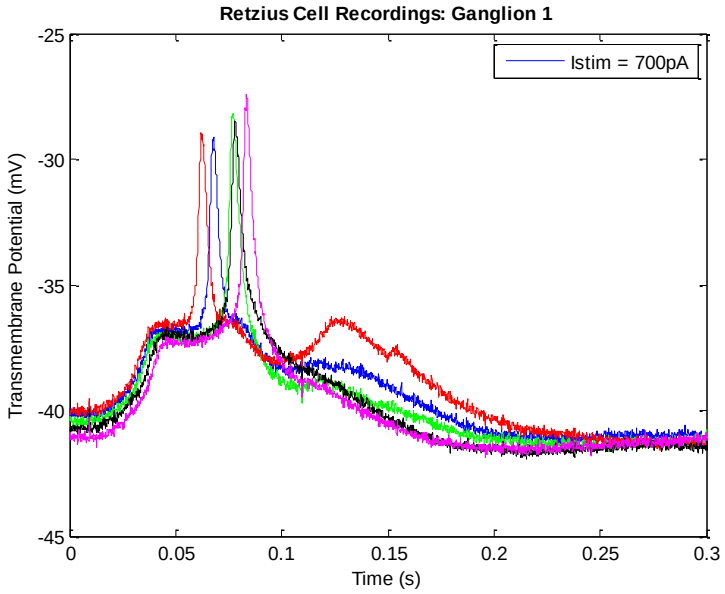

Figure 8.1. Retzius cell recordings in leech ganglion 1

TABLE 8.1

WAVEFORM CHARACTERISTICS OF THE RETZIUS CELL RECORDINGS DISPLAYED IN FIGURE 8.1

Ganglion 1					
Rz Cell Recording	1	2	3	4	5
Peak Potential (mV)	-29.11	-28.16	-28.96	-28.50	-27.43
Resting Potential (mV)	-39.88	-40.37	-40.01	-40.61	-41.02
Threshold Potential (mV)	-37.80	-37.05	-36.55	-36.85	-37.05
Peak Duration (s)	0.018	0.015	0.013	0.015	0.017

Figure 8.1 depicts five Retzius cell recordings from leech ganglia one, following a stimulation pulse with 700pA amplitude and 50ms duration. Table 8.1 describes the important waveform characteristics of each recording.

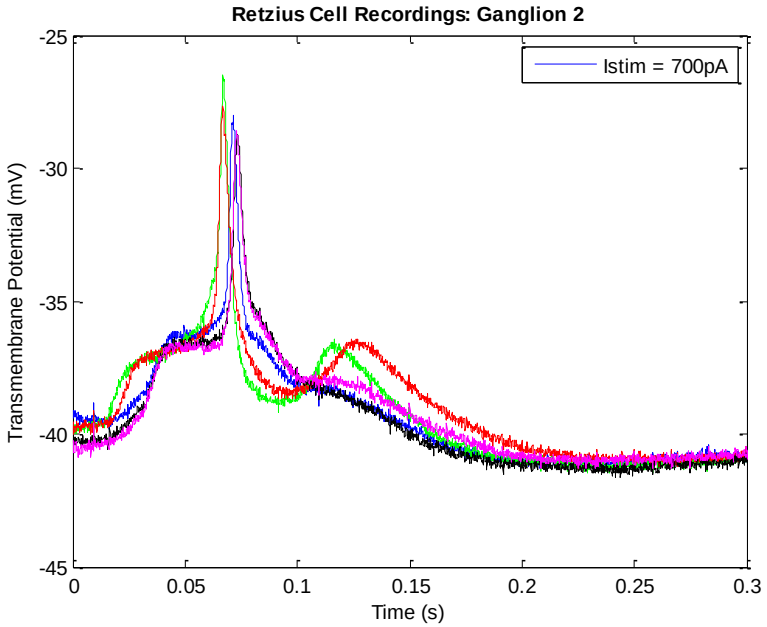

Figure 8.2. Retzius cell recordings in leech ganglion 2

TABLE 8.2

WAVEFORM CHARACTERISTICS OF THE RETZIUS CELL RECORDINGS DISPLAYED IN FIGURE 8.2

Ganglion 2					
Rz Cell Recording	1	2	3	4	5
Peak Potential (mV)	-28.01	-26.51	-27.67	-28.71	-28.59
Resting Potential (mV)	-39.42	-39.88	-39.55	-40.31	-40.25
Threshold Potential (mV)	-36.25	-36.75	-36.75	-36.5	-36.75
Peak Duration (s)	0.02	0.019	0.0175	0.0135	0.021

Figure 8.2 depicts five Retzius cell recordings from leech ganglia two, following a stimulation pulse with 700pA amplitude and 50ms duration. Table 8.2 describes the important waveform characteristics of each recording.

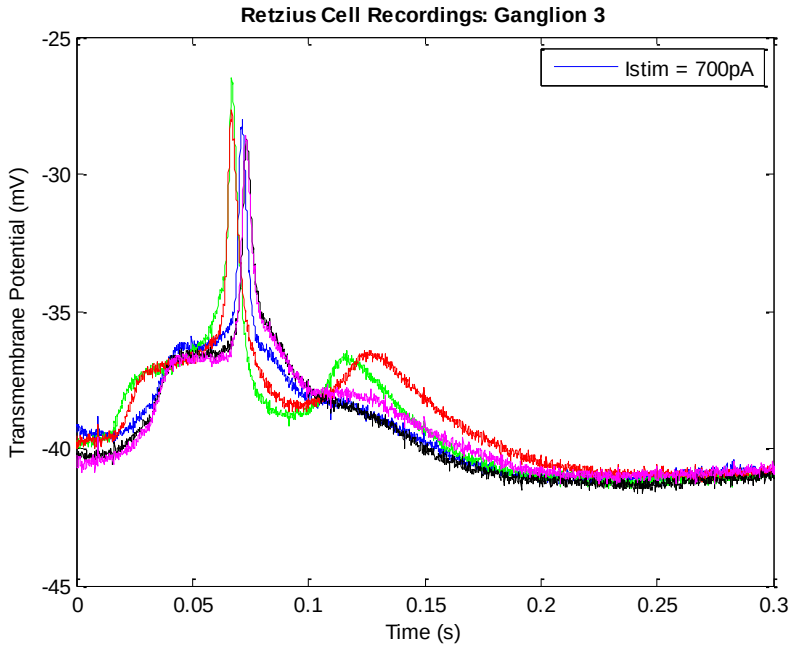

Figure 8.3. Retzius cell recordings in leech ganglion 3

TABLE 8.3

WAVEFORM CHARACTERISTICS OF THE RETZIUS CELL RECORDINGS DISPLAYED IN FIGURE 8.3

Ganglion 3					
Rz Cell Recording	1	2	3	4	5
Peak Potential (mV)	-28.01	-26.51	-27.67	-28.71	-28.59
Resting Potential (mV)	-39.42	-39.88	-39.55	-40.31	-40.25
Threshold Potential (mV)	-36.45	-37.05	-36.75	-36.55	-36.70
Peak Duration (s)	0.024	0.025	0.023	0.022	0.024

Figure 8.3 depicts five Retzius cell recordings from leech ganglia two, following a stimulation pulse with 700pA amplitude and 50ms duration. Table 8.3 describes the important waveform characteristics of each recording. An enhanced view a waveform peak is displayed in figure 8.4.

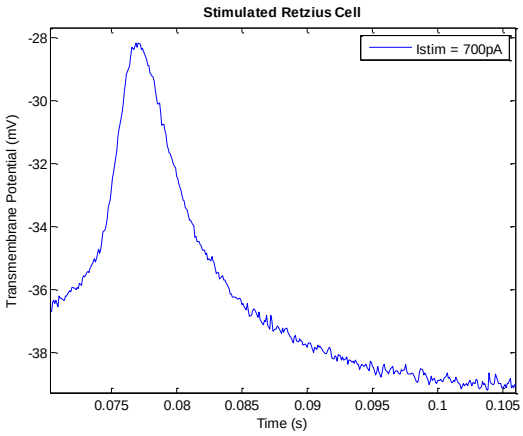

Figure 8.4 Enhanced individual Retzius cell recording 4 in leech ganglion 3

TABLE 8.4

AVERAGE VALUES OF RETZIUS CELL RECORDINGS IN LEECH GANGLIA 1-3

Rz Cell Mean Values	
Peak Potential (mV)	-28.072
Resting Potential (mV)	-40.047
Threshold Potential (mV)	-36.787
Peak Duration (s)	0.0191

Table 8.4 describes the average peak potential, resting potential, threshold potential and peak duration values for the recorded Retzius cell waveforms displayed in figure 8.1-8.3. These values will be used to accurately simulate a Retzius cell action potential.

CHAPTER IX: IMPLEMENTATION OF THE HODGKIN-HUXLEY MODEL IN *MATLAB*

9.1 Setup

The information obtained from the Hodgkin-Huxley Model permits the following simulation of transmembrane potential in an electrically small nerve cell when excited with a current pulse. The following conceptual representation of the electrophysiological setup and Hodgkin-Huxley model equivalent circuit were utilized in simulating a current clamped electrically small cell:

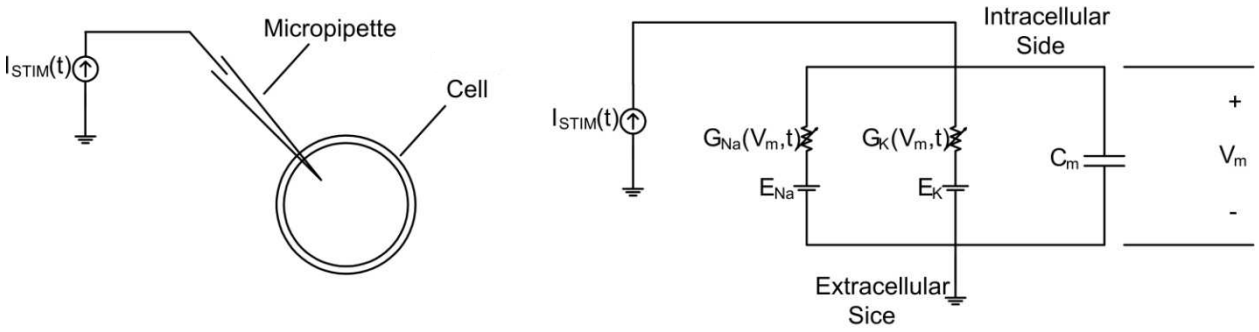

Figure 9.1. Conceptual representation of the electrophsysiological setup with an idealized cicuit, derived from the Hodgkin-Huxley Model

An idealized cicuit is derived from the Hodgkin-Huxley Model. The leak channels and their assosiated effects on V_m, *m, n,* and *h* are assumed to be negligible. Also represented is the conceptual setup. A current clamp micropipette is inserted into an electrically small cell allowing the stimulus current waveform, $I_{STIM}(t)$, to be passed into the cell. Simulating an electrically small cell justifies the use of the lumped parameter Hodgkin-Huxley membrane model shown above.

9.1.1 System of Nonlinear Ordinary Differential Equations

The following nonlinear ordinary differential equations represent the behavior of the *m, n,* and *h* gates:

$$\frac{\mathrm{d}m}{\mathrm{d}t} = a_m(1-m) - b_m m \tag{5.2}$$

$$\frac{\mathrm{d}h}{\mathrm{d}t} = a_h(1-h) - b_h h \tag{5.5}$$

$$\frac{\mathrm{d}n}{\mathrm{d}t} = a_n(1-n) - b_n n \tag{5.8}$$

These three equations are functions of membrane potential V_m. A fourth differential equation features the membrane potential as a differential variable and fully describes the nonlinear system.

The fourth equation is equivalent to a statement of Kirchoff's Current Law at the intracellular node of figure 9.1, shown below:

$$0 = C_m \frac{dV_m}{dt} + \overline{G_K} n^4(V_m, t)(V_m - V_K) + \overline{G_{Na}} m^3(V_m, t) h(V_m, t)(V_m - V_{Na}) - I_{STIM}(t) \tag{9.1}$$

Where $I_{STIM}(t)$ is a stimulus current pulse. Rearrangement of equation 9.1 will permit implementation in a nonlinear ordinary differential equations solver.

$$\frac{dV_m}{dt} = \frac{\overline{G_K} n^4}{C_m}(V_K - V_m) + \frac{\overline{G_{Na}} m^3 h}{C_m}(V_{Na} - V_m) - \frac{I_{STIM}(t)}{C_m} \tag{9.2}$$

Equations 5.6, 5.7, 5. 8 and 9.2 define a nonlinear system of ordinary differential equations that may be solved by a numerical solver.

9.1.2 Initial Conditions

The first step in solving this system of equations is defining the initial conditions. The behavior of this system specifies that each set of initial conditions will generate a unique solution. The initial conditions are the values of $V_m(t), m(t), h(t)$ and $n(t)$ at $t = 0$s. The value of $V_m(0)$ is assumed to be equal to the resting potential, Vr, and can be easily calculated using the Goldmann equation (equation 3.4).

The initial values of the gating variables are not so intuitively trivial. However, if we assume the membrane has been at rest for significantly long period of time, the gates of the voltage gated sodium and potassium channels should return to their original orientation, resulting in $x_\infty = x(0)$. We can now specify the initial conditions for the gating variables as:

$$m_\infty = m(0) = \frac{a_m(V_r)}{a_{m(V_r)} + b_m(V_r)} \tag{9.3}$$

$$h_\infty = h(0) = \frac{a_h(V_r)}{a_h(V_r) + b_{h(V_r)}} \tag{9.4}$$

$$n_\infty = n(0) = \frac{a_n(V_r)}{a_{n(V_r)} + b_{n(V_r)}} \tag{9.5}$$

The value of resting potential, V_r, is calculated in the same manner and implemented in the expressions of equations 9.3 to 9.5

9.1.3 MATLAB

MATLAB, or matrix laboratory, is a numerical computing environment and programming language developed by MathWorks. As its name suggests, *MATLAB* allows extensive matrix and algorithmic manipulation, including the implementation of ordinary differential equation solvers. *MATLAB* offers a variety of solvers which are designed to suit the stiffness and accuracy required by different types of problems; solver selection is extremely important for producing proper results.

9.1.4 MATLAB Ordinary Differential Equation Solvers

Selection of an ordinary differential solver is dependent on the stiffness and desired accuracy of the differential equation. Stiffness occurs when some components of the solution decay much more rapidly than others, requiring an extremely small step size in order to maintain numerical stability. In the context of circuit problems, stiffness can be attributed to the diverse order of magnitudes the time constants associated to the network. To account for stiffness, solver algorithm must take small step sizes.

Incremention levels of the solver step intervals constrain the accuracy of the solution generated. Often the higher the order of incremention, the more accurate the solution.

The ODE solvers *MATLAB* can be categorized based on their applicability to stiff and nonstiff as shown in tables 9.1 and 9.2.

TABLE 9.1.

MATLAB NONSTIFF SOLVERS

Solver	Order of Accuracy	Method	Applicability
ode45	Medium	Runge-Kutta	Nonstiff Differential Equations
ode23	Low	Runge-Kutta	Nonstiff Differential Equations
ode113	Low to High	Adams	Nonstiff Differential Equations

TABLE 9.2.

MATLAB STIFF SOLVERS

ode115s	**Low to Medium**	**NDFs (BDFs)**	**Stiff Differential Equations and Differential Algebraic Equations**
ode23s	Low	Rosenbrock	Stiff Differential Equations
ode23t	Medium	Trapezoidal Rule	Moderately Stiff Differential Equations and Differential Algebraic Equations
ode23tb	Low	Trapezoidal Rule-BDF2	Stiff Differential Equations

After consideration of the differential equations which will be implemented and solved, the ode45solver type was selected. The Hodgkin-Huxley model is a lumped parameter equivalent circuit

model, involving voltage or current clamp applications. Solutions of this type of system of differential equations do not typically contain unstable numerical regions, permitting the use of nonstiff solvers. Ode45 was selected for its versatility and applicability in certain Hodgkin-Huxley active membrane type problems.

9.2 Program Structure

Setting up the simulation program requires the following tasks to be achieved in a *MATLAB. m* file:

1. Establish circuit parameters in figure 9.1 (membrane capacitance, maximum conductances, etc) based on cell surface area.
2. Establish a vector of time points.
3. Determine initial conditions.
4. Call the ODE solver, ode45.
5. Display solver solutions of V_m, m, n and h as functions of time t.

9.2.1 Functions

The following functions must be implemented with the simulation program to return a solution:

1. The *odefunction* which defines the system of differential equations to be solved by the ode45 solver routine.
2. Computation of Vr by the Goldmann Equation.
3. Computation of $V_m(t), m(t), h(t)$ and $n(t)$ at $t = 0$s.
4. Computation of a_x and b_x.
5. Characterization of the stimulus pulse .

9.2.2 The ODE Function

The *odefun* function implements the system of nonlinear differential and returns a solution.

9.2.3 The Resting Potential Function

The *V_r* function calculates the initial value of $V_m(t)$ utilizing the Goldmann equation.

9.2.4 Initial Values of The Gating Variables

The functions *m_bound*, *h_bound* and *n_bound* compute the final value of each gating variable utilizing the membrane potential and equation 5.18.

9.2.5 Gating Variable Rate Constants

The functions *alpha_m, beta_m,alpha_h, beta_h, alpha_n,*and *beta_n* compute the gating variable rate constants from the membrane potential using equations 5.20-5.25.

9.2.6 Current

The *current* function describes the stimulus current waveform, $I_{STIM}(t)$.

$$I_{STIM}(t) = I_A \; 0 \leq t \leq 100\mu \quad \text{or} \quad t > 100\mu s \qquad \text{Eq. 9.6}$$

9.2.7 The Main Program

The main programs organizes all circuit and cell simulation parameters, initializes the time vector, computes and assigns the initial conditions to the initial conditions vector, calls the ode45 solver routine and formats the simulations results.

9.3 Results

Implementation of this program results in the waveforms depicted in figure 9.2 and 9.3.

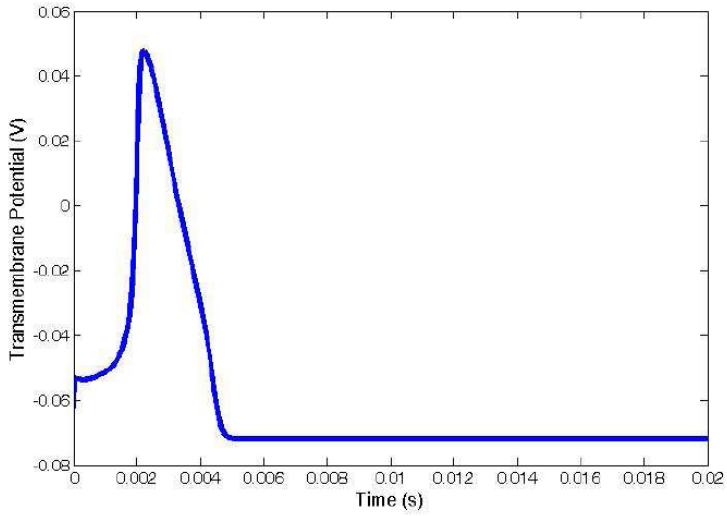

Figure 9.2. *MATLAB* simulation of an action potential waveform utilizing the Hodgkin-Huxley Model

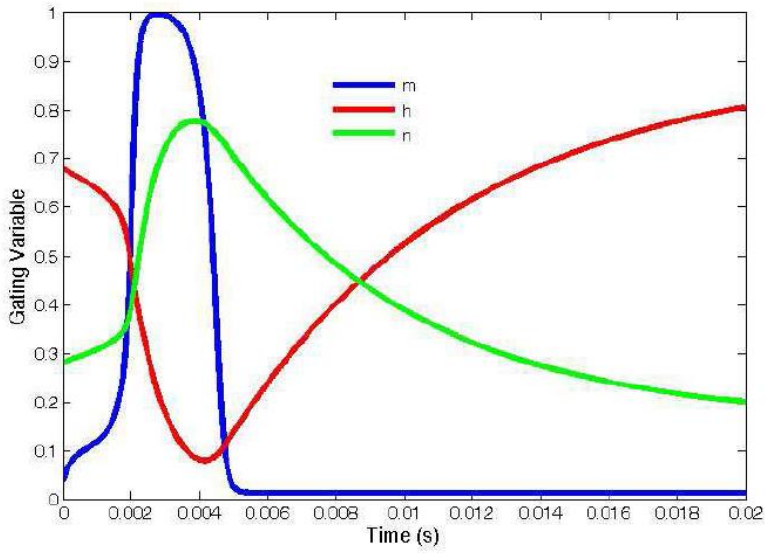

Figure 9.3. *MATLAB* simulation of an *m*, *h*, and *n* during an action potential waveform utilizing the Hodgkin-Huxley Model

Here, the behavior of the membrane potential and the gating variables over time is depicted; comparison of these plots to the results of the Hodgkin Huxley Model depicted figure 5.9 confirms the accuracy of this simulation. The scripts involved in this simulation are included in this document in Appendix A.

CHAPTER X: SIMULATING THE RETZIUS CELL

MATLAB simulation of the Retzius cell's action potential was developed based on the information gathered during the electrophysiological recordings shown in chapter 8. This simulation is based on the implementation of the Hodgkin-Huxley Model in *MATLAB* as depicted in chapter 9 and adjusted to suit Retzius cell characteristics. The following chapter will demonstrate how to modify the Hodgkin-Huxley model to simulate a desired nerve impulse. A simulation of the *Hirudo Medicinalis's* Retzius cell will be discussed in detail and compared with a simulation of the dissimilar P cell, also of the *Hirudo Medicinalis*. Simulations will be modeled after the Retzius cell's action potential waveforms found in Figure 10.1, and the P cell's action potential waveform illustrated in 10.2.

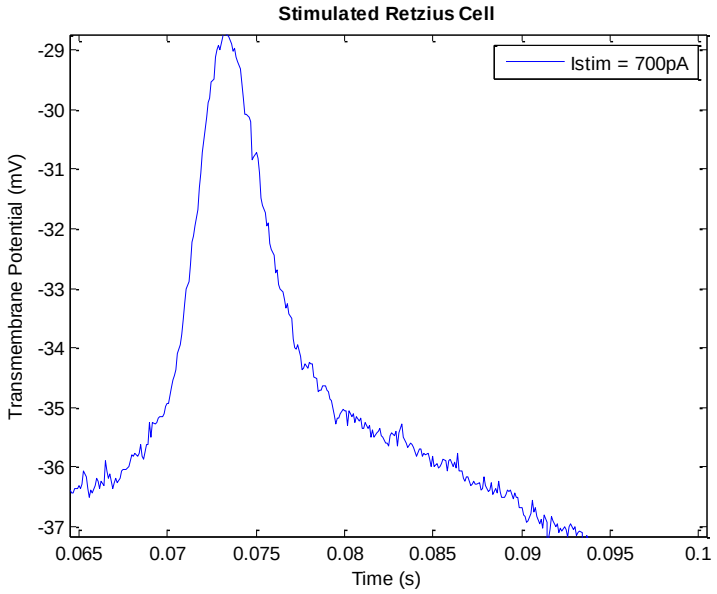

Figure 10.1. The Retzius cell action potential which will guide simulation parameters

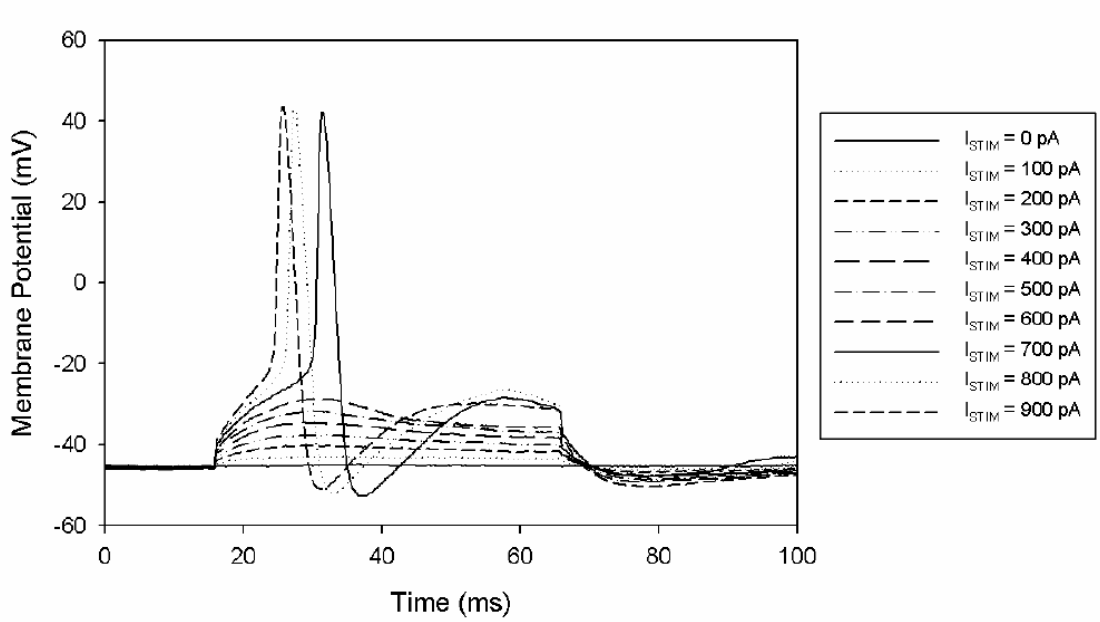

Figure 10.2. The P cell action potential will guide simulation parameters

These waveforms are quite different and will demonstrate the flexibility of this method. The *MATLAB* simulation of the Hodgkin Huxley model will be modified in three sections:

1. Initial conditions adjustment
2. Steady state analysis
3. Transient analysis

The scripts associated with these changes will be included in each section.

10.1 Initial Conditions Adjustments

Simulation initial conditions must be altered from the giant squid axon to suit the properties of the Retzius cell and P cell. This is essential to the relevance and accuracy of the resulting simulation.

10.1.1 Resting potential

Resting potential will be calculated according to the cellular parameters which are known. For example, the squid giant axon's intracellular and extracellular potassium and sodium concentrations are known, allowing the following function *V_r* to be utilized.

The function, *V_r*, calculates the values of resting membrane potential, sodium Nernst potential and potassium Nernst potential from sodium and potassium intracellular and extracellular concentrations according to the Goldmann and Nernst equations.

```
%% V_r
% author: Zechari Tempesta
% date: October 18th 2013

% inputs:
% co_Na = 491E-3;                    Extracellular Na concentration (M/L)
% %ci_Na = 50E-3;                    Intracellular Na concentration (M/L)
% co_K = 20.11E-3;                   Extracellular K concentration (M/L)
% ci_K = 400E-3;                          Intracellular K concentration (M/L)
% b                                  relative sodium to potassium conductance

% outputs:
% Vr                                       resting potential
% EK_nernst                          potassium Nernst potential
% ENa_nernst                                sodium Nernst potential

function [ Vr ] = V_r( coNa, ciNa, coK, ciK, T, b )

R = 8.314;
F = 9.648E4;
Z = 1;
TKelvin = 273.15 + T;

Vr = ((R*TKelvin)/(Z*F))*log((coK + b* coNa)/(ciK + b*ciNa));
EK_nernst = ((R*TKelvin)/(Z*F))*log((co_K)/(ci_K));
ENa_nernst = ((R*TKelvin)/(Z*F))*log((co_Na)/(ci_Na));


end
```

However, the values of intracellular and extracellular potassium and sodium concentration of the Retzius and P cells were not measured during the electrophysiology recordings and are not well documented in the literature. A literature review states the extracellular potassium concentration of a

Retzius cell is 3mM, and the intracellular sodium concentration is 10.7mM [22, 23]. To determine the remaining concentrations of intracellular potassium concentration and extracellular sodium concentration, the sodium Nernst potential and resting potential must be identified. The Retzius cell's resting potential was determined to be -40.05 mV according to the experimental averages in table 8.4. The Retzius cell sodium Nernst potential was determined to be +59 mV from Deitmer's experimental data [23].

The following function, *Nernst_from_Vr*, determines intracellular potassium concentration, extracellular sodium concentration and potassium Nernst potential under the cellular conditions defined by extracellular potassium concentration, intracellular sodium concentration, sodium Nernst potential and resting potential.

```
%% Nernst_from_Vr
% author: Zechari Tempesta
% date: October 18th 2013

% inputs:
% Vr                    resting potential
% ENa_nernst            sodium Nernst potential
% co_K                  extracellular K concentration (M/L)
% ci_Na                         intracellular Na concentration (M/L)
% b                             relative sodium to potassium conductance

% outputs:
% EK_nernst             potassium Nernst potential
% ci_K                  intracellular K concentration (M/L)
% co_Na                         extracellular Na concentration (M/L)


function [ co_Na ci_K EK_nernst ] = Nernst_from_V_r( Vr, ENa_nernst,ci_Na,co_K,b)

R = 8.314;
F = 9.648E4;
Z = 1;
T=6.3;
TKelvin = 273.15 + T;

ci_Na=co_Na/exp(ENa_nernst/((R*TKelvin)/(Z*F)));
ci_K=((co_K+ b* co_Na)/(exp(Vr*((Z*F)/(R*TKelvin)))))-b*ci_Na;
EK_nernst = ((R*TKelvin)/(Z*F))*log((co_K)/(ci_K));

end
```

With unknown values of intracellular and extracellular potassium and sodium concentrations of the P cell, we must rely on the electrophysiological recordings to determine the critical values which will guide simulation. The resting potential can be interpreted from electrophysiological recording data, the P cell's resting potential was determined to be -45mV by inspection of figure 10.2. With the sodium Nernst potential unknown, specification to a value just above the recorded waveform's maximum is appropriate. The sodium Nernst potential acts as an upper limit to rising membrane potential and can be used as a practical tool when refining peak characteristics. The P cell's sodium Nernst potential was determined to be +45mV, 5mV above the actual peak of +40mV, via inspection of figure 10.2. Implementing the same values of extracellular potassium concentration and the intercellular sodium concentration as the Retzius cell, we can simulate the cellular conditions of the P cell with the aforementioned *Nernst_from_Vr* Function.

10.1.2 Pulse Characteristics

The amount of current injected into the cell can be designed by adjusting the pulse width and pulse amplitude of $I_{STIM}(t)$. The Retzius and P cell were both stimulated at 700 pA for 50ms to match experimental values.

```
%% Pulse information
% author: Zechari Tempesta
% date: October 18th 2013
%
% inputs:
% pulse_width                    Stimulus pulse width (s)
% pulse_start                    Membrane potential at pulse start (mV)
% number_of_steps                        Stimulus pulse step
% pulse_step                     Stimulus pulse step amplitude (A)
%
% ouputs:
% pulse_amp                              Stimulus pulse amplitude
% Q                                      Stimulus charge (q)
% V_stim                                 Membrane potential increase
%
pulse_width = 50E-3;
pulse_start=-40.50e-3;                  pulse_start=((pulse_start-V_rest)*C)/pulse_width;
number_of_steps=1;
pulse_step=.7e-9;

%% Pulse steps
for j=1:number_of_steps
   pulse_amp(j) = pulse_start+(j)*pulse_step;

Q(j)=pulse_amp(j)*pulse_width;
V_delta(j)=Q(j)/C;
V_stim(j)=V_rest+V_delta(j);
...

...
end
```

10.1.3 Threshold Potential

The threshold potential can be specified by setting $I_{STIM}(t)$ to a magnitude which raises resting potential to the desired value of threshold potential. The function, *find_threshold*, uses the desired threshold potential, pulse width, the value of membrane potential when $I_{STIM}(t)$ is being applied and cellular capacitance to calculate the pulse amplitude required to raise membrane potential to the desired threshold potential. Sodium activation will be adjusted to initially elicit an action potential at this particular value of membrane potential.

```
%% find_threshold
% author: Zechari Tempesta
% date: October 18th 2013
%
% inputs:
% pulse_width                    Stimulus pulse width (s)
% pulse_start                    Membrane potential at pulse start (mV)
% C                                    Cell capacitance (F)

% ouputs:
% V_thresh                             Threshold potential

function [ pulse_step ] = find_threshold( pulse_start,pulse_width,C,V_thresh)

pulse_step=((V_thresh-pulse_start)*C)/pulse_width;

end
```

10.1.4 Gating Variable Initial Conditions

The initial conditions of the gating variables at resting potential must be determined to specify the initial conditions vector which will be implemented in the ODE solver; *x_bc*, *x_ac*, and *x_x* will be described later in steady state analysis.

```
% gating intial conditions
m_o_mod = m_bound(V_rest,V_rest,m_bc,m_ac,m_x);
h_o_mod = h_bound(V_rest,V_rest,h_bc,h_ac,h_x);
n_o_mod = n_bound(V_rest,V_rest,n_bc,n_ac,n_x);
```

10.2 Steady State Analysis

Modifying the Hodgkin-Huxley simulation in *MATLAB* at steady state allows alteration of rate equation behavior at important steady state values, such as resting potential, and response to initial conditions.

10.2.1 The Rate Equations and Resting Potential

The rate equations formulated by Hodgkin and Huxley describe the gating particle activity within the membrane during an action potential. The form of equations 5.19-5.25 can be adjusted for a given resting potential, where $\Delta V = V_m - V_{rest}$:

$$a_m = \frac{0.1(25-\Delta V)}{e^{(2.5-0.1(\Delta V)}-1} \tag{10.1}$$

$$b_m = 4e^{(-1/18)(\Delta V)} \tag{10.2}$$

$$a_h = 0.07e^{(-1/20)(\Delta V)} \tag{10.3}$$

$$b_h = \frac{1}{1+e^{(3-0.1(\Delta V)}} \tag{10.4}$$

$$a_n = \frac{0.01*(10-\Delta V)}{e^{(1-0.1(\Delta V))}-1} \tag{10.5}$$

$$b_n = 0.125e^{(-1/80)(\Delta V)} \tag{10.6}$$

Equations 10.1-10.6 are identical to equations 5.22-5.27when V_{rest} = -60mV. This altered form shifts the position of the rate equation waveform along membrane potential according to the variable, V_{rest}. Adjustment of this variable does not modify the temporal behavior of gating particle activity. This is demonstrated figure 10.3-10.6:

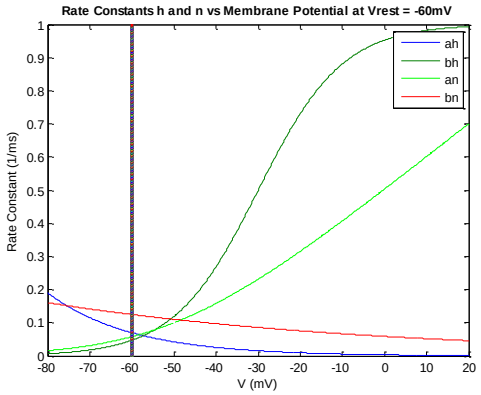

Figure 10.3. Steady state values of a_h, $b_{h,}a_n$, b_h at V_{rest}= -60mV

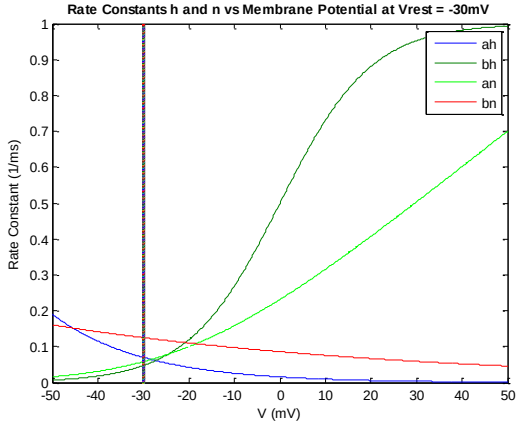

Figure 10.4 Steady state values of a_h, $b_{h,}a_n$, b_h at V_{rest}= -30mV

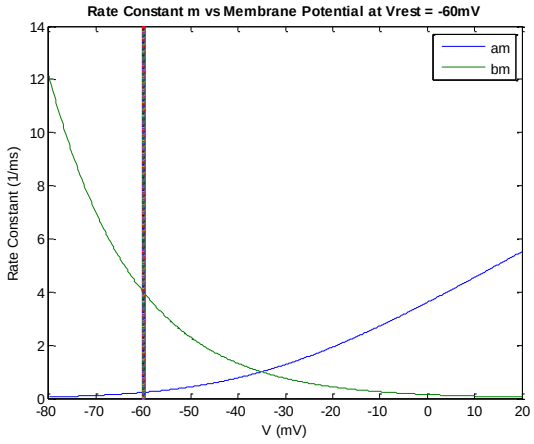

Figure 10.5. Steady state values of a_m, b_m at V_{rest}= -60mV

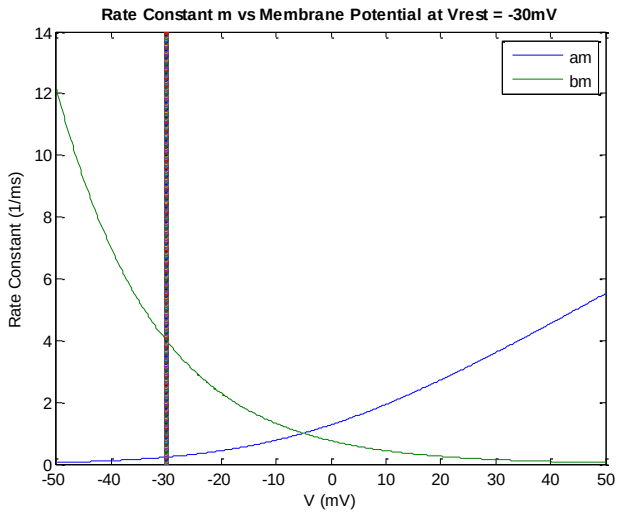

Figure 10.6. Steady state values of a_m, b_m at V_{rest} = -30mV

10.2.3 Time Constant and Gating Parameter Manipulation

The time constants,τ_m, τ_h, τ_n determine how quickly each gate responds to depolarization and the length of time gating activity will occur for. The gating parameters,m_∞, h_∞, n_∞, represent the position of their respective gates and the rate at which each will open or close. The time constants and gating parameters are list below.

$$m_\infty = \frac{a_m}{a_m + b_m} \tag{5.28}$$

$$h_\infty = \frac{a_h}{a_h + b_h} \tag{5.29}$$

$$n_\infty = \frac{a_n}{a_n + b_n} \tag{5.30}$$

$$\tau_m = \frac{1}{a_m + b_m} \tag{5.31}$$

$$\tau_h = \frac{1}{a_h + b_h} \tag{5.32}$$

$$\tau_n = \frac{1}{a_n + b_n} \tag{5.33}$$

With

$$m_\infty = \tau_m a_m \tag{5.34}$$

$$h_\infty = \tau_h a_h \tag{5.35}$$

$$n_\infty = \tau_n a_n \tag{5.36}$$

To simplify how the rate equations influence the time constant, each rate equation can be reduced into its fundamental exponential form. The opening of a gate is described by functions of exponential growth in the rate constants, a_m, $b_h$and a_n; the closing of a gate is described by functions of exponential decay in the rate constants, b_m, $a_h$and b_n. With this assumption, each time constant can be treated as a form on hyperbolic secant or inverse hyperbolic cosine:

$$\tau_x = \frac{1}{a_x + b_x} = \frac{1}{2}\left(\frac{2}{e^x + e^{-x}}\right) = \frac{1}{2}\left(\frac{1}{\cosh(x)^{-1}}\right) = \frac{1}{2}(\text{sech}(x)) \tag{10.7}$$

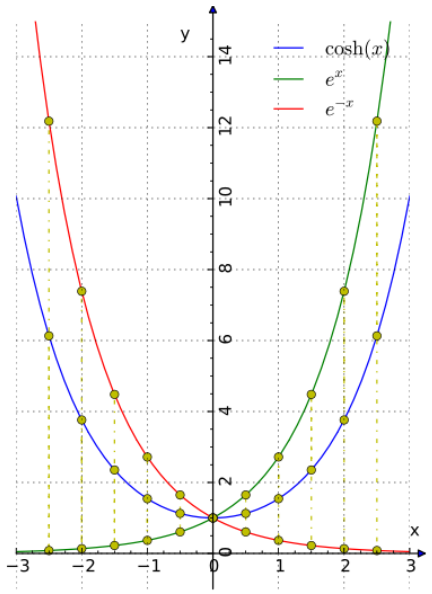

Figure 10.7. The relationship of $cosh(x)$, $e^x$and e^{-x}

The function $cosh(x)$ is the average of $e^x$and e^{-x}, with $\frac{e^x}{2}$representing the asymptote of the function's growing phase and $\frac{e^{-x}}{2}$ representing the asymptote of the function's decaying phase, illustrated in figures 10.7 and 10.8 [24].

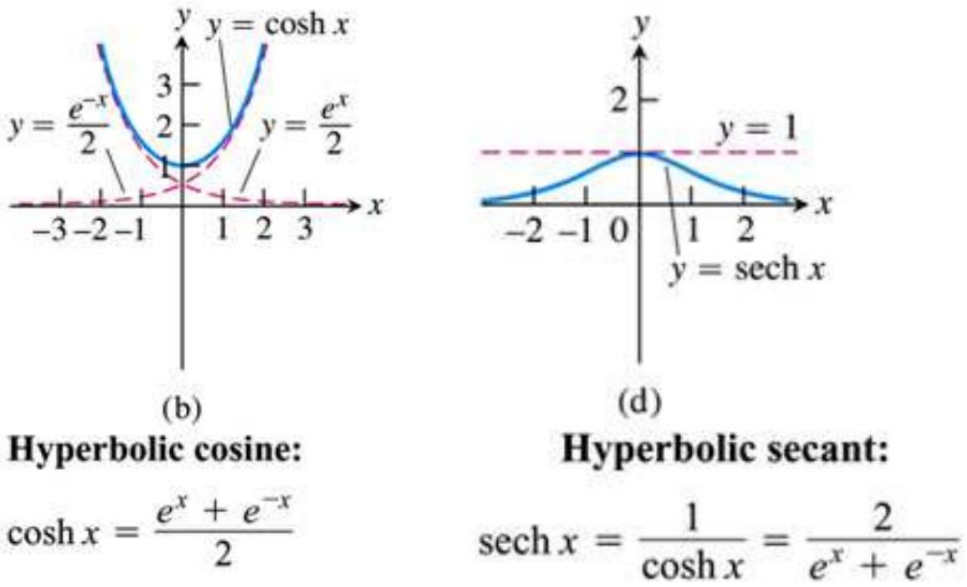

Figure 10.8. The relationship of $cosh(x)$ and $sech(x)$

$Sech(x)$ is the inverse of $cosh(x)$ and is symmetrical about the y=1 axis. This symmetry indicates that $\left(\frac{e^x}{2}\right)^{-1}$ and $\left(\frac{e^{-x}}{2}\right)^{-1}$ now represent the decaying and rising asymptotes [24]. This is illustrated in figure 10.9:

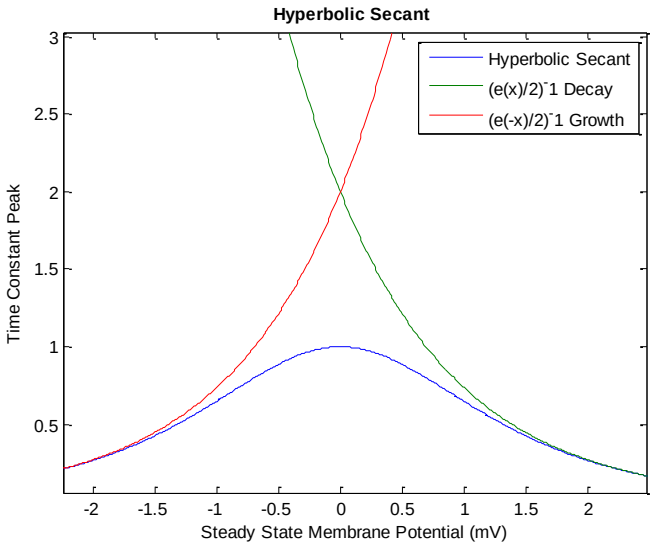

Figure 10.9. The relationship of $sech(x)$, $\left(\frac{e^x}{2}\right)^{-1}$ and $\left(\frac{e^{-x}}{2}\right)^{-1}$

The asymptotic relationship of $\left(\frac{e^x}{2}\right)^{-1}$ and $\left(\frac{e^{-x}}{2}\right)^{-1}$ to $sech(x)$ is analogous the inverse of the rate constants, $(a_x)^{-1}, (b_x)^{-1}$ to the time constant τ_x; the inversion of this relationship also holds true. These relationships are demonstrated in figure 10.10 and 10.11.

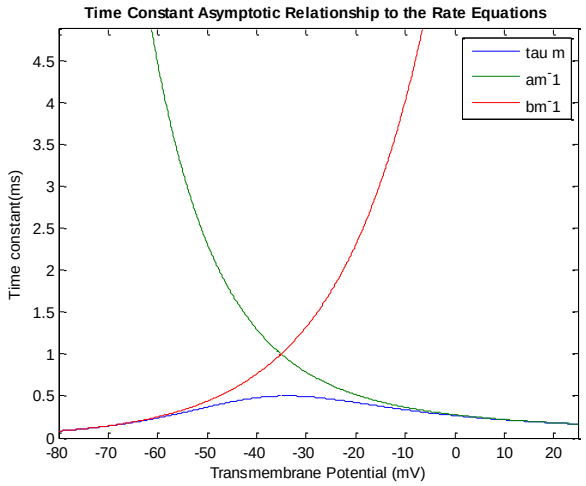

Figure 10.10. The relationship of τ_m, , $(a_m)^{-1}$ and $(b_m)^{-1}$

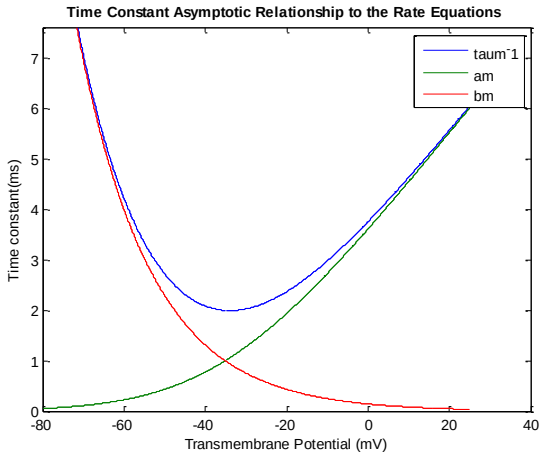

Figure 10.11. The relationship of $(\tau_m)^{-1}$, $(a_m)^{-1}$ and $(b_m)^{-1}$

This information can be used to manipulate each time constant into a form which better describes the characteristic of a waveform being simulated. The structure of $(a_x)^{-1}$ will be suited to fit the decaying phase of τ_x and the structure of $(b_x)^{-1}$ will be suited to fit the rising phase of τ_x.

With the shape of τ_x defined by the asymptotes, we can begin to alter its maximum value. The maximum corresponds to its $cosh(x)$ axis of symmetry; in the example above this was the y=1 axis, resulting in the maximum $sech(x)$ of 1. The symmetry axis can be expressed as, with $k = scaling\ constant$:

$$k^{-1}\ (sech(x)\ )$$

With asymptotes at:

$$\left(\frac{ke^{x}}{2}\right)^{-1} and \left(\frac{ke^{-x}}{2}\right)^{-1}$$

The time constant and rate equations can also be written in this form:

$$k^{-1}(\tau_x)$$

With asymptotes at:

$$(ka_x)^{-1} and\ (kb_x)^{-1}$$

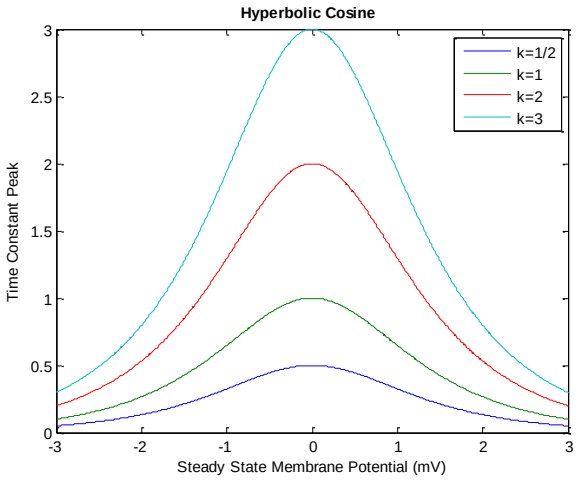

Figure 10.12. The function $k^{-1}(\tau_x)$ at steady state

Here the maximum value of τ_x is equal the scaling constant k^{-1}, positioned at a membrane potential value of zero. To adjust where the maximum occurs, the shift in membrane potential, h, can be included:

$$k^{-1}\ [sech(x-h)\ ]$$

With asymptotes at:

$$\left(\frac{ke^{x-h}}{2}\right)^{-1} and \left(\frac{ke^{-(x-h)}}{2}\right)^{-1}$$

The time constant and rate equations can also be written in this form:

$$k^{-1}\ (\tau_{x-h}) \ = \frac{1}{ka_{x-h}+kb_{x-h}} \qquad \text{Eq. 10.8}$$

With asymptotes at:

$$(ka_{x-h})^{-1} and\ (kb_{x-h})^{-1}$$

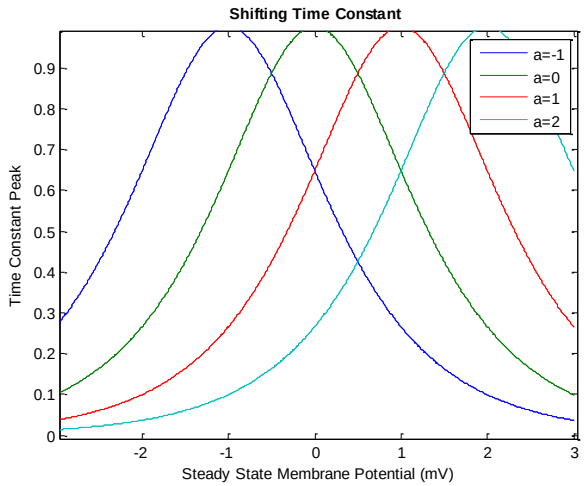

Figure 10.13. Shifting the time constant at steady state with varying values of *h* equal to *a*

Here, the time constant is shifted to values of membrane potential designated by the magnitude of a. The time constant can now be manipulated to suit any height or membrane potential position; however, the shape is limited to a symmetrical waveform with a fixed range of membrane potentials. In order to be unrestrained by symmetry, the functions of exponential growth and decay must cease to be symmetrical, with different values of decay and growth rates. The function $\mathrm{sech}(x)$ can no longer be used in its traditional form to describe the unsymmetrical time constant. The expression is modified to include horizontal and vertical adjustments, unique to the decaying (D_x) and rising (R_x) asymptotes.

$$D_x = k_d\, e_{decay}{}^{x-a_d} \tag{10.9}$$

$$R_x = k_r\, e_{rising}{}^{-(x-a_r)} \tag{10.10}$$

In equations 10.9 and 10.10, k_d , k_r and a_d , a_r are the vertical and horizontal scaling constants for the decaying and rising asymptotes of the time constants respectively. We can also include the rate of growth or decay in equations10.9 and 10.10:

$$D_x = k_d \, e_{decay}{}^{r_d \, (x - a_d)} \tag{10.11}$$

$$R_x = k_r \, e_{rising}{}^{-r_r \, (x - a_r)} \tag{10.12}$$

Here, r_d and r_r are the rate of growth and decay for the decaying and rising asymptotes of the time constant. A time constant may be able to be customized to suit any form with expression 10.13:

$$\tau_x \; = \; K_x \left[\frac{1}{D_x + R_x} \right] - A_x \tag{10.13}$$

Here, K_x and A_x represent the vertical and horizontal scaling constants of the time constant. D_x and R_x effectively represent the rate equations a_x and b_x. The expanded form is:

$$\tau_x \; = \; K_x \left[\frac{1}{k_d \, e_{decay}{}^{r_d \, (x - a_d)} + k_r \, e_{rising}{}^{-r_r \, (x - a_r)}} \right] - A_x \tag{10.14}$$

10.2.3 The Time Constant Relationship at Steady State

To effectively manipulate τ_x, we must investigate the properties of each gate's time constant at steady state. The time constant relationships are illustrated in figure 10.14.

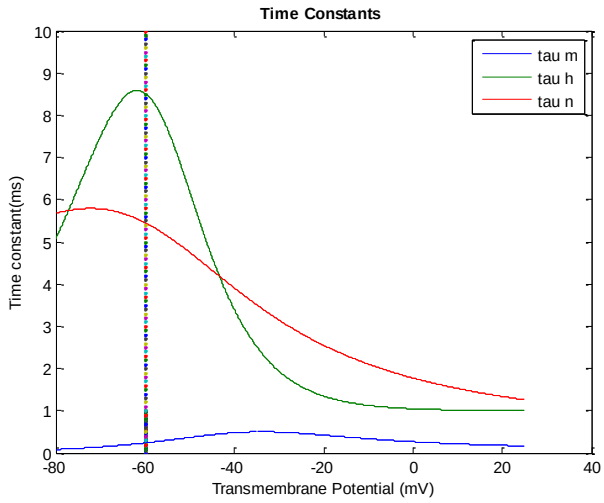

Figure 10.14. The relationship of τ_m, τ_h, and τ_n at steady state

Here, the time constants of *m, h,* and *n* are depicted over a linear increase in membrane potential with resting potential of -60mV. Together, these variables govern the temporal behavior of sodium and potassium conductance over the course of an action potential; it is possible to customize these constants to generate a waveform with desired characteristics in two ways: modifying the time constants as an entire system and modifying the interactions of individual time constants.

10.2.4 System Manipulation

System modification requires uniform changes across each time constant; this is achieved by adjusting maximum value of τ_x and the position at which it occurs. The maximum of each time constant indicates the speed at which each gate will respond to the initial depolarizing step. A uniform increase in the time constant results in an increased duration of the action potential with the fluctuations of *m, h,* and *n* remaining the same relative to one another; the opposite is true when the magnitude of the time constants is decreased. This behavior is demonstrated below:

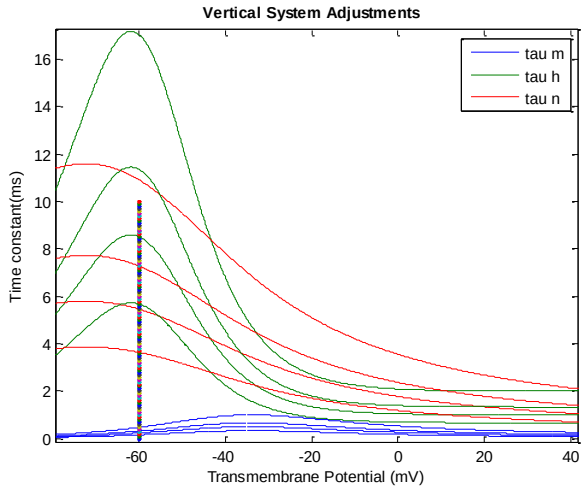

Figure 10.15. Uniform adjustment of τ_m, τ_h, and $\tau_n$at steady state using equations 10.8 for varying values of *k*

Here the maximum values of the time constants are altered uniformly; as the maximums increase, the time duration of the action potential lengthens. These maxima can also be shifted along the transmembrane potential axis, show in figure 10.16.

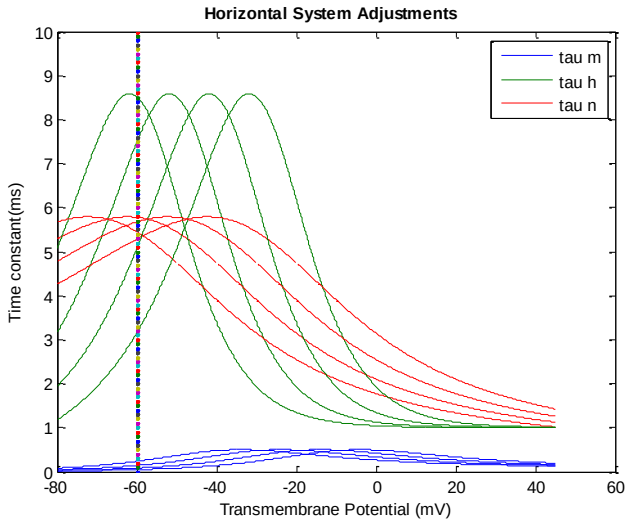

Figure 10.16 Uniform adjustment of τ_m, τ_h, and $\tau_n$at steady state using equations 10.8 for varying values of *h*

Modifying the membrane potential range for which the time constant occurs adjusts the position of each gate at resting potential. This is also illustrated in the gating parameters, shown in figure 10.17.

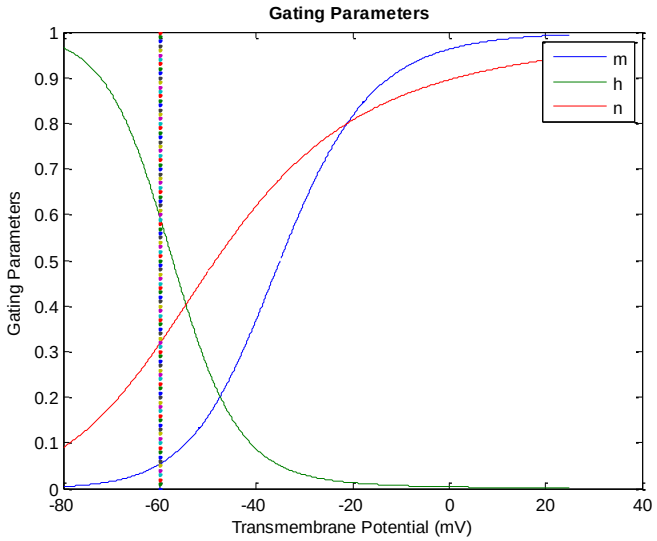

Figure 10.17 The gating parameters m_∞, h_∞, and n_∞ at steady state, with a resting potential of -60mV

Here the gating parameters m_∞, h_∞, and n_∞ are depicted over a linear increase in membrane potential with resting potential of -60mV. The values of m_∞, h_∞, and n_∞ at resting potential mark the initial position of the sodium and potassium gates before action potential generation. The time constant shift along the transmembrane potential axis orchestrates each gating position at resting potential.

Shifting the system of time constants to more negative values increases the resting to threshold potential magnitude. A negative shift causes the sodium inactivation gate to be in a more closed position at resting potential; in addition, the potassium activation gate is in a more open position at resting potential. These changes in initial gating position cause decreases in sodium permeability, requiring a stimulus current of greater magnitude to reach threshold potential.

Conversely, shifting the time constants to more positive values decreases the resting to threshold potential magnitude. A positive shift causes the position of the sodium inactivation gate to be in a more open position at resting potential; in addition, the potassium activation gate is in a more closed position. In this gating state, sodium can more easily enter the cell which requires a stimulus current of less magnitude to reach threshold potential.

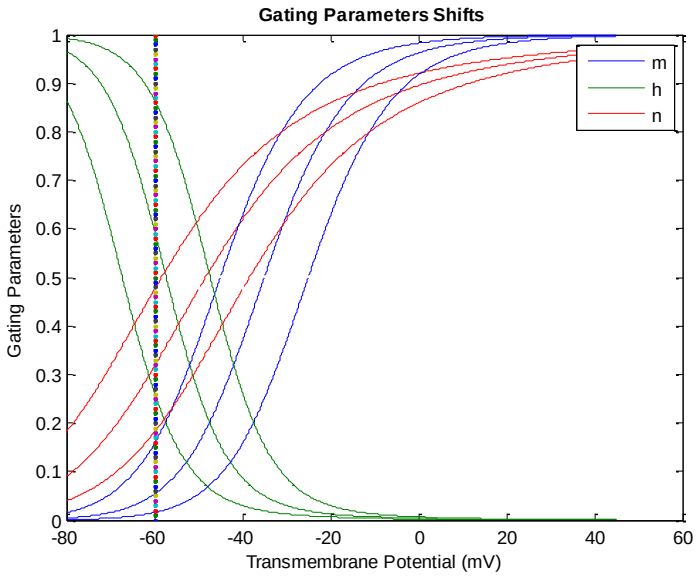

Figure 10.18. Uniform adjustment of m_∞, h_∞, and n_∞ at steady state using equations 10.8 for varying values of *h*.

Figure 10.18 includes positive and negative shifts of the time constants with a resting membrane potential of -60mV.

10.2.5 Interaction Manipulation

Once the system of time constants is appropriately adjusted, the manipulation of time constant interaction can begin. Uniform adjustment of the time constants maintains an interaction level among individual time constants; this is essential in determining bulk waveform characteristics but is limited in specificity. Time constant, and therefore rate equation, interaction allows an increased amount of precision in waveform simulation. Interaction can be defined as the portion of the waveform in which the rate equations of the time constants overlap and compete. The level of interaction among τ_m, $\tau_h$and τ_n indicate which gate will dominate a particular time interval of the action potential. Emphasis of a particular gate will highlight its effect on the action potential; when adjusting time constant interaction it is important to keep this point in mind. The following characteristics of the time constant can be directly manipulated to adjust the level interaction:

1. **The scaling constant of the decaying asymptote, k_d**
2. **The scaling constant of the rising asymptote, k_r**
3. **The membrane potential shift of τ_x max of the decaying asymptote**
4. **The membrane potential shift of τ_x max of the rising asymptote**
5. **τ_x at resting potential**
6. **$\tau_x$max**
7. The rate of decay of τ_x, r_d
8. The growth rate of τ_x, r_r

We will now analyze how to manipulate the characteristics listed in bold to customize each phase of the action potential, beginning with the initial sodium activation. The characteristics not listed in bold can be further manipulated to enhance the control of the simulation on its generated waveform, but are not included in this simulation. This simulation was designed to manipulate the equations of the Hodgkin-Huxley Model. A simulation which directly alters the decay and growth rate of the rate equations would be better served to begin with rate equations in their most fundamental form, similar to the hyperbolic secant.

10.3 Transient Analysis

The behavior of time constant interaction and its resulting effects on the action potential waveform is better understood and manipulated under transient analysis.

10.3.1 Sodium Activation

To depolarize the cell, the membrane potential must rise from resting potential to threshold potential. The magnitude of threshold potential is largely dependent on how easily sodium ions can enter the sodium channel. We are able to manipulate sodium entry in two ways:

1. Decrease $\tau_m$max relative to τ_h and τ_n max

2. Adjust τ_m max to occur when the *h gate* is in a more open state and the *n gate* is in a more closed state

The relative magnitude of τ_m max compared with τ_h and τ_n max indicates how sensitive the sodium activation gate is to changes in membrane potential. The smaller the relative magnitude of τ_m max, the more sensitive the sodium activation gate is to the depolarizing magnitude of stimulus current. Threshold potential and sodium activation can be manipulated by modifying the relative maximum of τ_m.

As mentioned in the *steady state* section, the positions of each gate at resting potential can influence the ease of sodium entry into the cell. Upon depolarization, sodium permeability dramatically increases, allowing a large influx of sodium ions into the cell. This dramatic change in sodium permeability happens at threshold potential, when the minimum amount sodium permeability is achieved in order to overcome the efflux of potassium ions and produce a net inward current. When the sodium activation gate fully opens, sodium permeability is limited by the position of the sodium inactivation and the amount of potassium entering the cell permitted by the position of the potassium activation gate. Shifting τ_m to peak at a membrane potential position where the *h gate* is in a more open state and the *n gate* is in a more closed state will lessen the resistance to sodium influx.

10.3.2 Waveform Duration

The period of the simulated action potential will be dependent on the maximum values of τ_m, τ_h and τ_n. Once sodium activation is achieved, the maximum of the time constants (including the adjustments made to τ_m,) can be uniformly adjusted to the desired period.

10.3.3 Action Potential Peak Adjustments

The maximum membrane potential an action potential will reach when depolarized is largely influenced by the sodium Nernst potential; this will be discussed in greater detail later. Here we will focus on manipulation of the time duration and height of the action potential peak.

The time duration of the action potential peak concerns the time interval between sodium activation and sodium inactivation. The maximum membrane potential occurs when the sodium activation gate is maximally open, identified when *m* reaches its maximum. The duration of this maximum is limited by the closure of the sodium inactivation gate, indicated by when *h* reaches its minimum. The time duration of the action potential peak can be adjusted by altering the time at which *m* reaches its maximum and *h* reaches its minimum. This can be achieved by varying the difference in τ_m and τ_h max. Increasing the difference in these maximums will create a longer, flatter peak, while decreasing the time constant difference will generate a shorter, sharper peak.

Adjusting the action potential height from this maximum impacts the level of sodium activation when sodium inactivation occurs. This is similar to adjusting the peak duration but instead of adjusting sodium inactivation with the maximum of *m*, sodium inactivation is adjusted to decreased level of *m.* The lower the value of *m* at sodium inactivation, the smaller the height of the action potential waveform.

10.3.4 Repolarization

During repolarization the sodium channel is inactivated by closure of the sodium inactivation gate; sodium's affect on membrane potential is now neutralized, permitting the potassium channel to exclusively determine membrane potential. The duration and decay rate of action potential repolarization can be manipulated by adjusting the maximum of τ_n . An increase in τ_n will lengthen the time duration of potassium activity and decrease the repolarization slope; decreasing τ_n will increase the repolarization slope and shorten the time duration of potassium activity.

10.4 Functions of Transient Analysis

10.4.1 Gating Behavior Manipulation

The gating behavior was manipulated with the following variables:

1. *V_rest*

2. *var_bc*
3. *var_ac*
4. *var_x*

Here, *var* can represent *m, h,* or *n*. The values of *V_rest, var_bc, var_ac, var_x* are used in determining rate equations, time constants, initial conditions of the gating variables, final conditions of the gating variables, and the ordinary differential equation solver. *V_rest* allows these variables to change in accordance to the initial condition: $V_m(0) = V_{rest}$. The scaling constants, *var_b* and *var_ac* and membrane potential shift, *var_x* , allow modification of the time constant maximum and the membrane potential at which it occurs. The following functions illustrate how these values are incorporated into each function set. Their corresponding functions are analogous in variable passage and execution.

```
% V_rest = resting potential
% m_bc = beta_m scaling constant
% m_ac = alpha_m scaling constant
% h_bc = beta_h scaling constant
% h_ac = alpha_h scaling constant
% n_bc = beta_n scaling constant
% n_ac = alpha_n scaling constant
% m_x = tau m shift
% h_x    = tau h shift
```

10.4.2 Rate Equation

```
% function: alpha_m
function [ am ] = alpha_m(Vm,V_rest,m_ac,m_x )

Vm = Vm/1.0E-3;
V_rest=V_rest/1.0E-3;
% orginal
if Vm ~= V_rest
   am = m_ac*((0.1*(25-(Vm-(V_rest+m_x))))./(exp(2.5-0.1*(Vm-(V_rest+m_x)))-1));

end
   if Vm == V_rest
   up = Vm + 1.0E-4;
   down = Vm - 1.0E-4;
   am =m_ac*(((0.1*(25-(up -(V_rest+m_x)))/(exp(2.5-0.1*(up-(V_rest+m_x)))-1)+(0.1)*(25-(down-
(V_rest+m_x)))/(exp(2.5-0.1*(down-(V_rest+m_x)))-1))/2));
   end

end
```

10.4.3 Time Constant

```
%function: tau_m
function [ tm ] = tau_m(Vm,V_rest,m_bc,m_ac,m_x)

tm = 1./(alpha_m(Vm,V_rest,m_ac,m_x)+beta_m(Vm,V_rest,m_bc,m_x));

end
```

10.4.4 Final Value of the Gating Variables

```
%function: m_bound

function [ mb ] = m_bound(Vm, V_rest,m_bc,m_ac,m_x)

mb = (alpha_m (Vm, V_rest,m_ac,m_x)./(alpha_m(Vm,V_rest,m_ac,m_x)+beta_m(Vm, V_rest,m_bc,m_x)));

end
```

10.4.5 Ordinary Differential Equation Solver

The solver routine *odefun* is called from the main program via ode45 and is passed the variables listed below.

```
%% Invoke ODE solver
[T,Y_Vr1] = ode45(@odefun_Vm_Vr1, t, y0, options, C, maxcond_Na, maxcond_K, Na_Battery, K_Battery,
pulse_width, pulse_amp(j), V_rest,m_bc,m_ac,h_bc,h_ac,n_bc,n_ac,n_x,m_x,h_x);
```

The solver routine, *odefun*, is called from the main program. The following variables are passed to the solver, which runs and returns the solution to the set of ordinary differential equations.

```
%

% Function: odefun
% Revision Date: 12/11/09
% Author: Robert B. Szlavik
%
% Modified Date: October 18th, 2013
% Author: Zechari R. Tempesta
%
%
%
% USES FUNCTIONS: m_bound
% h_bound
% n_bound
% tau_m
% tau_h
% tau_n
% Current
%
% Inputs: t = current time point being evaluated in (s)
% y = previous value of the ODE variables, VECTOR
% Cm = membrane capacitance in (F)
% GNamax = maximum sodium conductance in (S)
% GKmax = maximum potassium conductance in (S)
% VNa = sodium Nernst potential in (V)
% VK = potassium Nernst potential in (V)
% pw = stimulus pulse width in (s)
% amp = stimulus pulse amplitude in (A)
%
% V_rest = resting potential
% m_bc = beta_m scaling constant
% m_ac = alpha_m scaling constant
% h_bc = beta_h scaling constant
% h_ac = alpha_h scaling constant
% n_bc = beta_n scaling constant
% n_ac = alpha_n scaling constant
% m_x = tau m shift
% h_x    = tau h shift
% n_x    = tau n shift
%
% Returns: dy = first derivative value of ODE variables
```

```
%
% Internal: mf = step bounded value of m gating variable
% hf = step bounded value of h gating variable
% nf = step founded value of n gating variable
% taum = step rise time value of m gating variable
% tauh = step rise time value of h gating variable
% taun = step rise time value of n gating variable
%
%%%%%%%%%%%%%%%%%%%%%%%%%%%%%%%%%%%%%%%%%%%%%%%%%%%%%%%%%%%
%%%%%%%%%%%%%%%%%%
function dy = odefun(t, y, Cm, GNamax, GKmax, VNa, VK, pw,
amp,V_rest,m_bc,m_ac,h_bc,h_ac,n_bc,n_ac,n_x,m_x,h_x)


mf = m_bound(y(1),V_rest,m_bc,m_ac,m_x);
hf = h_bound(y(1),V_rest,h_bc,h_ac,h_x);
nf = n_bound(y(1),V_rest,n_bc,n_ac,n_x);
taum = tau_m(y(1),V_rest,m_bc,m_ac,m_x);
tauh = tau_h(y(1),V_rest,h_bc,h_ac,h_x);
taun = tau_n(y(1),V_rest,n_bc,n_ac,n_x);
dy = [-(GKmax/Cm)*((y(4))^4)*(y(1)-VK)-(GNamax/Cm)*((y(2))^3)*y(3)*(y(1)-VNa)+Current(t,pw,amp)/Cm;
(mf-y(2))/taum;
(hf-y(3))/tauh;
(nf-y(4))/taun];
```

10.4.6 Sodium Activation

Depolarization at a designated threshold potential can only occur if the sodium gates are in appropriate positions. When the initial conditions of this problem is modified, it is important to determine which positions will begin to depolarize the cell at the chosen threshold potential. This determination can be made by shifting τ_m along the steady state membrane potential axis until a depolarization is observed. This can be done as described in equation 10.14, however, following this shift, τ_m becomes disproportionately scaled to τ_h and τ_n. Instead we will use a new approach to shift τ_m utilizing the scaling constants of the decaying and rising phase of the time constants, *m_bc* and *m_ac*.

Decreasing *m_bc* while increasing *m_ac* will move the time constant to more negative values of steady state membrane potential; increasing *m_bc* while decreasing *m_ac* moves the time constant to more positive values of steady state membrane potential. The shifts produced by values of *m_bc* and *m_ac* which resulted in a τ_{shift} max equal to τ_m max were recorded. We now have an array of *m_bc* and

m_ac values which shift the time constant along the steady state membrane potential axis and can be scaled as shown in Table 10.1.

TABLE 10.1

VALUES OF *M_BC* AND *M_AC* WHICH SHIFT THE TIME CONSTANT ALONG THE STEADY STATE MEMBRANE POTENTIAL AXIS

$\tau_{shift}(mV)$	m_bc	m_ac
-20.4	1.84	0.62
-21.4	1.76	0.64
-22.4	1.68	0.66
-25.8	1.44	0.74
-30.6	1.16	0.88
-31.8	1.1	0.92
-33.8	1	1
-36	0.9	1.1
-36.6	0.88	1.12
-38	0.82	1.2
-40.8	0.72	1.36
-41.4	0.7	1.4
-42	0.68	1.44
-42.6	0.66	1.48
-43.8	0.62	1.58
-46	0.56	1.76
-47.4	0.52	1.9

The procedure for gathering the values listed in table 10.1 is demonstrated in the *tau_m_shift* script.

```
%% tau_m_shift
% author: Zechari Tempesta
% date: October 18th 2013

% inputs:
% V_rest                                    resting potential
% range_m_bc                          range of the scaling constant m_bc
% range_m_ac                          range of the scaling constant m_ac
% desired_tau_max                           maximum value of taum

% outputs:
% tau_m_b_coeff_within_range          m_bc value at desired_tau_max
% tau_m_a_coeff_within_range          m_ac value at desired_tau_max
% tau_m_vmax_within_range             shift of new time constant from rest
%
%

clear all
Vm=-80:.2:20;
V_rest=-62.4929;

% Finding which tau max
range_m_bc=0:.001:2;
range_m_ac=0:.001:2;
for n=1:length(rangea)
for i=1:length(rangeb)
a(n)=range_m_ac(n);
b(i)=range_m_bc(i);

bm1(:,i,n) = b(i)*(4*exp(-(Vm-(V_rest))/18))+...
   a(n)*((0.1*(25-(Vm-(V_rest))))./(exp(2.5-0.1*(Vm-(V_rest)))-1));
tau_m=1./bm1;
tau_m_maxes(:,i,n)= max(tau_m(:,i,n));

fo(:,i,n)=find(tau_m(:,i,n)==tau_m_maxes(:,i,n));

end
end
max_index(:,:)=fo(1,:,:);
v_at_max(:,:)=Vm(max_index);
tau_m_max(:,:)=tau_m_maxes(1,:,:);

fee=zeros([length(a) length(b)]);
for n=1:length(a)
desired_tau_max=0.50143;

low_range= desired_tau_max-0.005;
high_range= desired_tau_max+0.005;

below=length(find(tau_m_max(:,n)>low_range));
diff_below=length(a)-below;
```

```
below_index(:,n)=[find(tau_m_max(:,n)>low_range)', zeros([1 diff_below])]';

above=length(find(tau_m_max(:,n)<high_range));
diff_above=length(a)-above;
above_index(:,n)=[zeros([1 diff_above]), find(tau_m_max(:,n)<high_range)'];

end

range_index=below_index.*above_index;
tau_m_within_range_index=find(range_index);
tau_m_values_within_range=tau_m_max(tau_m_within_range_index);
tau_m_vmax_within_range=v_at_max(tau_m_within_range_index);

fo=ones([length(a) length(a)]);
a_coeff=fo(:,1)*a;
b_coeff=a_coeff';

tau_m_a_coeff_within_range=a_coeff(tau_m_within_range_index);
tau_m_b_coeff_within_range=b_coeff(tau_m_within_range_index);

tau_m_critical_points=[tau_m_values_within_range tau_m_vmax_within_range...
   tau_m_b_coeff_within_range tau_m_a_coeff_within_range tau_m_within_range_index];
```

The values of *m_bc* and *m_ac* which shift the time constant are now applied to the beta_m and alpha_m until depolarization is observed. We are interested in the *m_bc* and *m_ac* pair which elicits an action potential with the minimum value of *m_ac*. This pair will permit the pulse parameters, set in the initial conditions, to raise membrane potential from resting potential to the desired threshold potential.

```
%% Sodium activation
% author: Zechari Tempesta
% date: October 18th 2013

% inputs:
% m_bc_tau_scaled                    value of m_bc at scaled tau m
% m_ac_tau_scaled                    value of m_ac at scaled tau m
% selected_tau_m                     scale of tau_m
% selected_tau_h                     scale of tau_h
% selected_tau_n                     scale of tau_n
% V_rest                             resting potential
% m_x                                tau m shift
% h_x                                tau h shift
% n_x                                tau n shift

% outputs:
% T                                  time
% Y_Vr1                              membrane potential, m, h, n

%% Shifitng m_bc and m_ac

m_bc_tau_scaled=[1.84 1.76 1.68 1.44 1.23 1.16 1.1 1 0.9 ...
   0.88 0.82 0.72 0.7 0.68 0.66 0.62 0.56 0.52...
   .64 .62 .6 .58];

m_ac_tau_scaled =[0.62 0.64 0.66 0.74 .84 0.88 0.92 1 1.1 ...
   1.12 1.2 1.36 1.4 1.44 1.48 1.58 1.76 1.9 1.52...
   1.56 1.6 1.64];

for x=1:length(m_bc_tau_scaled)

selected_tau_m=[1 1];
selected_tau_h=[1 1];
selected_tau_n=[1 1];

m_x=0;
m_bc= m_bc_tau_scaled(x)*selected_tau_m(1);
m_ac= m_bc_tau_scaled(x)*selected_tau_m(2);

h_x=0;
h_bc=selected_tau_h(1);
h_ac=selected_tau_h(2);

n_x=0;
n_bc=selected_tau_n(1);
n_ac=selected_tau_n(2);

m_o_mod = m_bound_mod(V_rest,V_rest,m_bc,m_ac,m_x);
h_o_mod = h_bound_mod(V_rest,V_rest,h_bc,h_ac,h_x);
n_o_mod = n_bound_mod(V_rest,V_rest,n_bc,n_ac,n_x);

%% Specify the inital conditions vector
y0 = [V_rest, m_o_mod, h_o_mod, n_o_mod ];
```

```
options = odeset();

%% Invoke the solver
[T,Y_Vr1] = ode45(@odefun_Vm_Vr1, t, y0, options, C, maxcond_Na,...
    maxcond_K, Na_Battery, K_Battery, pulse_width, pulse_amp(j),...
    V_rest,m_bc,m_ac,h_bc,h_ac,n_bc,n_ac,n_x,m_x,h_x);

colors={'b','g','r','k','m','c','y'};

%% Plot solution
figure(1)
plot(T,Y_Vr1(:,1),colors{x})
hold on
axis([0 max_time EK_nernst ENa_nernst]);
title('Shifting Tau M','FontWeight','bold')
xlabel('Time(s)')
ylabel('Membrane Potential (V)')
hold on
legend ('Istim 700pA')
hold on
```

The membrane potential generated while shifting τ_m is plotted in figure 10.19.

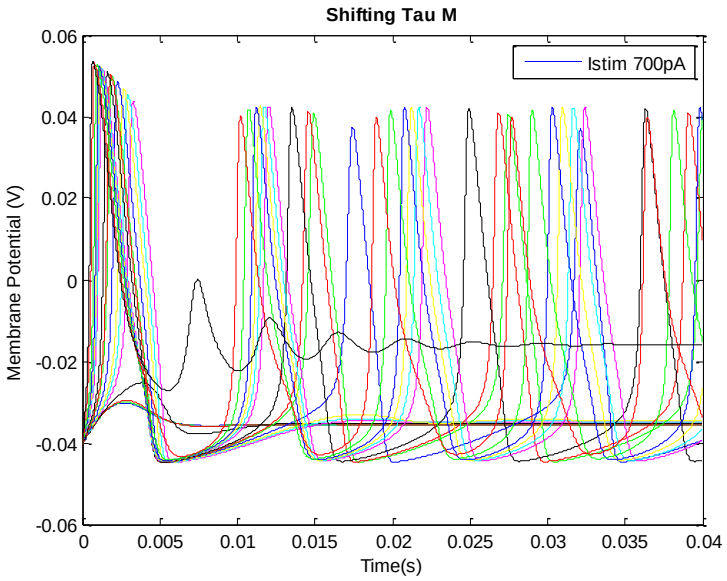

Figure 10.19. The Retzius cell membrane potential generated while shifting τ_m using the Sodium activation function

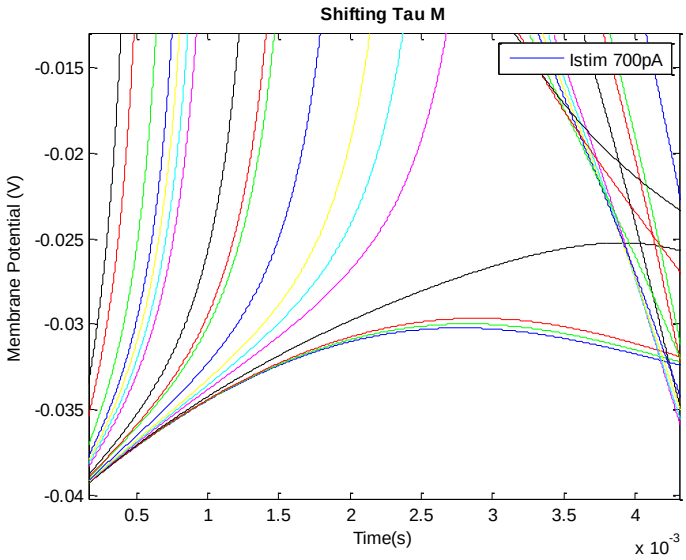

Figure 10.20. An enhanced look at figure 10.19 where the initial activation of an action potential of the Retzius cell is observed

Here, we can observe the initial depolarization, displayed above in magenta. The values of *m_bc* and *m_ac* which elicited this action potential will be used to simulate the Retzius cell waveform.

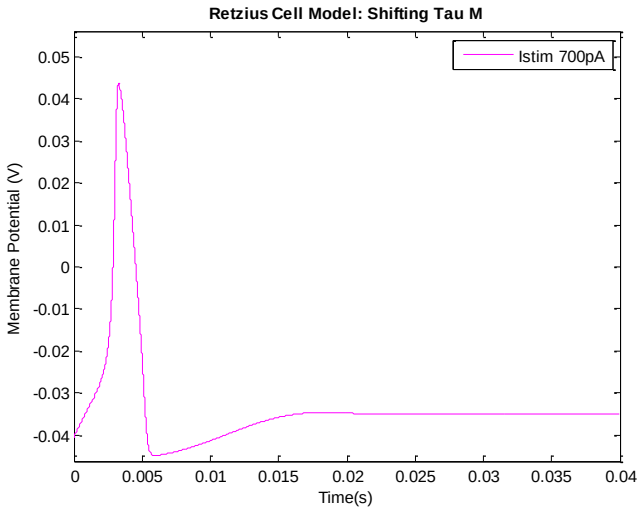

Figure 10.21. The initially activated action potential form figures 10.19 and 10.20 of the Retzius cell

The Retzius cell action potential from figures 10.19 and 10.20 is isolated in figure 10.21. The values of *m_bc* and *m_ac* which elicited this action potential are 1.23 and 0.84 respectively.

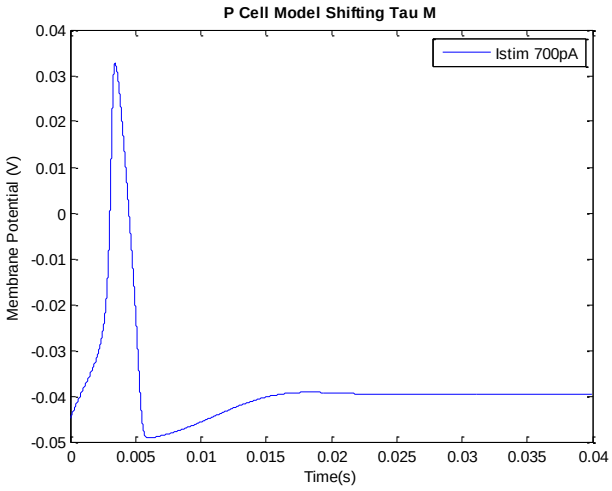

Figure 10.22. The initially activated action potential of the P cell.

The same method was followed with the initial conditions of the P cell, resulting in the isolated P cell waveform displayed above in figure 10.22. The P cell values of *m_bc* and *m_ac* which elicited this action potential were also 1.23 and 0.84 respectively. Note the differences in resting potential and action potential maximum from the Retzius cell.

10.4.7 Period Extension

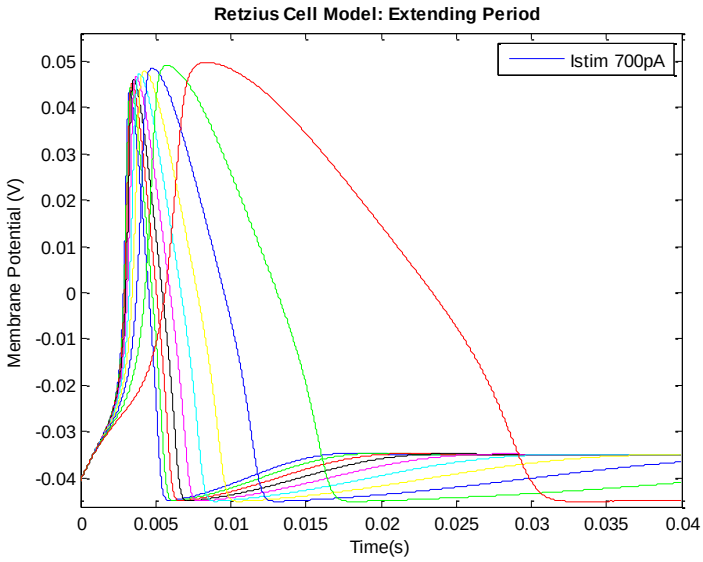

Figure 10.23. Extension of the action potential period observed in the Retzius cell

Here, the period of the Retzius cell is extended using the following script:

```
%% Period Extension
%%

duration_range=.1:.1:1;
duration_range =fliplr(duration_range);

for x=1:length(duration_range)

duration=duration_range(x);

selected_tau_m=[1.23* duration 0.84* duration];
selected_tau_n=[duration duration];
selected_tau_h=[duration duration];

m_x=0;
m_bc= m_bc_tau_scaled(x)*selected_tau_m(1);
m_ac= m_bc_tau_scaled(x)*selected_tau_m(2);

h_x=0;
h_bc=selected_tau_h(1);
h_ac=selected_tau_h(2);

n_x=0;
n_bc=selected_tau_n(1);
n_ac=selected_tau_n(2);

m_o_mod = m_bound_mod(V_rest,V_rest,m_bc,m_ac,m_x);
h_o_mod = h_bound_mod(V_rest,V_rest,h_bc,h_ac,h_x);
n_o_mod = n_bound_mod(V_rest,V_rest,n_bc,n_ac,n_x);

%% Specify the inital conditions vector
y0 = [V_rest, m_o_mod, h_o_mod, n_o_mod ];
options = odeset();

%% Invoke the solver
[T,Y_Vr1] = ode45(@odefun_Vm_Vr1, t, y0, options, C, maxcond_Na,...
    maxcond_K, Na_Battery, K_Battery, pulse_width, pulse_amp(j),...
    V_rest,m_bc,m_ac,h_bc,h_ac,n_bc,n_ac,n_x,m_x,h_x);

colors={'b','g','r','k','m','c','y'};

%% Plot solution
plot(T,Y_Vr1(:,1),colors{x})
hold on
axis([0 max_time EK_nernst ENa_nernst]);
title('Retzius Cell Model: Extending Period ','FontWeight','bold')
xlabel('Time(s)')
ylabel('Membrane Potential (V)')
hold on
legend ('Istim 700pA')
hold on
```

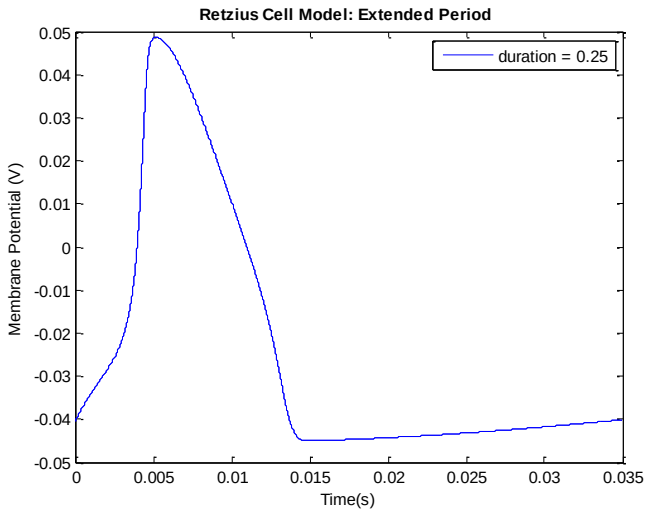

Figure 10.24. Extension of the action potential period observed in the Retzius cell to a *duration* value of 0.25

The *duration* value of 0.25 was chosen to match the experimental recordings of the Retzius cell. If the maximum of the simulated action potential must be reduced, it is important to choose a period length about 10% longer than desired. This compensation accounts for the increase in period length which will happen during peak reduction.

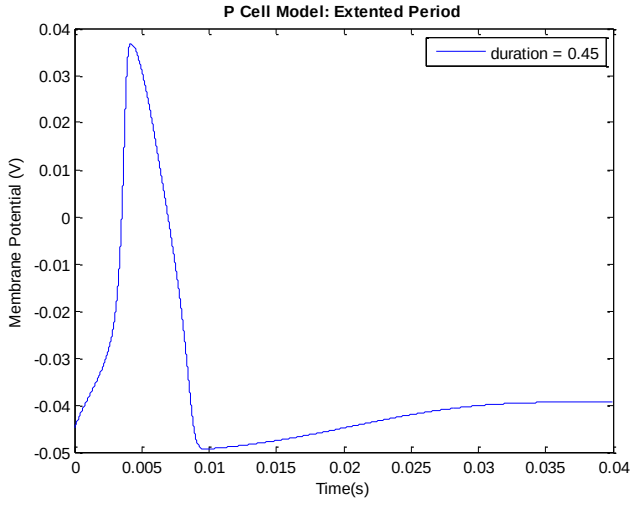

Figure 10.25. Extension of the action potential period observed in the P cell to a *duration* value of 0.45

10.4.8 Reducing Maximum

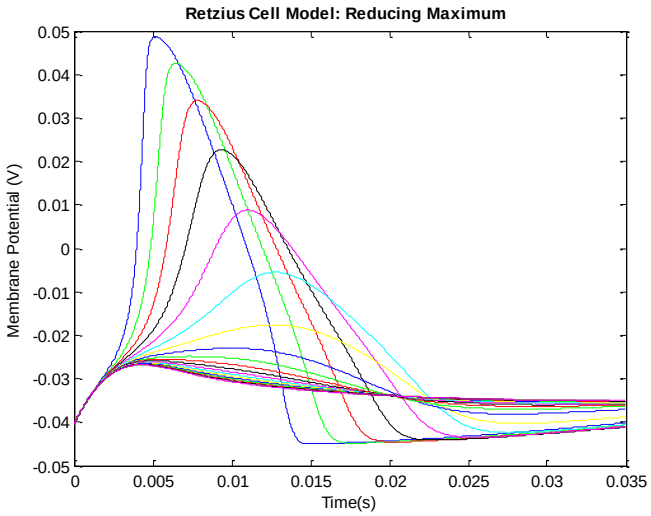

Figure 10.26. Peak reduction of the action potential observed in the Retzius cell

The peak height of the action potential is reduced by diminishing the magnitude of τ_x,using the following script.

```
%% Reducing Maximum
%%

duration_range=.1:.1:1;
duration_range =fliplr(duration_range);

tau_m_reduction=1:.5:10;

for x=1:length(tau_m_reduction)

duration=0.25;
red_max=tau_m_reduction(x);

selected_tau_m=[(1.23*duration)/red_max (0.84*duration)/red_max];
selected_tau_n=[duration duration];
selected_tau_h=[duration duration];

m_x=0;
m_bc= m_bc_tau_scaled(x)*selected_tau_m(1);
m_ac= m_bc_tau_scaled(x)*selected_tau_m(2);

h_x=0;
h_bc=selected_tau_h(1);
h_ac=selected_tau_h(2);
```

```
n_x=0;
n_bc=selected_tau_n(1);
n_ac=selected_tau_n(2);

m_o_mod = m_bound_mod(V_rest,V_rest,m_bc,m_ac,m_x);
h_o_mod = h_bound_mod(V_rest,V_rest,h_bc,h_ac,h_x);
n_o_mod = n_bound_mod(V_rest,V_rest,n_bc,n_ac,n_x);

%% Specify the inital conditions vector
y0 = [V_rest, m_o_mod, h_o_mod, n_o_mod ];
options = odeset();

%% Invoke the solver
[T,Y_Vr1] = ode45(@odefun_Vm_Vr1, t, y0, options, C, maxcond_Na,...
   maxcond_K, Na_Battery, K_Battery, pulse_width, pulse_amp(j),...
   V_rest,m_bc,m_ac,h_bc,h_ac,n_bc,n_ac,n_x,m_x,h_x);

colors={'b','g','r','k','m','c','y'};

%% Plot solution
plot(T,Y_Vr1(:,1),colors{x})
hold on
axis([0 max_time EK_nernst ENa_nernst]);
title('Retzius Cell Model: Reducing Maximum ','FontWeight','bold')
xlabel('Time(s)')
ylabel('Membrane Potential (V)')
hold on
legend (duration = 0.25)
hold on
```

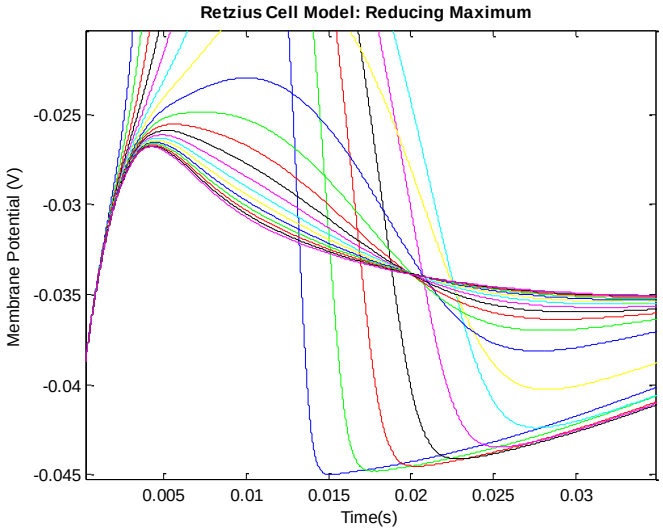

Figure 10.27. An enhanced depiction of figure 10.26

Figure 10.27 is an enhanced view of the reduced action potentials. If the peak duration of an action potential must also be reduced, following maximum reduction, it is important its maximum be

reduced to about 10% greater than the desired final height; reducing the peak duration will also slightly decrease the maximum. For this reason the *tau_m_reduction* value of 8.5 was chosen.

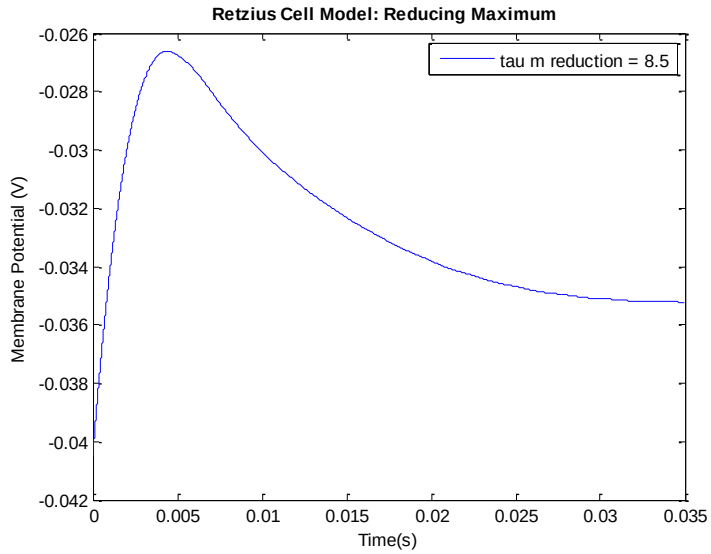

Figure 10.28. Peak reduction of the action potential observed in the Retzius cell to a *tau_m_reduction* of 8.5

The *tau_m_reduction* value of 0.9 was chosen for the P cell to increase the action potential maximum.

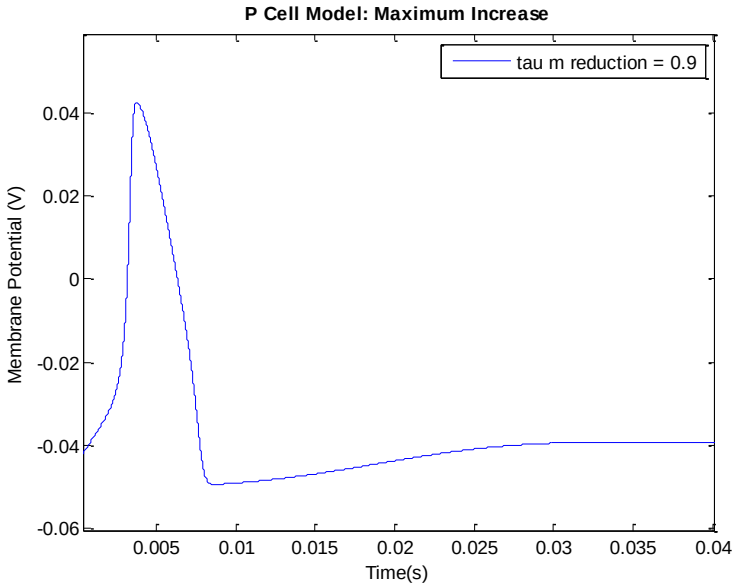

Figure 10.29. Peak reduction of the action potential observed in the P cell to a *tau_m_reduction* of 0.9

10.4.9 Reducing Peak Duration

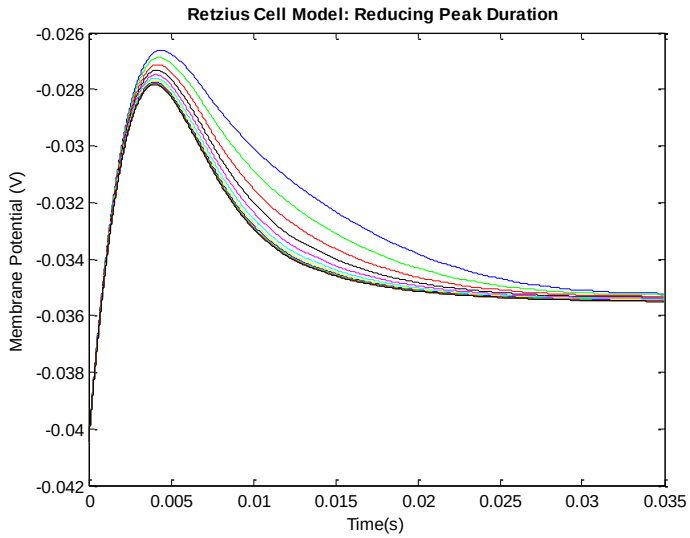

Figure 10.30. Peak duration reduction of the action potential observed in the Retzius cell

Figure10.30 illustrates the peak duration reduction of the Retzius cell. The peak duration is reduced by negatively shifting *h_x* with the following script:

```
%% Reducing Peak Duration
%%

duration_range=.1:.1:1;
duration_range =fliplr(duration_range);
tau_m_reduction=1:.5:10;

tauh_shift=0:-3:-30;

for x=1:length(tauh_shift)

duration=0.25;
red_max =8.5;

selected_tau_m=[(1.23*duration)/red_max (0.84*duration)/red_max];
selected_tau_n=[duration duration];
selected_tau_h=[duration duration];

m_x=0;
m_bc= m_bc_tau_scaled(x)*selected_tau_m(1);
m_ac= m_bc_tau_scaled(x)*selected_tau_m(2);

h_x= tauh_shift(x);
h_bc=selected_tau_h(1);
h_ac=selected_tau_h(2);
```

```
n_x=0;
n_bc=selected_tau_n(1);
n_ac=selected_tau_n(2);

m_o_mod = m_bound_mod(V_rest,V_rest,m_bc,m_ac,m_x);
h_o_mod = h_bound_mod(V_rest,V_rest,h_bc,h_ac,h_x);
n_o_mod = n_bound_mod(V_rest,V_rest,n_bc,n_ac,n_x);

%% Specify the inital conditions vector
y0 = [V_rest, m_o_mod, h_o_mod, n_o_mod ];
options = odeset();

%% Invoke the solver
[T,Y_Vr1] = ode45(@odefun_Vm_Vr1, t, y0, options, C, maxcond_Na,...
   maxcond_K, Na_Battery, K_Battery, pulse_width, pulse_amp(j),...
   V_rest,m_bc,m_ac,h_bc,h_ac,n_bc,n_ac,n_x,m_x,h_x);

colors={'b','g','r','k','m','c','y'};

%% Plot solution
plot(T,Y_Vr1(:,1),colors{x})
hold on
axis([0 max_time EK_nernst ENa_nernst]);
title('Retzius Cell Model: Reducing Peak Duration ','FontWeight','bold')
xlabel('Time(s)')
ylabel('Membrane Potential (V)')
hold on
```

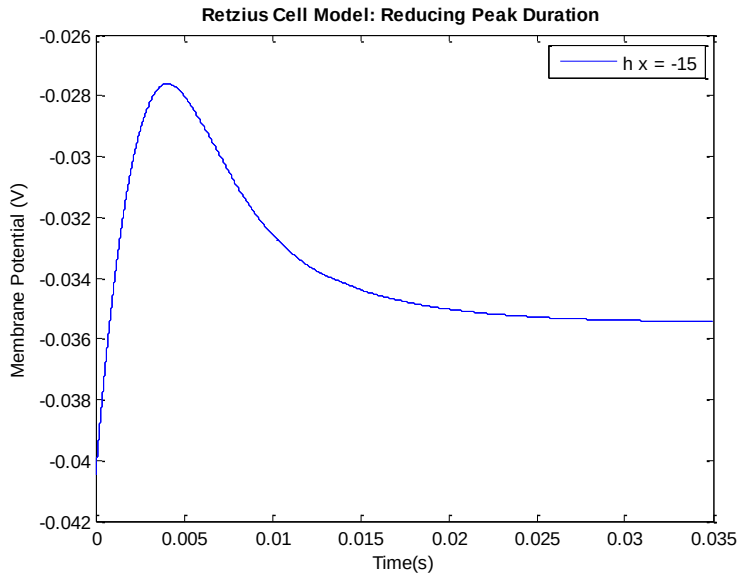

Figure 10.31. Peak duration reduction of the action potential observed in the Retzius cell to *h* value of -15

The peak duration of the Retzius cell depicted in figure 10.31 is reduced to a *h_x* value of -15. The peak duration of the P cell is slightly increase to a *h_x* value of 1.

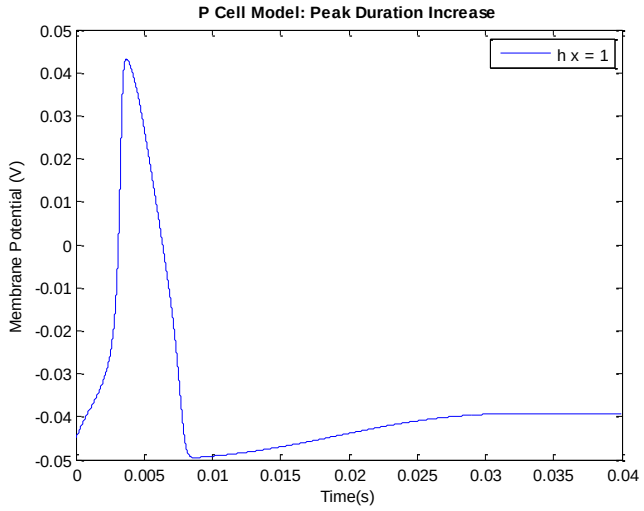

Figure 10.32. Peak duration reduction of the action potential observed in the P cell to *h* value of -1

10.4.10 Repolarization Increase

The repolarization of the Retzius cell matches the experimental recordings without any adjustment. However, the repolarization of the P cell was adjusted, shown in figure 10.33.

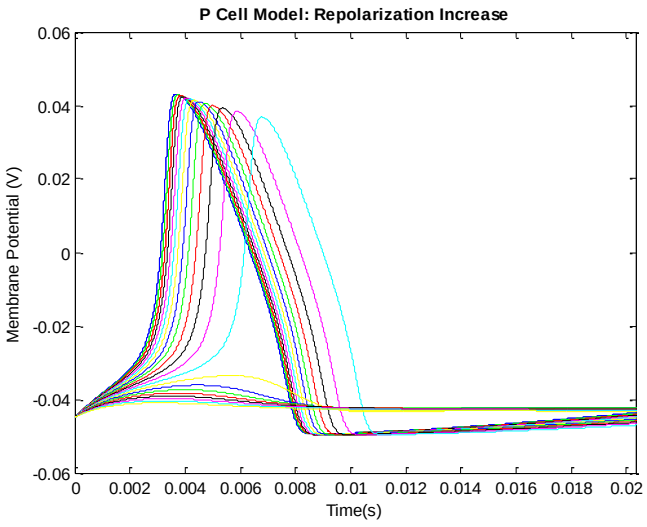

Figure 10.33. Repolarization increase of the P cell

The P cell's repolarization phase was increased by reducing *n_x* to -0.0061 with the following script. The resulting waveform is shown in figure 10.34.

```
%% Repolarization Increase
duration_range =fliplr(duration_range);
tau_m_reduction=1:.25:8;
tauh_shift=0:-1:-10;
taun_shift=0:-5e-4:-10e-3;

for x=1:length(taun_shift)

duration=0.45;
red_max =0.9;

selected_tau_m=[(1.23*duration)/red_max (0.84*duration)/red_max];
selected_tau_n=[duration duration];
selected_tau_h=[duration duration];

m_x=0;
m_bc= m_bc_tau_scaled(x)*selected_tau_m(1);
m_ac= m_bc_tau_scaled(x)*selected_tau_m(2);

h_x=1;
h_bc=selected_tau_h(1);
h_ac=selected_tau_h(2);

n_x= taun_shift(x);
n_bc=selected_tau_n(1);
n_ac=selected_tau_n(2);

m_o_mod = m_bound_mod(V_rest,V_rest,m_bc,m_ac,m_x);
h_o_mod = h_bound_mod(V_rest,V_rest,h_bc,h_ac,h_x);
n_o_mod = n_bound_mod(V_rest,V_rest,n_bc,n_ac,n_x);
%% Specify the inital conditions vector
y0 = [V_rest, m_o_mod, h_o_mod, n_o_mod ];
options = odeset();

%% Invoke the solver
[T,Y_Vr1] = ode45(@odefun_Vm_Vr1, t, y0, options, C, maxcond_Na,...
    maxcond_K, Na_Battery, K_Battery, pulse_width, pulse_amp(j),...
    V_rest,m_bc,m_ac,h_bc,h_ac,n_bc,n_ac,n_x,m_x,h_x);

colors={'b','g','r','k','m','c','y'};

%% Plot solution
plot(T,Y_Vr1(:,1),colors{x})
hold on
axis([0 max_time EK_nernst ENa_nernst]);
title('Retzius Cell Model: Repolarization increase ','FontWeight','bold')
xlabel('Time(s)')
ylabel('Membrane Potential (V)')
hold on
legend (n x =-0.0061)
```

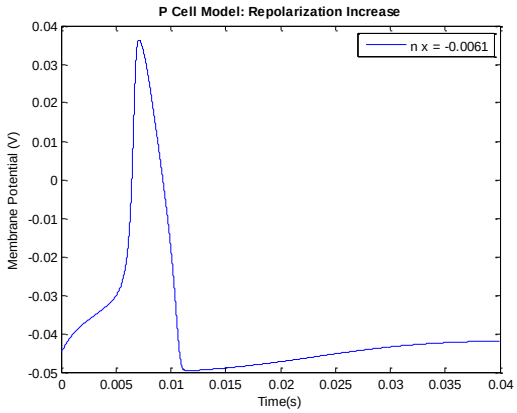

Figure 10.34. Repolarization increase of the P cell with the value of *n_x* equal to -0.0061

CHAPTER XI: RESULTS AND CONCLUSIONS

MATLAB simulation of the Retzius cell action potential was achieved through modification of the Hodgkin-Huxley model rate equations. A P cell action potential was also successfully simulated using the same methodology, demonstrating the ability to simulate diverse waveforms. The final simulations of the Retzius cell and P cell are compared to actual electrophysiological recordings in figures 11.1-11.5.

11.1 Results

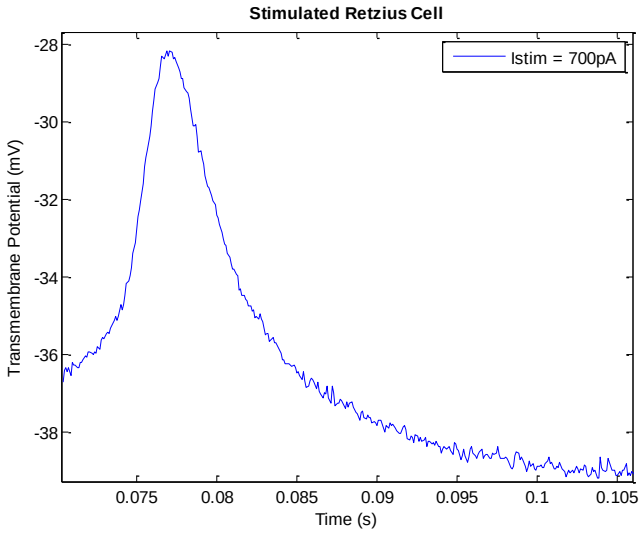

Figure 11.1. An experimental recording of a Retzius cell action potential from the data gathered in Chapter 8

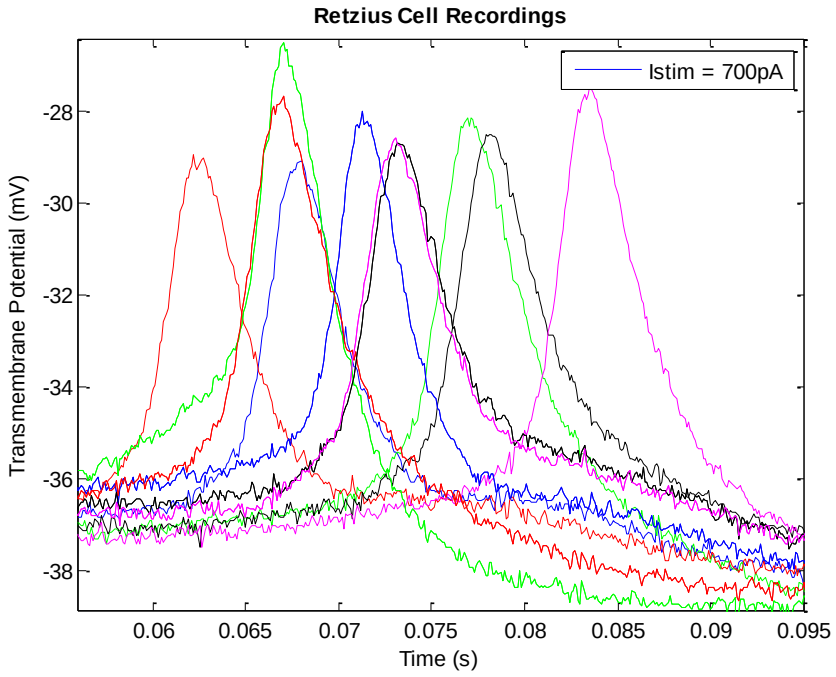

Figure 11.2 Multiple experimental recordings of a Retzius cell action potentials from the data gathered in Chapter 8

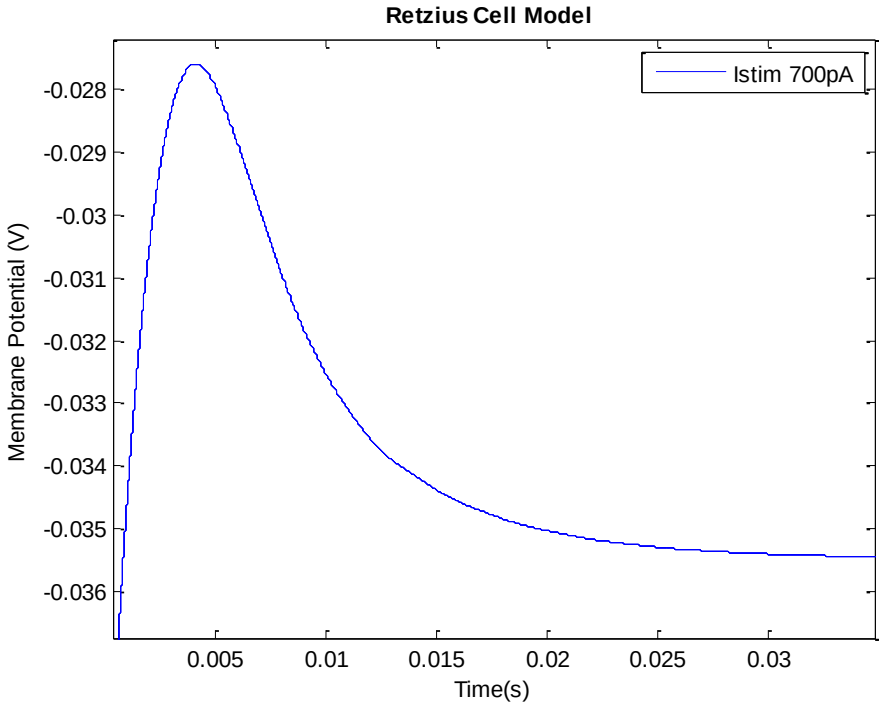

Figure 11.3. The stimulated action potential of a Retzius cell

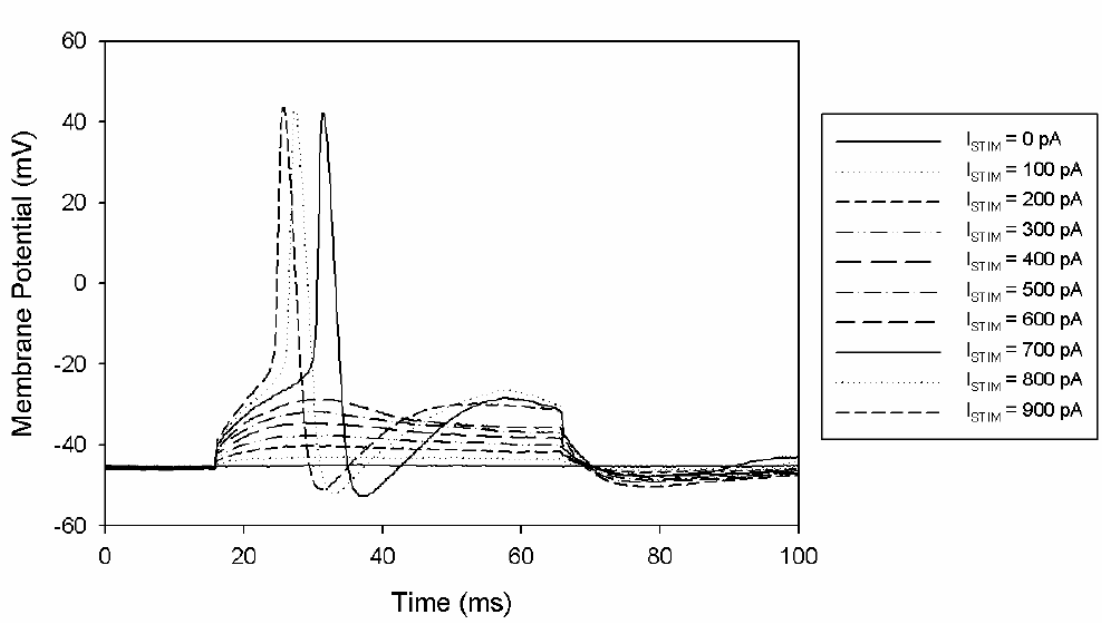

Figure 11.4 Recording of a P cell action potential

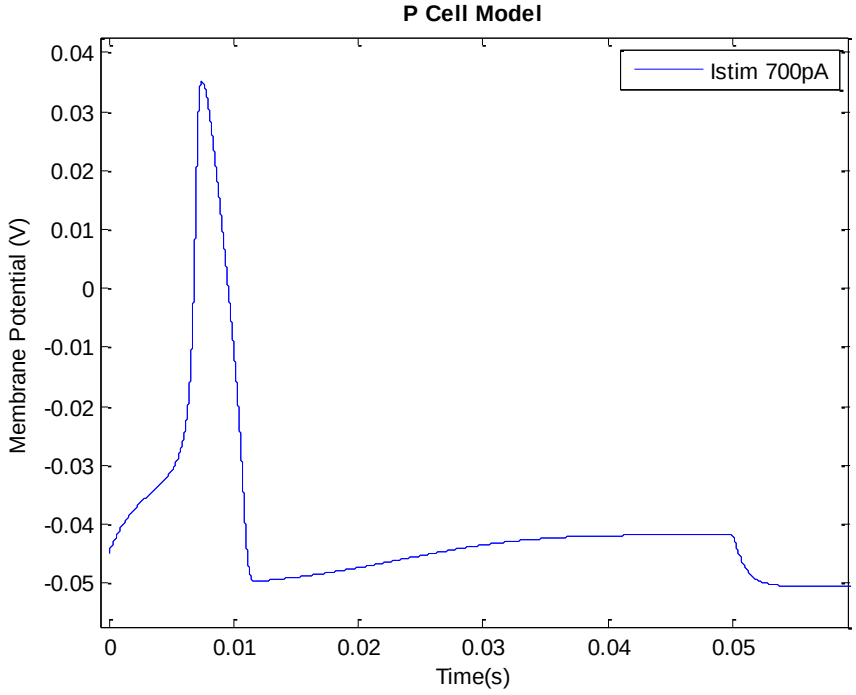

Figure 11.5. The simulated action potential of a P cell

11.2 Conclusions

The simulated Retzius cell waveform is able to accurately represent many aspects of actual Retzius cell electrophysiological recordings, including: waveform amplitude, period, peak duration and decay. This waveform is generated under analogous conditions to those found in the Retzius cell, such as cellular dimension, intracellular and extracellular ionic concentrations, ionic electrochemical grandients, ionic membrane permeabilies, membrane capacitance, stimulation parameters, threshold potential and function of voltage-gated ion channels.

This simulation was implemented through the alteration of votlage-gated sodium and potassium channel behavior via Hodgkin-Huxley rate equation modification. This methodology proves to have diverse application in waveform simulation, accurately simulating action potentials recorded in the Retzius and P cell of the *Hirudo Medicinalis.* Further refinement of this technique should allow for the voltage-gated behavioral based simulation of any action potential-like waveform with simulation conditions analogous to the cellular environment. Eventually, simulations of this nature could provide helpful insight regarding the voltage sensitivity and dependence of voltage-gated ion channels in an array of organisms.

REFERENCES

[1] Fox, S.I., *Human Physiology,* 5th ed. Boston, Mass: Wm. C. Brown Publishers. 1996.

[2] Waxman, S.G., *Clinical Neuroanatomy,* 26th ed. San Francisco: McGraw Hill Medical, 2010.

[3] Aidley, D.J., *The Physiology of Excitable Cells,* 4th ed. Cambridge, UK: Cambridge University Press, 1998.

[4] Matthews, Gary G. *Cellular Physiology of Nerve and Muscle,* 4th ed. Boston: Blackwell Scientific Publications, 2001.

[5] Weiss, T. F., *Cellular Biophysics Volume 2,* Cambridge, Mass: MIT Press, 1997.

[6] Purves D., Augustine G.J., Fitzpatrick D., *Neuroscience,* 2nd ed. Sunderland, Mass: Sinauer Associates; 2001.

[7] Xu, Z.J., Adams, D.J., "Resting membrane potential and potassium currents in cultured parasympathetic neurons from rate intracardiac ganglia,*"J. Physiol.,*no. 456, pp. 405-424. October, 1992.

[8] Cholette, M. "Membrane Channel Properties," California Polytechnic State University- San Luis Obispo, BMED 450: Neuroengineering Lecture Slides. Fall 2011.

[9] Cholette, M. "Membrane Potential," California Polytechnic State University- San Luis Obispo, BMED 450: Neuroengineering Lecture Slides. Fall 2011.

[10] Cholette, M. "The Action Potential," California Polytechnic State University- San Luis Obispo, BMED 450: Neuroengineering Lecture Slides. Fall 2011.

[11] Saladin, Kenneth S. *Anatomy & Physiology: The Unity of Form and Function*, 4th ed. Georgia College and State University. New York: McGraw Hill Companies, 2007.

[12] Cholette, M. "Neurotransmission," California Polytechnic State University- San Luis Obispo, BMED 450: Neuroengineering Lecture Slides. Fall 2011.

[13] Nobel Media. (Oct 2013) *The Nobel Prize in Physiology or Medicine 1963* [Online]. Available:http://www.nobelprize.org/nobel_prizes/medicine/laureates/1963/

[14] Hodgkin, A. L. and Huxley, A. F., "A quantitative description of membrane current and its application to conduction and excitation in nerve," *J. Physiol,* vol. 117, no. 4, pp. 500-544, Aug. 1952.

[15] Hodgkin, A. L. and Huxley, A. F., "The dual effect of membrane potential on sodium conductance in the giant axon of Loligo," *J. Physiol,* vol. 116, no. 4, pp. 497-506, Apr. 1952.

[16] Hodgkin, A. L. and Huxley, A. F., "Currents carried by sodium and potassium ions through the membrane of the giant axon of Loligo," *J. Physiol*, vol. 116, no. 4, pp. 449-472, Apr. 1952.

[17] Hodgkin, A. L. and Huxley, A. F., "The components of membrane conductance in the giant axon of Loligo," *J. Physiol*, vol. 116, no. 4, pp. 473-496, Apr. 1952.

[18] Hodgkin, A. L. and Huxley, A. F., and Katz, B., "Measurement of current-voltage relations in the membrane of the giant axon of Loligo," *J. Physiol*, vol. 116, no. 4, pp. 424-448, Apr. 1952.

[19] Catterall, W.A., Raman, I.M., Robinson, H., Sejnowski, T.,Paulsen, O., "The Hodgkin-Huxley Heritage: From Channels to Circuits," *J.Neurosci,* vol. 32, no. 41, pp. 14064-14073. November, 2012.

[20] Muller, K.J., Nicholls, J.G. and Stent, G.S. Neurobiology of the Leech. Cold Spring Harbor Laboratory, New York, 1981, pp. 51-78.

[21] "The Axon Guide," MDS Analytical Technologies, 3rd edition. Sunnyvale, California. 2008.

[22] Deitmer, J.W., Schlue, W.R., "Measurements of the intracellular potassium activity of Retzius cells in the leech central nervous system," *J. Exp. Bio.,*vol 91, pp 87-101. 1981. Great Britain.

[23] Deitmer, J.W., Schlue, W.R., "Intracellular Na+ and Ca+ in leech Retzius neurons during inhibition of the Na+ -K+ pump," *Euro. J. Phys.*vol. 397, pp. 195-201. 1983.

[24] Becker, G. F., Orstrand., C.E. *Hyperbolic Function,* Washington: Smithson. Institution, 1931.

[25] Terlau, H., Stuhmer, W., "Structure and function of voltage-gated ion channels," *Nature,* vol. 85 no. 85. Pp. 437-44. 1998.

APPENDIX A

MATLAB scripts and functions referenced in Chapter IX

```
%%%%%%%%%%%%%%%%%%%%%%%%%%%%%%%%%%%%%%%%%%%%%%%%%%%%%%%%%%%%%%%%%%%%%%%%%%%%%%%%%%%%%%%%%%%%%%%%%%%%%%%%%%%%%%%%%%%%%%%%%%%%%%%%%%%%%%%%%%%%%%%%%%%%%%%%%%%%%%%%%%%
%%%%
%
% Function: odefun
% Revision Date: 12/11/09
% Author: Robert B. Szlavik
%
% Implement the system of nonlinear ordinary differential equations
% associated with the problem presented in Section 6.1.
%
% USES FUNCTIONS: m_bound
% h_bound
% n_bound
% tau_m
% tau_h
% tau_n
% Current
%
% Inputs: t = current time point being evaluated in (s)
% y = previous value of the ODE variables, VECTOR
% Cm = membrane capacitance in (F)
% GNamax = maximum sodium conductance in (S)
% GKmax = maximum potassium conductance in (S)
% VNa = sodium Nernst potential in (V)
% VK = potassium Nernst potential in (V)
% pw = stimulus pulse width in (s)
% amp = stimulus pulse amplitude in (A)
%
% Returns: dy = first derivative value of ODE variables
%
% Internal: mf = step bounded value of m gating variable
% hf = step bounded value of h gating variable
% nf = step founded value of n gating variable
% taum = step rise time value of m gating variable
% tauh = step rise time value of h gating variable
% taun = step rise time value of n gating variable
%
%%%%%%%%%%%%%%%%%%%%%%%%%%%%%%%%%%%%%%%%%%%%%%%%%%%%%%%%%%%%%%%%%%%%%%%%%%%%%%%%%%%%%%%%%%%%%%%%%%%%%%%%%%%%%%%%%%%%%%%%%%%%%%%%%%%%%%%%%%%%%%%%%%%%%%%%%%%%%%%%%%
%%%%

function dy = odefun(t, y, Cm, GNamax, GKmax, VNa, VK, pw, amp);
mf = m_bound(y(1));
hf = h_bound(y(1));
nf = n_bound(y(1));
taum = tau_m(y(1));
tauh = tau_h(y(1));
taun = tau_n(y(1));
dy = [-(GKmax/Cm)*(y(4)^4)*(y(1)-VK)-(GNamax/Cm)*(y(2)^3)*y(3)*(y(1)-VNa)+Current(t,pw,amp)/Cm;
(mf-y(2))/taum;
(hf-y(3))/tauh;
(nf-y(4))/taun];



%%%%%%%%%%%%%%%%%%%%%%%%%%%%%%%%%%%%%%%%%%%%%%%%%%%%%%%%%%%%%%%%%%%%%%%%%%%%%%%%%%%%%%%%%%%%%%%%%%%%%%%%%%%%%%%%%%%%%%%%%%%%%%%%%%%%%%%%%%%%%%%%%%%%%%%%%%%%%%%%%%
%%%%
%
% Function: V_r
% Revision Date: 12/11/09
% Author: Robert B. Szlavik
%
% Find the resting membrane potential for sodium and potassium using
% the Goldmann Equation.
```

```
%
% Inputs: coNa = Extracellular sodium concentration in
% (moles/liter)
% ciNa = Intracellular sodium concentration in
% (moles/liter)
% coK = Extracellular potassium concentration in
% (moles/liter)
% ciK = Intracellular potassium concentration in

% T = Temperature in degrees (Celsius)
% b = Relative permeability of sodium to potassium
%
% Returns: Vr = Resting transmembrane potential in (V)
%
% Internal: R = Reiberg Gas Constant in (joules/(mole*kelvin))
% F = Faraday's Constant in (coulombs/mole)
% Z = Sodium and potassium ionic valence
% TKelvin = Temperature in degrees (Kelvin)
%
%%%%%%%%%%%%%%%%%%%%%%%%%%%%%%%%%%%%%%%%%%%%%%%%%%%%%%%%%%%%%%%%%%%%%%%%%%%
%%%%
function Vr = V_r(coNa,ciNa,coK,ciK,T,b)
R = 8.314; % Reiberg gas constant (joules/(mole*kelvin)).
F = 9.648E4; % Faraday's constant (coulombs/mole).
Z = 1; % Sodium and potassium ionic valence.
TKelvin = 273.15 + T;
Vr = ((R*TKelvin)/(Z*F))*log((coK + b*coNa)/(ciK + b*ciNa));

%%%%%%%%%%%%%%%%%%%%%%%%%%%%%%%%%%%%%%%%%%%%%%%%%%%%%%%%%%%%%%%%%%%%%%%%%%%
%%%%
%
% Function: m_bound
% Revision Date: 12/14/09
% Author: Robert B. Szlavik
%
% Computes the final value of the m gating variable given a step
% excitation.
%
% USES FUNCTIONS: alpha_m
% beta_m
%
%
% Inputs: Vm = Membrane Potential (V)
%
% Returns: mb = Final value of m gating variable given a step
% excitation
%
%%%%%%%%%%%%%%%%%%%%%%%%%%%%%%%%%%%%%%%%%%%%%%%%%%%%%%%%%%%%%%%%%%%%%%%%%%%
%%%%
function mb = m_bound(Vm)
mb = alpha_m(Vm)/(alpha_m(Vm)+beta_m(Vm));



%%%%%%%%%%%%%%%%%%%%%%%%%%%%%%%%%%%%%%%%%%%%%%%%%%%%%%%%%%%%%%%%%%%%%%%%%%%
%%%%
%
% Function: alpha_m
% Revision Date: 12/14/09
% Author: Robert B. Szlavik
%
% Computes the value of the alpha rate constant for the m gating
% variable. The function error traps for the denominator singularity
% condition.
%
% Inputs: Vm = Membrane Potential (V)
%
% Returns: am = Returns the alpha rate constant for the m
% gating variable (1/ms)
```

```
%
%%%%%%%%%%%%%%%%%%%%%%%%%%%%%%%%%%%%%%%%%%%%%%%%%%%%%%%%%%%%%%%%%%%%%%%%%%%%%%%%%%%%%%%%
%%%%
function am = alpha_m(Vm)
Vm = Vm/1.0E-3;
if Vm ~= -35
am = -0.1*(Vm+35)/(exp(-0.1*(Vm+35))-1);
end
if Vm == -35
up = Vm + 1.0E-4;
down = Vm - 1.0E-4;
am =(-0.1*(up+35)/(exp(-0.1*(up+35))-1)+(-0.1)*(down+35)/(exp(-0.1*(down+35))-1))/2;
end

%%%%%%%%%%%%%%%%%%%%%%%%%%%%%%%%%%%%%%%%%%%%%%%%%%%%%%%%%%%%%%%%%%%%%%%%%%%%%%%%%%%%%%%%
%%%%
%
% Function: alpha_h
% Revision Date: 12/14/09
% Author: Robert B. Szlavik
%
% Computes the value of the alpha rate constant for the h gating
% variable.
%
% Inputs: Vm = Membrane Potential (V)
%
% Returns: ah = Returns the alpha rate constant for the h
% gating variable (1/ms)
%
%%%%%%%%%%%%%%%%%%%%%%%%%%%%%%%%%%%%%%%%%%%%%%%%%%%%%%%%%%%%%%%%%%%%%%%%%%%%%%%%%%%%%%%%
%%%%
function ah = alpha_h(Vm)
Vm = Vm/1.0E-3;
ah = 0.07*exp(-0.05*(Vm+60));

%%%%%%%%%%%%%%%%%%%%%%%%%%%%%%%%%%%%%%%%%%%%%%%%%%%%%%%%%%%%%%%%%%%%%%%%%%%%%%%%%%%%%%%%
%%%%
%
% Function: alpha_n
% Revision Date: 12/14/09
% Author: Robert B. Szlavik
%
% Computes the value of the alpha rate constant for the n gating
% variable. The function error traps for the denominator singularity
% condition.
%
% Inputs: Vm = Membrane Potential (V)
%
% Returns: an = Returns the alpha rate constant for the n
% gating variable (1/ms)
%
%%%%%%%%%%%%%%%%%%%%%%%%%%%%%%%%%%%%%%%%%%%%%%%%%%%%%%%%%%%%%%%%%%%%%%%%%%%%%%%%%%%%%%%%
%%%%
function an = alpha_n(Vm)
Vm = Vm/1.0E-3;
if Vm ~= -50
an = -0.01*(Vm+50)/(exp(-0.1*(Vm+50))-1);
end
if Vm == -50
up = Vm + 1.0E-4;
down = Vm - 1.0E-4;
an = (-0.01*(up+50)/(exp(-0.1*(up+50))-1) + -0.01*(down+50)/(exp(-0.1*(down+50))-1))/2;
end

%%%%%%%%%%%%%%%%%%%%%%%%%%%%%%%%%%%%%%%%%%%%%%%%%%%%%%%%%%%%%%%%%%%%%%%%%%%%%%%%%%%%%%%%
%%%%
%
% Function: beta_m
% Revision Date: 12/14/09
```

```
% Author: Robert B. Szlavik

%

% Computes the value of the beta rate constant for the m gating
% variable.
%
% Inputs: Vm = Membrane Potential (V)
%
% Returns: bm = Returns the alpha rate constant for the m
% gating variable (1/ms)
%
%%%%%%%%%%%%%%%%%%%%%%%%%%%%%%%%%%%%%%%%%%%%%%%%%%%%%%%%%%%%%%%%%%%%%%%%%%%%%%%%%%%%%%%%%%%%%%%%%%%%%
%%%%
function bm = beta_m(Vm)
Vm = Vm/1.0E-3;
bm = 4.0*exp(-(Vm+60)/18);

%%%%%%%%%%%%%%%%%%%%%%%%%%%%%%%%%%%%%%%%%%%%%%%%%%%%%%%%%%%%%%%%%%%%%%%%%%%%%%%%%%%%%%%%%%%%%%%%%%%%%
%%%%
%
% Function: beta_h
% Revision Date: 12/14/09
% Author: Robert B. Szlavik
%
% Computes the value of the beta rate constant for the h gating
% variable.
%
% Inputs: Vm = Membrane Potential (V)
%
% Returns: bh = Returns the alpha rate constant for the h
% gating variable (1/ms)
%
%%%%%%%%%%%%%%%%%%%%%%%%%%%%%%%%%%%%%%%%%%%%%%%%%%%%%%%%%%%%%%%%%%%%%%%%%%%%%%%%%%%%%%%%%%%%%%%%%%%%%
%%%%
function bh = beta_h(Vm)
Vm = Vm/1.0E-3;
bh = 1/(1+exp(-0.1*(Vm+30)));

%%%%%%%%%%%%%%%%%%%%%%%%%%%%%%%%%%%%%%%%%%%%%%%%%%%%%%%%%%%%%%%%%%%%%%%%%%%%%%%%%%%%%%%%%%%%%%%%%%%%%
%%%%
%
% Function: beta_n
% Revision Date: 12/14/09
% Author: Robert B. Szlavik
%
% Computes the value of the beta rate constant for the n gating
% variable.
%
% Inputs: Vm = Membrane Potential (V)
%
% Returns: bn = Returns the alpha rate constant for the n
% gating variable (1/ms)
%
%%%%%%%%%%%%%%%%%%%%%%%%%%%%%%%%%%%%%%%%%%%%%%%%%%%%%%%%%%%%%%%%%%%%%%%%%%%%%%%%%%%%%%%%%%%%%%%%%%%%%
%%%%
function bn = beta_n(Vm)
Vm = Vm/1.0E-3;
bn = 0.125*exp(-0.0125*(Vm+60));

%%%%%%%%%%%%%%%%%%%%%%%%%%%%%%%%%%%%%%%%%%%%%%%%%%%%%%%%%%%%%%%%%%%%%%%%%%%%%%%%%%%%%%%%%%%%%%%%%%%%%
%%%%
%
% Function: Current
% Revision Date: 12/14/09
% Author: Robert B. Szlavik
%
% Computes the value of the beta rate constant for the m gating
% variable.
```

```
%
% Inputs: t = Time in (s)
% pw = Stimulus pulse width in (s)
% amp = Stimulus current pulse amplitude in (A)
%
% Returns: I = Returns the stimulus current value in (A)
%
%%%%%%%%%%%%%%%%%%%%%%%%%%%%%%%%%%%%%%%%%%%%%%%%%%%%%%%%%%%%%%%%%%%%%%%%%%%
%%%%
function I = Current(t,pw,amp)
if t >= 0.0 & t <= pw
I = amp;
else
I = 0.0;
End

%%%%%%%%%%%%%%%%%%%%%%%%%%%%%%%%%%%%%%%%%%%%%%%%%%%%%%%%%%%%%%%%%%%%%%%%%%%
%%%%
%
% Program: Main_Program
% Revision Date: 12/22/09
% Author: Robert B. Szlavik

% Current clamped electrically small cell solution.
%
% USES FUNCTIONS: odefun
% V_Na
% V_K
% V_r
% m_bound
% h_bound
% n_bound
% ode45
%
% Internal: a = Cell radius (m)
% d = Cell diameter (m)
% L = Cell length (m)
% temp = Temperture (deg. C)
% gmax_Na = Maximum sodium conductance per unit area
% (S/m^2)
% gmax_K = Maximum potassium conductance per unit area
% (S/m^2)
% co_Na = Extracellular Na concentration (M/L)
% ci_Na = Intracellular Na concentration (M/L)
% co_K = Extracellular K concentration (M/L)
% ci_K = Intracellular K concentration (M/L)
% C_m = Membrance capacitance per unit area (F/m^2)
% b = Relative sodium to potassium conductance
% delta_t = Time step (s)
% max_time = Maximum time (s)
% pulse_width = Stimulus pulse width (s)
% pulse_amp = Stimulus pulse amplitude (A)
% Area = Cell surface area (m^2)
% C = Cell capacitance (F)
% maxcond_Na = Maximum sodium conductance (S)
% maxcond_K = Maximum potassium conductance (S)
% Na_Battery = Sodium Nernst potential (V)
% K_Battery = Potassium Nernst potential (V)
% V_rest = Resting membrane potential (V)
% m_o = m gating variable initial value
% h_o = h gating variable initial value
% n_o = n gating variable initial value
% t = Vector of time points (s)
% y0 = Vector of initial conditions
% opions = default solver options data structure
%
%%%%%%%%%%%%%%%%%%%%%%%%%%%%%%%%%%%%%%%%%%%%%%%%%%%%%%%%%%%%%%%%%%%%%%%%%%%
%%%%
% Variable declerations
```

```
a = 20E-6; % Cell radius (m)
d = 2*a; % Cell diameter (m)
L = 40.0E-6; % Cell length (m)
temp = 6.3; % Temperature (deg. C)
gmax_Na = (120E-3)*100^2; % Maximum sodium conductance per unit area (S/m^2)
gmax_K = (36E-3)*100^2; % Maximum potassium conductance per unit area (S/m^2)
co_Na = 491E-3; % Extracellular Na concentration (M/L)
ci_Na = 50E-3; % Intracellular Na concentration (M/L)
co_K = 20.11E-3; % Extracellular K concentration (M/L)
ci_K = 400E-3; % Intracellular K concentration (M/L)
C_m = (1.0E-6)*100^2; % Membrane capacitance per unit area (F/m^2)
b = 0.02; % Relative sodium to potassium conductance
delta_t = 1.0E-6; % Time step (s)
max_time = 20.0E-3; % Maximum time (s)
pulse_width = 10E-6; % Stimulus pulse width (s)
pulse_amp = 53E-9; % Stimulus pulse amplitude (A)

% Compute cell parameter values

Area = 2*(pi*a^2) + 2*pi*a*L;
C = Area*C_m;
maxcond_Na = Area*gmax_Na;
maxcond_K = Area*gmax_K;
Na_Battery = V_Na(co_Na, ci_Na, temp);
K_Battery = V_K(co_K, ci_K, temp);
V_rest = V_r(co_Na, ci_Na, co_K, ci_K, temp, b);
m_o = m_bound(V_rest);
h_o = h_bound(V_rest);
n_o = n_bound(V_rest);
% Set up the time vector
t = zeros(floor(max_time/delta_t),1);
for i = 1:floor(max_time/delta_t)
t(i) = (i-1)*delta_t;
end
% Specify the initial conditions vector
y0 = [V_rest, m_o, h_o, n_o];
options = odeset();
% Invoke the solver
[T,Y] = ode45(@odefun, t, y0, options, C, maxcond_Na, maxcond_K, Na_Battery, K_Battery,
pulse_width, pulse_amp);
% Plot the solution
figure(1)
plot(T,Y(:,1))
grid
figure(2)
plot(T,Y(:,2))
hold on
plot(T,Y(:,3),'r')
hold on
plot(T,Y(:,4),'g')
grid
```